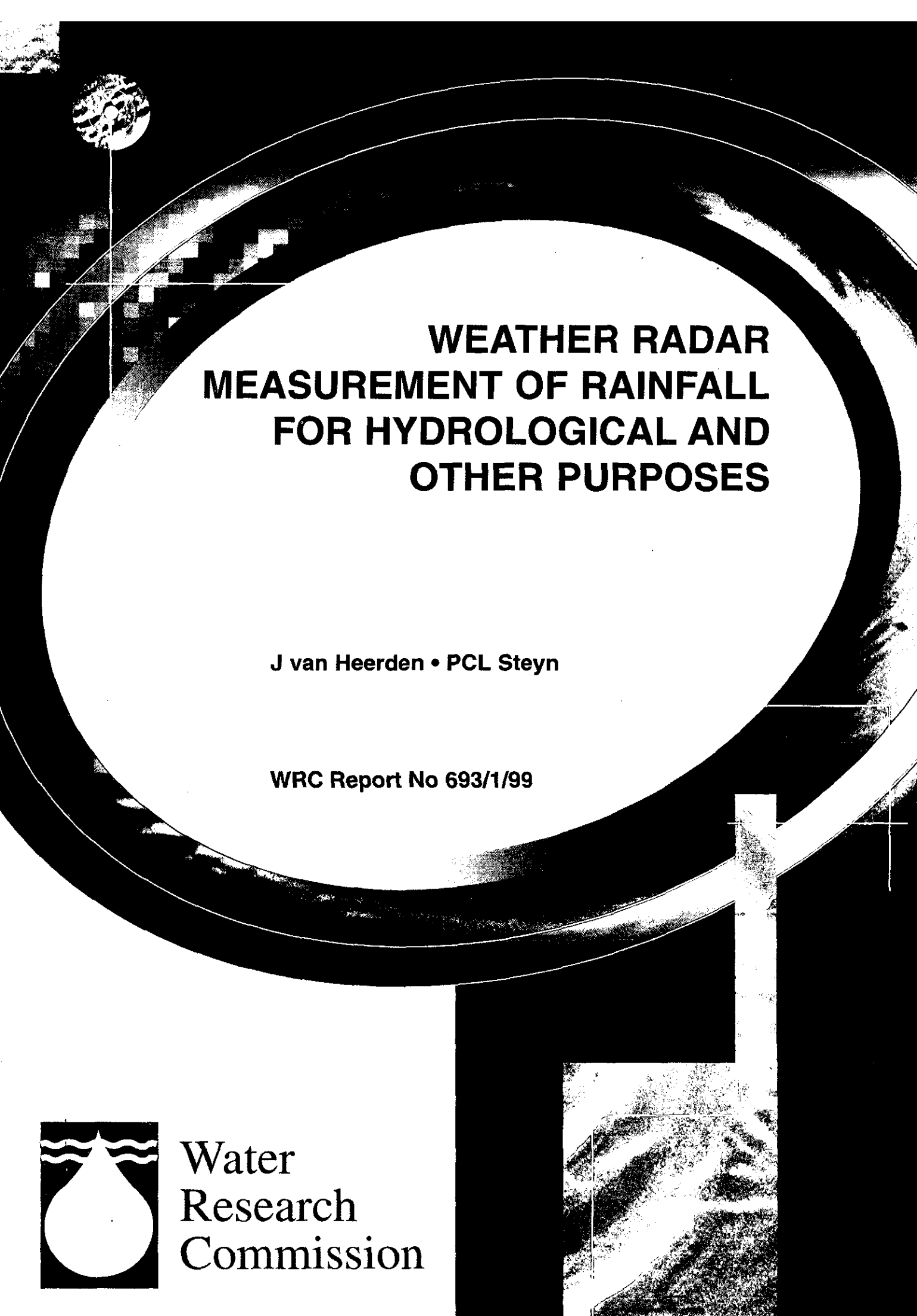

WEATHER RADAR MEASUREMENT OF RAINFALL FOR HYDROLOGICAL AND OTHER PURPOSES

J van Heerden • PCL Steyn

WRC Report No 693/1/99

Water Research Commission

Weather Radar Measurement of Rainfall for Hydrological and other purposes

J van Heerden • PCL Steyn

Final report to the Water Research Commission on the project:
"Research into the weather radar measurement of rainfall
as well as hydrological applications of weather radar"
Department of Earth Sciences
University of Pretoria

WRC Report No 693/1/99
ISBN No 1 86845 5386

PROJECT TEAM

University of Pretoria

Prof J van Heerden

Mr P C L Steyn

Dr C J de W Rautenbach

Ms L L Dyson

Mrs H Kenyon

Mr M M Truter

Bethlehem Precipitation Research Project (Weather Bureau)

Mr N J Kroese

Dr D E Terblanche

Mr D J Dicks

Ms M P Mittermaier

Mr F O Hiscutt

Mr H K P de Waal

Mr F Stuart

Mr P Visser

ACKNOWLEDGEMENTS

The project "Research into the weather radar measurement of rainfall as well as hydrological applications of weather radar" (RADARAIN), would not have been possible without the support of three institutions:

- The Water Research Commission (WRC) purchased the MRL-5 radar and funded the RADARAIN project.
- The Weather Bureau's Bethlehem Precipitation Research Project made personnel, equipment and infrastructure available.
- The University of Pretoria (UP) made infrastructure and staff available.

The WRC Steering Committee provided guidance and encouragement. The following persons, team members excluded, all participated in several of the Steering Committee activities:

Dr GC Green	Water Research Commission (Chairman)
Mr H Maaren	Water Research Commission
Mr DJ Marais	Water Research Commission (Committee Secretary)
Mrs CM Smit	Water Research Commission (Committee Services)
Dr MC Hodson	CSIR (retired)
Prof GCS Pegram	University of Natal
Mr G C Schulze	South African Weather Bureau (Chief Director)
Prof WJR Alexander	University of Pretoria
Mr KA Monnik	Agricultural Research Council (ISCW)
Mr S van Biljon	Department of Water Affairs & Forestry

In the compilation of the report several team members provided contributions and allowed us to use and adapt from their published material. Much of the detail provided in Chapters 1, 2 and 4 provide background and explain the use, in RADARAIN, of research work by:

Dr D E Terblanche, Mr P J M Visser and Ms M Mittermaier.

It would have been impossible to compile this report without using some of their work. A special word of thanks to Mr F Stuart who spent many days in preparing computer programmes for use in RADARAIN. His dedication made it possible to compute the SSS, CAPPI and other fields from meteorological data volume (**mdv**) files. Mr H K P de Waal performed a vital role in providing all the radar data used in this project. Computing the **mdv** formatted files required a vast amount of work, which in part required the revamping of the BPRP archival system.

Our special appreciation also to all the team members and students who participated in RADARAIN. Operating the rainfall network involved considerable travel on farm roads and digging and pushing vehicles out of the mud happened often.

The owners of the farms Liefde, Rust, Slangfontein, Eureka, Truia, Somerslus, Prosperity, Tweespruit, Sweetwaters, Welverdiend, and Vrede who allowed us to install tipping bucket rain gauges and to travel on their farms deserve our special thanks. We were welcomed into their homes and all assisted to make operation of the rain gauge network a success. The Tipping bucket data logger combination worked very well and Mr Hiscutt should be congratulated for the development of such a stable system.

Our thanks to Mrs H Kenyon who spent many hours in front of the computer compiling this document. The support by Ms C du Preez and Ms I Booysen by providing the figures, is appreciated.

ABBREVIATIONS

AGL	Above General Level
ASL	Above Sea Level
BEWMEX	Bethlehem Weather Modification Experiment
BPRP	Bethlehem Precipitation Research Project
CAPPI	Constant Altitude Plan Position Indicator
CSIR	Council for Scientific and Industrial Research
DISPLACE	Digital Signal Processing for Logarithmic, Linear and Quadratic Responses
DVA	Displace Variate Averaging
DSD	Drop Size Distribution
EDL	Event Data Logger
LINUX	PC version of UNIX
LWC	Liquid Water Content
"mdv"	Meteorological Data Volume
NPRP	National Precipitation Research Programme
NTW	Network
PEP	Precipitation Enhancement Programme
PPI	Plan Position Indicator
PRF	Pulse Repetition Frequency
RCC	Radar Control Card
RDAS	Radar Data Acquisition System
RF	Radio Frequency
SAST	South African Standard Time
SAWB	South African Weather Bureau
SSS	Storm Structure Severity
TITAN	Thunderstorm Identification Tracking and Nowcasting
UP	University of Pretoria
UT	Universal Time
WMO	World Meteorological Organisation
WRC	Water Research Commission

TABLE OF CONTENTS

EXECUTIVE SUMMARY

1. INTRODUCTION

The difficulty and cost in maintaining a rainfall gauge network country wide, as well as the increasing unwillingness of lay-observers to report daily rainfall, demand the investigation of alternative methods of recording rainfall. Radar based rainfall estimates are a viable alternative. Enough experience in this field existed to launch the project "Research into the weather radar measurement of rainfall as well as hydrological applications of weather radar (RADARAIN)".

The RADARAIN Project has four main components:

- The MRL-5 radar, data transmission analysis and archival system.
- The rainfall gauge network operated by University of Pretoria (UP) RADARAIN project personnel. Up to 16 automatic gauges were deployed.
- A research component comprising researchers from UP and the Bethlehem Precipitation Research Project (BPRP) including recent work by Visser (1999) on the Storm Structure Severity (SSS) method and work by Mittermaier (1999) on the bright band.
- The Thunderstorm Identification Tracking and Nowcasting (TITAN) (Dixon and Wiener, (1993) software as well as radar data in Meteorological Data Volume (**mdv**) format.

The objectives of the RADARAIN project can be summarised as:

- *To develop greater understanding of the space-time characteristics of convective precipitation over the highveld regions of South Africa using the MRL-5 10/3 cm and other radar data.*

- *Develop and apply measuring techniques based on 10 and 3 cm radar data in order to measure storm rainfall accurately at scales varying from cloud scale to catchment scale.*

- *Refine the inter-calibration links between S-, X- and C- band radar's for quantitative rainfall measurement. (Use of the attenuation of X-band data for cloud and rainfall research).*

- *To develop the means of communicating experimental radar/satellite based rainfall data to potential users, with a view to satisfying hydrological requirements.*

The research conducted to attain these objectives covered a period of more than 4 years.

In May 1994 the installation of the MRL-5 radar on the Witbanksfontein site (approximately 20 km north west of Bethlehem), took place. By the end of the 1994/95 summer season this system started to produce useful data after fairly comprehensive upgrades and performance testing were completed.

2. THE MARSHALL PALMER Z-R RELATIONSHIP

Quantitative measurements of precipitation are based on the work of Marshall et al. (1947) and Marshall and Palmer (1948). They showed that the rain rate and radar reflectivity could be related by a simple power law, called a Z-R relationship, which assumes an exponential drop size distribution (DSD). The M-P exponential drop size distribution has held its own throughout the years as the simplest and adequate description of average drop spectra. When precipitation particles are small with respect to the radar transmitter wavelength, the backscattered power is proportional to the reflectivity factor (Z). Empirical studies have shown a relation between Z and the rain rate, (R measured in mm h^{-1}). The relationship used in RADARAIN is:

$$Z=200\,R^{1.6}$$

3 THE MRL-5 RADAR, SIGNAL PROCESSING

This dual wavelength MRL-5 radar which operates at S- and X-band is of Russian origin. The system operates at both these wavelengths through a unique antenna system designed to match the beam patterns at the two wavelengths.

The Digital Signal Processing for Logarithmic, Linear and Quadratic Responses (DISPLACE) processing algorithm, developed by Terblanche (1996, 1997), allows flexible processing of the MRL-5 logarithmic receiver output. Using this computationally efficient processing algorithm it became possible to speed up the signal processing and to avoid bias correction. The DISPLACE algorithm also formed the basis of the method developed by Mittermaier and Terblanche (1997) of more accurate Constant Altitude Plan Position Indicators (CAPPIs), on which the rainfall computation was done. The BPRP team also developed a state-of-the-art Radar Data Acquisition System (RDAS) which ensures that the calibration process is standard.

4. THE RADARAIN NETWORK

The rainfall network, generally referred to at the RADARAIN network (figure 1), is approximately 60 km east of the MRL-5 and 40 km from the Enterprise Radars. Sixteen tipping bucket rain gauges fitted with BPRP designed event dataloggers were deployed in the network.

5. RADAR ANALYSIS METHODS

5.1 CONSTANT ALTITUDE PLAN POSITION INDICATOR FIELDS

The grid points of the Constant Altitude Plan Position Indicator Fields (CAPPI) matrix have a 1 minute longitude by 1 minute latitude horizontal resolution and a 1 km vertical resolution. The CAPPI levels are calculated in a 201 by 201 horizontal grid, centred on the radar, with 15 vertical levels, starting at 2 km and ending at 16 km above sea level. The lowest CAPPI possible for the MRL-5 radar, at altitude 1712 m, is 4km above sea level. Twenty CAPPI pixels which cover the RADARAIN network, were extracted for analysis.

5.2 STORM SEVERITY STRUCTURE

The Storm Severity Structure (SSS) Method, derived from volumetric radar data, determines the structure and intensity of convective storms. The vertical distribution of the liquid water content is used to define the structure of a convective storm. Visser (1999) classified the vertical structure according to TOP, VOLUME or BASE based on the height of the maximum reflectivity.

Table 1: The SSS classification. Numbers 1-9 are the SSS class number.

	Weak	**Moderate**	**Severe**
Base	Weak Base (WB) 1	Moderate Base (MB) 4	Severe Base (SB) 7
Volume	Weak volume (WV) 2	Moderate Volume (MV) 5	Severe Volume (SV) 8
Top	Weak Top (WT) 3	Moderate Top (MT) 6	Severe Top (ST) 9

Use of conventional CAPPI data provides little information on the storm structure or its evolution. The SSS method developed by Visser (1999) provides a means to classify a storm at radar pixel level in terms of its structure and intensity. Classification can be accomplished in near real time for incorporation in a rainfall computation scheme. In several case studies use was made of the SSS classification. It appears that the most rainfall events occurred when the water mass in the storm descended to lower levels during the dissipating stage of the storm and when SSS class 1 weak base (WB) was identified. Fairly high rainfall rates occurred when a class 4 moderate base (MB) occurred, as depicted in the second case study.

5.3 THE BRIGHT BAND

The layered structure of stratiform precipitation near the freezing level causes the reflectivity to be enhanced by radar since the reflectivity of melting snow aggregates is much higher than that of water drops. This bright band results in an over-estimation of rainfall totals. Mittermaier (1999) uses a convective-stratiform classification algorithm combined with an objective mathematical technique to improve the quality of radar- rainfall estimates where a bright band is possible.

6. RAINFALL GAUGE NETWORK

Radar rainfall rates were calculated at radar bins which correspond with the geographical positions of the rainfall gauges depicted in figure 1. Following this procedure mean radar rainfall was calculated for an area of approximately 4 x 5 km and used for comparison with the point rainfall measurements from the rain gauge sites.

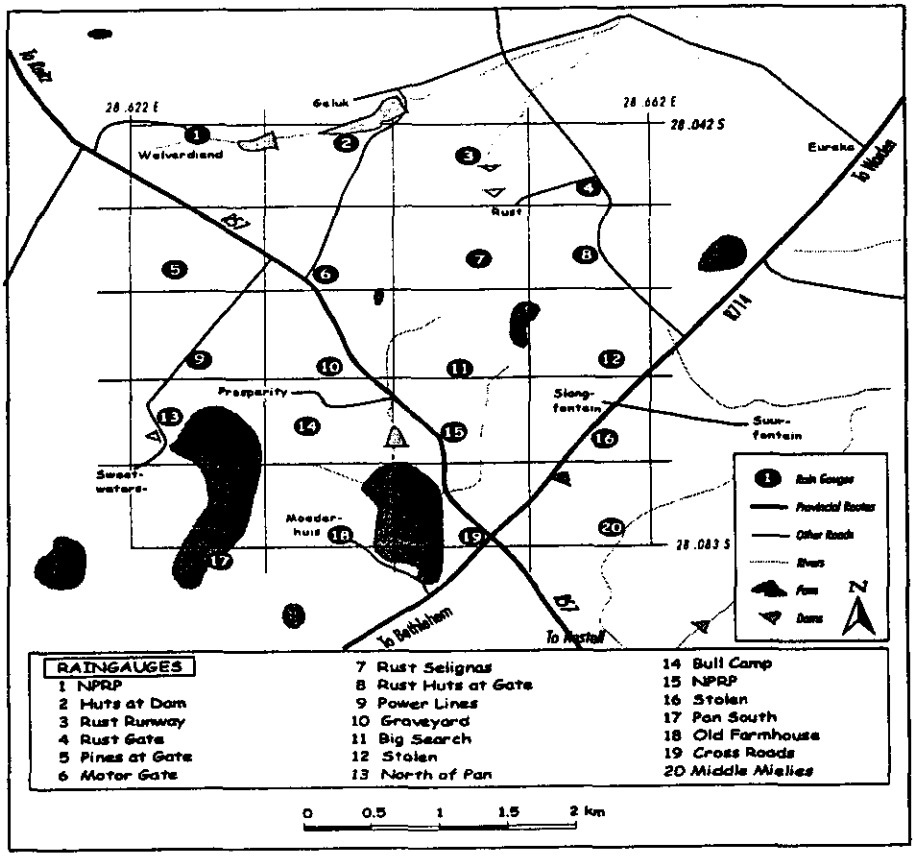

Figure 1: The RADARAIN network. The gridlines delimit the radar pixels.

7. RADAR AND GAUGE-DERIVED RAINFALL INTER COMPARISONS

7.1 SEASONAL INTER COMPARISONS

Figure 2 shows a scatter plot on a logarithmic scale of radar and gauge derived daily rainfall for the three seasons. A total of 118 days were available when both radar and rain gauge data could be used. The data are clustered fairly closely around the diagonal. Large deviations, however, are also evident.

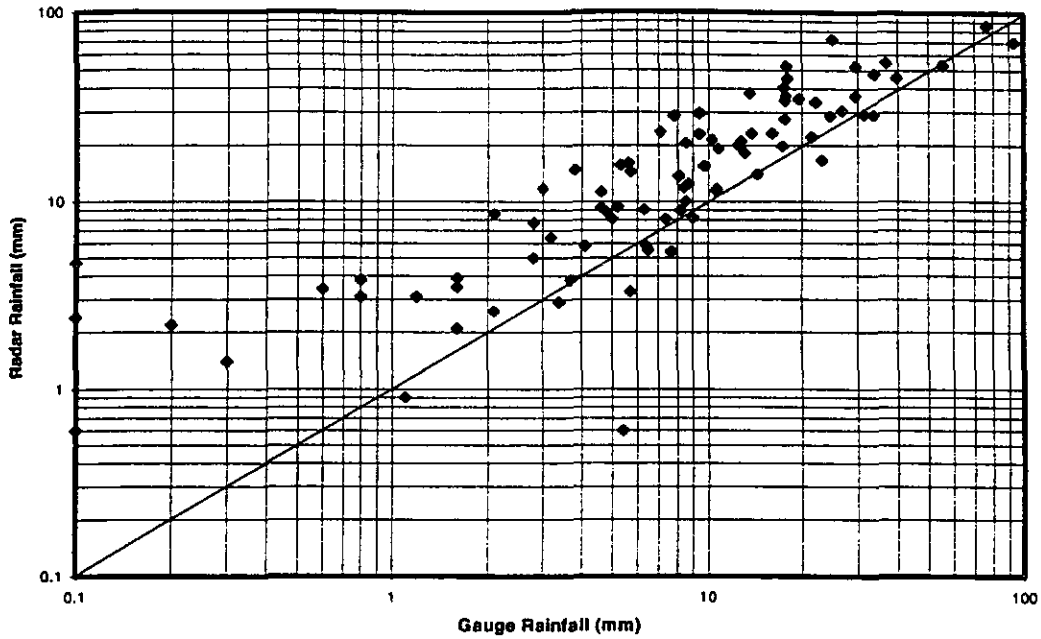

Figure 2: Scatter plot of radar-derived rainfall and gauge-derived daily rainfall for the three summer seasons October to March 1995/96, 1996/97 and 1997/98.

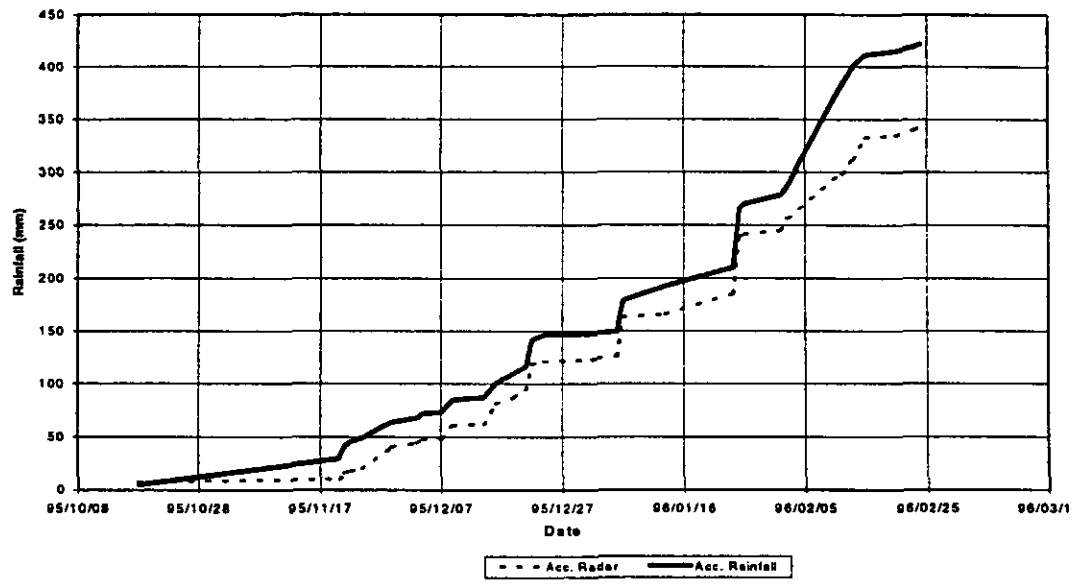

Figure 3: Accumulated radar-derived and gauge-derived rainfall for the RADARAIN network summer 1995/96. Only days with both radar and gauge rainfall are included in the figure.

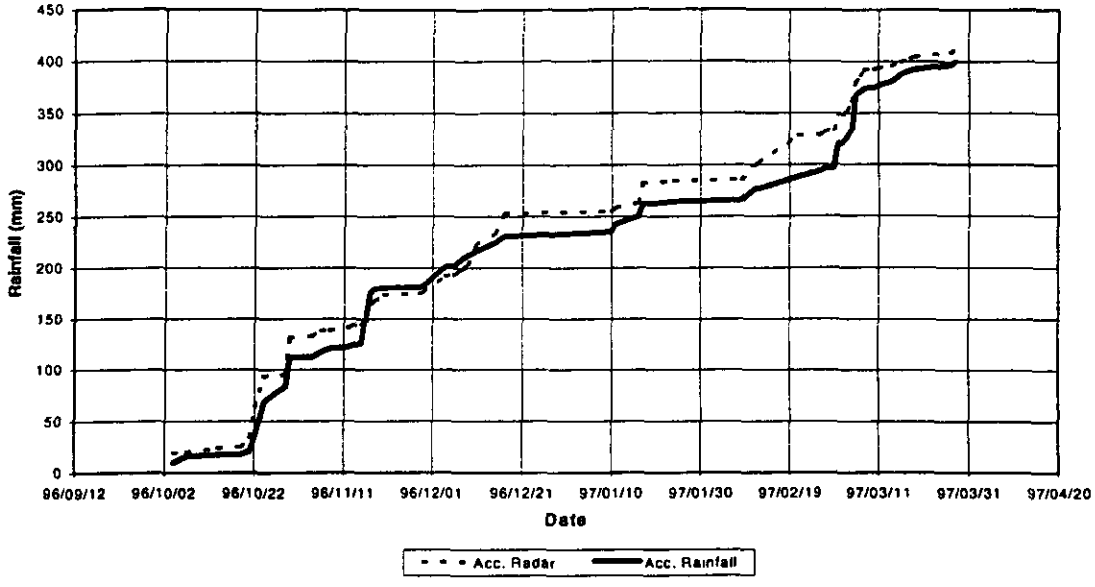

Figure 4: As for figure 3, but for the 1996/97 summer season.

Figures 3 to 5 compare the accumulated rainfall (radar and gauge) for the three seasons. The ratio (gauge/radar) was 1.2 for the 1995/96 season, indicating that the radar underestimated the rainfall. The 1996/97 season (figure 4) shows a very good comparison, a ratio of 0.9 at the end of the season. The 1997/98 season shows a deviation between the two curves during the early season, followed by a good comparison towards the end of January, and then a deviation in mid January and towards the end of the season. Noticeable in figure 5 is the good comparison of the heavy rainfall at the beginning of January 1998.

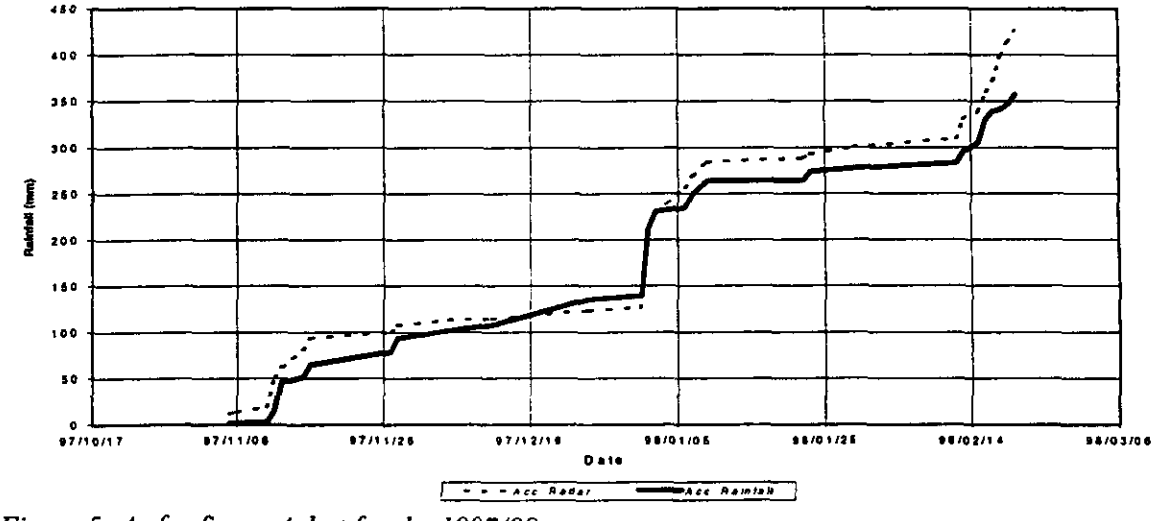

Figure 5: As for figure 4, but for the 1997/98 summer season.

7.2 CLASSIFICATION OF RADAR IMAGES

The TITAN (version 5) system allowed the authors to view and classify each rainfall system as it moved over the RADARAIN network. In all, 32 576 radar scans were available. Table 1 depicts the distribution between isolated, clusters, large clusters and general rain.

Table 1. Contribution of the different classes of days to the Total Rainfall.

	Percentage of total rainfall	Number of cases
Isol	18.7	103
Clusters	20.4	61
Large Clusters	38.8	66
General Rain	22.1	85

The biggest contribution to the rainfall during the periods of the classification came from the large cluster cases and the least is from the isolated cases.

7.3 CASE STUDIES.

One case study for general rain is described, showing good radar/rainfall relationship.

7.3.1 Case Study 1: 1997-12-31 – 1998-01-02

The rain event started at 21h00 on 31 December 1997 and lasted until 16h00 on 2 January 1998. This rain event started off as isolated rain over the network, developing to large clusters with high rainfall intensities during the morning of 1 January 1998 and finally to general rain from the night of the 1st lasting until the end of the event on the 2nd.

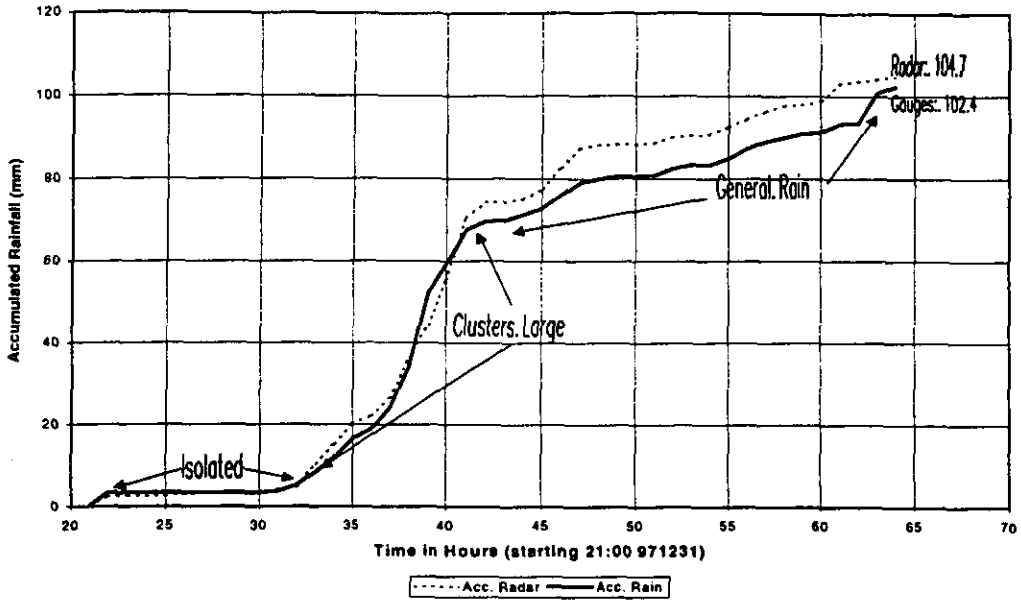

Figure 6: Accumulated radar and gauge rainfall for the period 1997-12-31 to 1998-01-02.

The rainfall comparisons (figure 6) between the radar and the rain gauges on this occasion were very good, ending with a ratio of 0.98. Noticeable are the very good comparisons during the high rainfall intensities. The authors are of the opinion that in this case a bright band did not occur, or was not present near the RADARAIN network

7.3.2 Case Study 2: 1997-03-08

This day was classified as a day with predominantly isolated convective systems over the network. Figure 7 shows the result of the sudden onset of intense showers over pixels 2, 5 and 13 at about 14h30 UT. The rain gauges at stations 2 and 5 (figure 1) recorded the sudden onset of the showers at this time, while the rain gauge at station 13 missed the shower altogether. Gauge 13 and the associated CAPPI show good correspondence with the shower which started at about 17h00 UT. Both CAPPI's 13 and 2 recorded an intense shower which started about 21h30 UT, lasting for about 30 minutes.

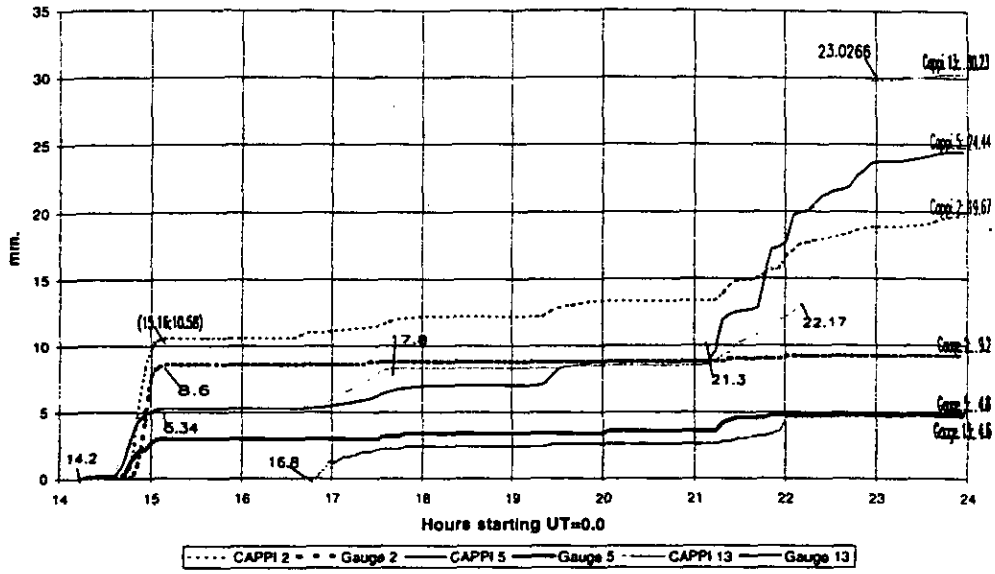

Figure 7: Accumulated CAPPI and Gauge rainfall at pixels/gauges 2, 5 and 13 on 1997-03-08. The values are either time or rainfall.

Considering the accumulations it is obvious that the totals computed from the CAPPI's overestimated with ratio's between 2.3 (2) and 6.57 (13). In this case it is clear from the rain rates and the onset and stop times of the showers that the CAPPI data may in fact do much better than the rain gauges.

8. CONCLUSIONS AND RECOMMENDATIONS

Only the most important conclusions and recommendations are listed here.

8.1 CONCLUSIONS

The first objective of RADARAIN was achieved in that considerable understanding of the space-time characteristics of convective precipitation over the northeastern Free State has been gained. The potential of the S band MRL-5 radar to measure rainfall down to pixel scale has been adequately demonstrated. Under conditions when a bright band or large melting spheres are **absent** the accuracy of the S band CAPPI data was surprisingly good. The best results were obtained under conditions of **general rain** or when large well-organised **cloud clusters** were present. It is precisely these systems which produce hydrologically significant rainfall. On time scales extending to a season the comparison between the CAPPI derived rainfall totals and the

gauge date shows that radar does have the potential to provide accurate seasonal rainfall distribution.

With respect to the second RADARAIN objective, results from the large number of case studies and analysis of the data supported the use of the conventional Marshall-Palmer Z-R relationship. The classification of rainfall producing systems over the network provided little motivation for any modification of this relationship. A classification may be useful to assign reliability to the CAPPI derived rainfall.

The commissioning, calibration and other operational constraints relative to the MRL-5 radar made the operation of the MRL-5 at X band wavelengths, during the RADARAIN project impossible. Research to deal with the third RADARAIN objective therefore never got off the ground.

With respect to the fourth objective we report that the authors did not attempt communicating radar based rainfall information. Soon after the start of this project developments within the BPRP itself saw the establishment and refinement of methods of communicating radar-based rainfall information to users. For the project team to have undertaken development in this regard would have meant an unwarranted duplication of effort. Efforts were consequently focussed on more comprehensive achievement of the first two objectives.

8.2 RECOMMENDATIONS

Based on the experience gained during RADARAIN we feel free to make the following recommendations with respect to the operation of an S band radar for hydrological operations.

- It is of absolute fundamental importance to have an experienced professional meteorologist to provide overall project leadership and be supported by competent radar technicians in order to ensure that the radar(s) stay operational.

- It is of fundamental importance to have a data archival and retrieval system operating in near real time.

- A research team utilising this system remains the best guarantee for quality of the output.

- The classification of rainfall systems and the SSS system could be adapted and computerised for active convective systems in order to provide error bars to the computed radar rainfall.

- It is recommended that the "bright band" algorithm of Mittermaier be tested thoroughly.

- It is recommended that a small rain gauge network, producing **real time rainfall rates**, be operated at a suitable distance from the radar. Data from this network should be used to identify anomalous radar derived rainfall and maintain ongoing research on radar based rainfall.

REFERENCES

Dixon M and Wiener G, 1993.
TITAN: Thunderstorm Identification, Tracking, Analysis and Nowcasting – A Radar-based Methodology. *J. Atmos. Ocean Tech. 10 (6), 785-797.*

Marshall J S and Palmer W Mc K, 1948.
The distribution of raindrops with size. *J. Meteorol., 5, 165-166.*

Marshall J S., Lagille R C and Palmer W Mc K, 1947.
Measurement of rainfall by radar. *J. Meteor. 4, 186-192*

The National Precipitation Research Programme, Final Report: 1993-1996. *WRC Report No. 726/1/97*

Mittermaier M.P., 1999.
Characteristics of the radar vertical reflectivity profile. *Unpublished Msc Eng dissertation.* University of Natal, Durban.

Mittermaier M P and Terblanche D E, 1997.
Converting weather radar data to Cartesian space: A new approach using DISPLACE averaging. *Water SA, 23(1), 45-50.*

Terblanche D E, 1996.
A Simple Digital Signal Processing Method to Simulate Linear and Quadratic Responses from a Radar's Logarithmic Receiver. *J. Atmos. Oceanic. Technol., 10, 785-797.*

Terblanche D E, 1997.
Digital signal processing of data from conventional weather radar: The DISPLACE method. *PhD Thesis, Faculty of Engineering, University of Pretoria, 86pp.*

Visser P J M, 1999.
The use of Volumetric Scanned Weather Radar Reflectivities for the identification of Convective Storm Characteristics. *Unpublished MSc dissertation.*

CHAPTER 1: INTRODUCTION

1.1. OBJECTIVES AND COMPONENTS OF RADARAIN

RADARAIN is the acronym for the project "Research into the weather radar measurement of rainfall as well as hydrological applications of weather radar".

It is only by the most judicious management of water resources that the water requirements of our growing population will be satisfied. In addition to supply-demand imbalances, managers have to contend with an extremely variable precipitation climate, with droughts and floods a regular occurrence. Hydrologists have, over the years, developed many modelling tools to assist water resources managers. Beneficial application has, however, almost as a rule been hampered by a lack of suitable precipitation data, particularly real-time data and spatially distributed (areal) data. Inadequate rain gauge networks can be complemented by satellite and radar data, and this report describes methods to compute rainfall from radar data.

The WRC acquired, as a national research facility, a dual wavelength (10/3 cm) research radar, in order to obtain the best possible rainfall data base for water resources applications.

This report details the use of the MRL-5 radar and a surface rain gauge network in the Bethlehem area, to generate vital knowledge and information. This includes an accurate characterisation of the development and occurrence, spatially and temporally, of precipitation in the area of 10 cm radar coverage and over the rainfall network. Ideally, this is the type of information needed to establish true links between rainfall and hydrological response.

During 1994 Dr D E Terblanche suggested that radar determined rainfall and gauge rainfall over a dense (1km x 1km) network should be attempted in South Africa. This suggestion plus the commissioning of the MRL-5 radar, eventually let to the Water Research Commission funded project: Research into the Weather Radar Measurement of Rainfall as well as Hydrometeorological Applications of Weather Radar, referred to as the RADARAIN Project.

RADARAIN has four main components:

(i) The MRL-5 radar, data transmission analysis and archival system.

(ii) The rainfall gauge network operated by the University of Pretoria (UP) RADARAIN project personnel. Up to 16 automatic gauges were supplied and calibrated by the Bethlehem Precipitation Research Programme (BPRP) staff who also supplied the Event Data Loggers (EDL). Gauge rainfall data collection and analysis remained the responsibility of the UP team.

(iii) The research component during which researchers from UP investigated relationship between the gauge network rainfall and rainfall figures originating from the MRL-5 S-band radar.

(iv) The Thunderstorm Identification Tracking and Nowcasting (TITAN) (Dixon and Wiener, 1993), software became available to the UP team towards the end of 1998. After an initial familiarisation period the team investigated all the available radar files in Meteorological Data Volume (**mdv**) format in order to classify each rainfall system which passed over the rainfall network on days with **mdv** radar data. The TITAN system is such a powerful radar image and analysis display system that the project team decided to use the opportunity to conduct a rainfall system classification for all available **mdv** formatted images. Research by Visser (1999) also indicated that information on the storm structure can be obtained using a Storm Structure Severity (SSS) method. The calculation of these SSS fields became possible to UP team members on the TITAN system using programmes developed and adapted from Visser (1999) by Stuart.

Good co-operation existed between all the team members throughout the project. The BPRP team provided support and guidance. Apart from the Steering Committee meetings when progress reports were detailed, the UP and BPRP teams had several research meetings to discuss research results. However the research was somewhat hampered by the fact that many of the components as well as most of the **mdv** format data only became available in 1998 and 1999. Because the availability of **mdv** formatted files was dependent on the proper functioning of the BPRP radar archival system, it took a tremendous effort by the BPRP team to provide the **mdv** data used in this report.

The objectives of the RADARAIN project can be summarised as:

- *To develop greater understanding of the space-time characteristics of convective precipitation over the Highveld regions of South Africa using the MRL-5 10/3 cm and other radar data.*

- *Develop and apply measuring techniques based on 10 and 3 cm radar data in order to measure storm rainfall accurately at scales varying from cloud scale to catchment scale.*

- *Refine the inter-calibration links between S-, X- and C- band radar's for quantitative rainfall measurement. (Use of the attenuation of X-band data for cloud and rainfall research).*

- *To develop the means of communicating experimental radar/satellite based rainfall data to potential users, with a view to satisfying hydrological requirements.*

X-band radar data remained unavailable during the project. Therefore the third objective could not be accomplished. The first two objectives were researched and detailed in this report

With respect to the fourth objective we report that the authors did not attempt communicating radar based rainfall information. Soon after the start of this project developments within the BPRP itself saw the establishment and refinement of methods of communicating radar-based rainfall information to users. For the project team to have undertaken development in this regard would have meant an unwarranted duplication of effort. Efforts were consequently focussed on more comprehensive achievement of the first two objectives.

In order to provide areal information of a rainfall event using radar reflectivities the operator must start at radar pixel resolution. To investigate the reliability of the MRL-5 at pixel resolution several case studies were completed at radar pixel resolution. Some of these describe days when the MRL-5 CAPPI derived rainfall did very well while poor correspondence with measurements derived from a single rain gauge at pixel resolution are also illustrated.

In order to perform this research it was decided to use the "**mdv**" format radar images provided by the BPRP staff. These radar "**mdv**" files comprise a vast number of images all in **mdv** format.

Unfortunately the BPRP staff were unable to provide all of the **mdv** formatted radar files for all of the days during the three project seasons. The BPRP processing and archival system only became fully operational during 1998. Eventually a cut-off data for computation of **mdv** files, using Displace Variate Averaging, was set for end June 1999. This left the UP team very little time to complete the analysis. Analysis of the **mdv** formatted files comprised the classification of rainfall / cloud systems over the project rain gauge network using the TITAN system as well as:

(i) CAPPI data at 4 km ASL
(ii) Storm Severity Structure (SSS) data
(iii) Maximum dBz values above network grid point.
(iv) Rainfall rates based on (iii)

In order to do this the UP team had to acquire a working knowledge of LINUX and the TITAN system. To perform these tasks Mr F Stuart from the BPRP developed the programmes in accordance with our specifications. He also devoted more than a week to training the project leader in the use of the TITAN 5 software and the running of the programme system. This process is quite complicated but fortunately LINUX allows for multi processing and all programmes ran simultaneously. These processing tasks started in January 1999 and continued, as **mdv** files became available following the storm classification. Table 5.3.1 lists all the days per season for which "**mdv**" files became available. Appendix B details the storm classification per day per hour.

The storm classification was used with the areal analysis while the new CAPPI, SSS, Max dBz and rain rate data were used in case studies at pixel resolution.

1.2 BRIEF HISTORY OF RADAR MEASUREMENT OF RAINFALL IN SOUTH AFRICA

The weather-radar infrastructure in South Africa represents a capital investment of about twenty million Rand (Terblanche, 1996). The South African Weather Bureau (SAWB) operates nine Enterprise C-band radars. The Water Research Commission (WRC) owns a Pacer C-band radar and a Russian built MRL-5 dual-wavelength radar.

Since the beginning of this decade the BPRP was central to most basic radar meteorological research and development in South Africa. The BPRP focussed on improving the performance of their radars. This included modernising the processing, display and storage of radar data and doing thorough performance testing. As BPRP personnel are actively using radar data as part of the precipitation enhancement research programme, they are in a position to identify areas where improvements can be made. As part of the preparations for area radar rainfall experiments, extended rain-gauge networks were deployed for radar-rain-gauge comparisons.

An in-house developed radar data acquisition system (RDAS) was introduced on all meteorological radars in South Africa. The system led to standard radar formats and calibration methods across the country. Radar meteorology is now seen as a multifaceted technology that can benefit science and the people of South Africa and provide the basic infrastructure which made this project possible. This is however only possible if adequate manpower and funding are provided.

1.3 HISTORICAL PERSPECTIVE

The development of radar technology grew from the theories of Maxwell, describing the interaction between magnetic and electric waves and their relationship with one another. Heinrich Hertz in 1886, showed that radio waves could be reflected by dielectric bodies. Rayleigh (1871) showed that the scattering of light is proportional to the sixth power of the object diameter and inversely to the fourth power of wavelength. Mie (1908) expanded on this by looking at the case where particle diameter (D) and wavelengths (λ) led to $\pi D/\lambda$ exceeding 0.22. Mie and Rayleigh scattering still form the foundation of understanding the scattering of electromagnetic waves by droplets. The pulse technique, with which Radio Frequency (RF) waves are transmitted in very short duration pulses to determine the distance of an object, was first used by Breit and Tuve (1926). By 1935 the United Kingdom had a pulse radar able to detect targets at a range of 40 miles, using a frequency of 25 MHz.

Leading up to, and during World War 2, radar was developed primarily to detect and determine the range and position of aircraft for military applications. The acronym radar, for radio detection and ranging, was coined in the 1940's. Through increased output power, improved sensitivity and refinements to antennae and receivers, this technology soon found applications in other fields including meteorology. The radar beam penetrates clouds, is reflected by the precipitation which

ultimately reveals the internal cloud structures. A thorough treatment of the development and use of radar in meteorology can be found in Atlas (1990). Textbooks on the theory and applications of weather radar are those by Atlas (1964), Skolnik (1970, 1981), Battan (1973) and Doviak and Zrnic (1984).

The highly secret invention of the resonant cavity magnetron at the University of Birmingham in Britain paved the way for the development of microwave (centrimetric) radar. The first working examples (S-band) were produced in the middle of 1940. It was through using radar operating at these wavelengths that storms and precipitation were observed for the first time. The first reported radar observation of a rain shower was made in Britain in February 1941. The foundations for radar meteorology were laid by Ryde (1941). His and other's research was in anticipation of the widespread use of micro-wave radar and the effects weather would have at these short wavelengths. Their work included theoretical and observational studies on the reflectivity and attenuation of rain and hail as a function of precipitation rate and wavelength, as well as studies on the 'bright band'.

Pulsed weather radar systems transmit brief pulses of electromagnetic energy. The energy is focussed by an antenna system into the atmosphere at a high frequency of between 3 and 30 GHz. These pulses are propagated at the speed of light ($c \approx 3 \times 10^8$ m s $^{-1}$). The incident electromagnetic wave induces electric and magnetic dipoles on the cloud particles, assumed to be spherical, oscillating them at the frequency of the wave. Some of the energy is absorbed as heat and some is scattered back towards the antenna of the radar. The amount of backscattered energy is dependent on the radar cross section of the droplets. When the droplet diameter is smaller than 0.07λ, where λ is the wavelength of the radar, the Rayleigh approximation for scattering is assumed. However many cloud particles such as hail and snow, might not resemble a sphere or might consist of both ice and liquid water, which forms due to melting of ice particles or the accretion of hail and droplets. When the following occur the Rayleigh scattering approximation becomes invalid: i) Large hailstones; ii) A thin coating of water around an ice sphere dramatically increases the reflectivity of the ice sphere which then resembles the reflectivity from a liquid sphere of the same size (Langleben and Gunn, 1952); iii) With large spheres where $D > 0.08\lambda$, the onset of melting results in a decrease in reflectivity, due to Mie scattering.

The ratio between power transmitted (P_t) and power received back, together with characteristics of the radar and of target interactions with electromagnetic energy, provide information on the

size of precipitation particles observed by the radar. Radar reflectivity is related to the sixth power of drop size diameter for a Rayleigh scattering approximation. If a Gaussian profile for the antenna gain G is assumed and losses due to receiver (L_r), waveguide (L_m) and atmospheric attenuation (L_a) are incorporated, the weather radar equation can be derived as (Smith 1986):

$$\overline{P}_r = \frac{\Pi^3 c}{1024 \ln 2} \left| \frac{P_t \tau G^2 \theta \phi L_m L_r}{\lambda^2} \right| \left| \frac{|K|^2 Z_e L_a}{r^2} \right| \qquad (1.3.1)$$

Where $\overline{P}_r$ is the back scattered power received from targets within the contributing region of the radar pulse, τ the pulse duration, ϕ and θ radar beam width in the vertical and horizontal, r the range of the target and K is proportional to the complex index of refraction. The radar reflectivity factor in dBZ is determined from the logarithmic form of equation (1.3.1)

$$10 \log Z_e = 10 \log P_r + 20 \log r - C \qquad \text{with dBZ defined as:} \quad dBZ = 10 \log Z_e \qquad (1.3.2)$$

This is the general term to define the intensity of the returned echo from a scattering volume in the atmosphere.

1.4 SOUTH AFRICAN DEVELOPMENTS

The first South African radar was built in 1939 under the leadership of Dr Basil Schonland of the Bernard Price Institute of Geophysical Research at the University of the Witwatersrand. Dr Schonland and his Institute (which at the time fell under the Department of Defence), set out, using local components, to build South Africa's first radar. The first radar echo was observed on 16 December 1939 and was thought to be from the Northcliff Water Tower in Johannesburg.

After the war, in 1946, two members of Dr Schonland's team formed the basis of the Telecommunications Research Laboratory of the Council for Scientific and Industrial Research (CSIR) of which he was the first president. The CSIR, in association with the South African Air Force and the Weather Bureau, and inspired by the then recent cloud seeding results in the USA, conducted a glaciogenic seeding experiment on the Highveld in an attempt to enhance rainfall during the summer of 1947/1948 (CSIR, 1948). An X-band radar based at the Laboratory's

premises in Johannesburg was used to monitor the seeding effects - one of the first times radar was utilised in this role.

In 1970, the CSIR acquired a Mitsubishi S-band weather radar which was installed at Houtkoppen, near Johannesburg. A large number of documented studies were done using data collected by this system (Held and Carte, 1973; Carte and Held, 1978 and Held 1978 and 1982). Severe hail-producing storms over the Highveld were documented which highlighted some of the differences between these storms and storms in other parts of the world. One was the low frequency of large steady-state storms, also referred to as super cells, which are more common in the Northern Hemisphere.

The first hydrological use of weather radar was in 1975 when observations from the CSIR's radar at Houtkoppen were used in real time for the prediction of severe floods in the Vaal River catchment upstream of Vaal Dam (Alexander, 1990).

Later in 1975 data from the operational cloud seeding project at Nelspruit were used for the determination of the depth-area-duration properties of storm rainfall. This information was required for flood frequency analyses (Alexander, 1990).

The SAWB started using radar for upper-air balloon tracking in 1952/53 using British made GL3 S-band radars initially installed in Pretoria and Maun, Botswana. The authors were quite familiar with their use during the 1960's. Similar systems were later introduced at the weather offices in Cape Town, Durban and Alexander Bay. The Pretoria GL3 set was modified in 1959 to provide PPI's and was thereafter used for the observation of storms (du Toit, 1996 - personal communication). In the second half of the 1950's a Decca X-band weather radar was installed at the then Jan Smuts Airport but was constantly plagued by gearbox problems. During 1962 two Selenia X-band weather radars were purchased, the one for Pretoria and the other for Durban while a third one was installed at Port Elizabeth in 1963. These radars were used for weather observations and balloon tracking. In the first half of 1964 a Mitsubishi RC 4B C-band radar was installed in Bloemfontein and used for meteorological observations before being moved to Bethlehem in 1971 as part of the Bethlehem Weather Modification Experiment (BEWMEX). An introduction to this programme, listing the equipment in use in the early years, is given in Harrison (1974). Fleischer (1980) compiled a report on the radar storm observations in the north-eastern Free State from data collected by this system during the 1978/79 summer season.

The Enterprise WSR-81 C-band radar, installed in Bethlehem during 1982, has been used for the acquisition of reflectivity data from weather targets in volume-scan mode as part of the research effort in precipitation enhancement. The radar was used to monitor the effects of glaciogenic cloud seeding, complementing the data acquired by three instrumented research aircraft. Analyses carried out on data captured by this radar include studies of first echoes and storm climatologies (Steyn and Bruintjes, 1990; Mather and Terblanche, 1993); radar responses of glaciogenic cloud seeding (Krauss et al., 1987; Gagin et al., 1986); the effects of evaporation of precipitation between cloud base and the ground (Rosenfeld, 1988) and the rainfall yield from convective storms (Rosenfeld and Gagin, 1989).

CHAPTER 2: RADAR SYSTEMS

2.1 THE MARSHALL PALMER Z-R RELATIONSHIP

Quantitative measurements of precipitation gained momentum after World War 2 with the work of Marshal et al. (1947) and Marshall and Palmer (1948) from the Stormy Weather Group in Canada. Their work indicated that the rain rate and radar reflectivity could be related by a simple power law, called a Z-R relationship, which assumes an exponential drop size distribution (DSD). Although measurements around the world soon proved that a wide range of Z values could represent the same rain rate, the universal Z-R relationship suggested by Marshall and Palmer did however invigorate radar measurements and research. The M-P exponential drop size distribution has held its own throughout the years as the simplest and adequate description of average drop spectra. In this project attempts to modify this relationship did not provide conclusive results.

When precipitation particles are small with respect to the radar transmitter wavelength, the backscattered power is proportional to the reflectivity factor (Z). A great number of empirical studies have shown a relation between Z and the rain rate (R in mm h^{-1}). This then implies that radar can be employed to estimate rainfall at a radar pixel. The best known and widely used empirical relationship between Z and R is that of Marshall and Palmer (1948) who found, based on measurements of Z and the drop-size distribution (DSD), that:

$$Z=200\ R^{1.6} \tag{2.1.1}$$

An exponential DSD – often a good approximation for precipitation is given by:

$$N(D) = N_o \exp -(\Lambda D) \tag{2.1.2}$$

where

$$N_o = 0.08\ cm^{-4} \tag{2.1.3}$$

and

$$\Lambda = 41\ R^{-0.21} \tag{2.1.4}$$

The fact that Z-R relationships, based on exponential DSD's, have been widely investigated is reflected in Battan (1973). A list of more than 60 of these relationships is given. These Z-R relationships were obtained in different parts of the world, using different equipment and for

various rainfall types. The large variety of Z-R relationships is partially due to the fact that reflectivity alone does not describe a precipitation dropsize distribution explicitly. In this study we found that the Marshall-Palmer Z-R relationship provides remarkably accurate radar-rainfall measurements using the calibrated MRL-5 S-band radar. Terblanche (1996, personal communication) indicated that other factors, not related to the DSD, have a much larger effect on errors in radar-rain-gauge comparisons. The team therefore decided to stick to the Marshall-Palmer relationship except where otherwise indicated.

2.2 THE MRL-5 RADAR

The dual wavelength MRL-5 radar which operates at S- and X-band is of Russian origin. It was originally designed to assist in the extensive hail research and suppression efforts which conducted in many states of the former USSR. Two versions of the MRL-5 radar are available, one for permanent siting and the other a mobile version. The system operates at S- and X-band through a unique antenna system designed to match the beam patterns at the two wavelengths. Although many of these radars are in use in Eastern Europe, their applications in the western hemisphere have been limited. An MRL-5 system was used in the multi-national Precipitation Enhancement Programme (PEP) in Spain organised by the World Meteorological Organisation (WMO) during the 1980's. During PEP the rugged construction and suitability for extended operations of the system were demonstrated. During 1992, the project leader, acting on the advice of Seed and Austin, amongst others, recommended the purchase of the MRL-5 mobile radar to the WRC. Once funds became available in 1992 and after an inspection visit to the radar factory at Gorky in Russia, the WRC purchased the MRL-5. The system was installed approximately 20 km north west of Bethlehem at Witbanksfontein (28° 05's, 28° 10' E) altitude 1712 metres, on a site that provides much improved coverage of the BPRP research area. The characteristics of the MRL-5 radar are summarised in Table 2.1 by Terblanche (1996).

Table 2.1 Characteristics of the MRL-5 radar.

	X-Band		S-Band	
Receiver sensitivity	- 104 dBm		- 106 dBm	
Receiver dynamic range	70 dB		70 dB	
Transmitter frequency	9.603 GHz		2.954 GHz	
Pulse duration	2 μs	1 μs	2 μs	1 μs
Peak transmitter power	200 kW	200 kW	600 kW	600 kW
Pulse Repetition Frequency	250 Hz	500 Hz	250 Hz	500 Hz
	± < 5 %		± < 5 %	
Pulse coincidence	Within 0.2 μs		Within 0.2 μs	
Antenna gain	40 dB		39 dB	
Side lobes	> 22 dB down		> 22 dB down	
Polarisation	Vertical		Horizontal	
Beam-width	1.5° at 3 dB one-way points		1.5° at 3 dB one-way points	

An option available on the MRL-5 radar is to use the X-band with the 4.5m antenna. This results in a 0.5° beam-width and an antenna gain of 49 dB. An 18 dB two-way gain and improvement in performance is achieved.

A PC-based Radar Data Acquisition System (RDAS) allowing digitising and processing of the receiver output in sync with the PRF trigger in a user defined manner as well as control over the antenna for programmable volume-scan operation, was developed. This system was installed on the Bethlehem Enterprise C-band radar and thorough performance testing initiated. This system, measurements and the tests conducted were described by Terblanche et al. (1994). These tests included antenna beam pattern measurements, accurate determination of all losses in the radar system and verification of radar estimated rainfall using tipping bucket rain gauges in the Kransfontein area equipped with loggers on loan from the Department of Water Affairs and Forestry.

RDAS performs analogue to digital conversion on the receiver output in synch with the pulse repetition frequency pulses and then carries out the DISPLACE procedure (Terblanche, 1997). The result from the RDAS processing is a 12 bit digitised value per range bin that can be related to received power from the calibration tables. The radar was set to execute 18 elevation steps with base scan at 1.5° and top scan at 55°. Received power integration over four range and eight azimuth samples is done to produce 224 range bins. Each of the 224 range bins has a length of 600 m, totalling to a radar range of 134.4 km for data storage along a beam path. A skip of 80 μs

is used, resulting in a blank range 12 km around the radar, extending the range to 146.4 km. The skip assures that the top scan at 55 ° reaches the top of the tropopause and that 3 dimensional structures of convective storms further than 12 km range will be completely observed by the radar. At ranges closer than 12 km, a blank radar cone exists, making the use of vertical reflectivity profiles impossible. The rotation speed is also set to 5.2 rpm.

Towards the end of 1995 an uninterruptable power supply system integrated with an automated diesel generator was commissioned to solve the problem of electrical interruption at the site. Facilities for remote controlling and system monitoring were developed (Radar Control card – RCC). A 128 kBits s^{-1} microwave link was installed for data transfer to and from the Bethlehem offices towards the end of 1995. During the 1995/96 summer season these developments resulted in the collection of about 2000 hours (100 gigabyte) of volume-scan data. All the main rain events of the season were captured and the system proved its reliability and stability.

Further information on the commissioning of the MRL-5 is given in the WRC Report No. 726/1/97, available at the WRC. During 1995 the DISPLACE averaging method for radar signals, developed by Dr D E Terblanche, became operational. A new approach employed to convert radar data to cartesian space was also developed by Ms M P Mittermaier under the guidance of Dr D E Terblanche. These developments were finalised towards the end of 1995. Publications describing these developments are detailed in the WRC Final Report (1993-1996) of the BPRP (WRC Report No. 726/1/97). CAPPI data resulting from the new approach became available to the project only towards the middle of 1996. Therefore the CAPPI data compiled using Seed's (1998) approach were utilised in the development of radar/rainfall algorithms.

The WRC's MRL-5 radar upgraded with hard- and software, developed in-house, has proved itself since 1994. This is in no small measure due to the dedicated efforts of Messrs Dennis Dicks and Farren Hiscutt and all others that played a role in the development of this system which is now recognised internationally for the quality of its data.

2.3 RADAR PERFORMANCE TESTING

Since the early 1990's an increasing need for high quality radar data has emerged within the Bethlehem Precipitation Research Project (BPRP) in order to convince hydrologists, especially, about radar's ability for areal rainfall estimation in real-time. The first real attempt at this was a

paper presented at the South African Hydrological Symposium (Terblanche et al., 1993). The cloud seeding experiments, using the newly developed hygroscopic flare seeding technology (Mather et al., 1997a), also showed a lot of potential and it was envisaged that radar would have to play a central role in any future areal applications. The need to upgrade to S-band measurements had been identified on several occasions by that stage. Previously, (C-band) radar data were used more in a relative sense, for comparisons between seeded and non-seeded storms in randomised experiments and had been sufficient to show that there was no statistically significant difference in the average range from the radar of the two groups. At about the same time Mr Dennis Dicks (ex-CSIR) joined the BPRP on a WRC contract, providing much needed radar expertise to the group. Hardware and software design capabilities were provided by Mr Farren Hiscutt, also on contract to the WRC.

Terblanche et al. (1994) identified the following as further areas of research and development:

(i) **Improved signal processing techniques to avoid the standard (2.5 dB) bias correction applied when simply averaging the output from the radars logarithmic receiver, especially under convective conditions with its steep reflectivity gradients; and allowing the compilation of more accurate Constant Altitude Plan Position Indicators (CAPPIs).**

The DISPLACE processing algorithm, developed by Terblanche (1996, 1997) and detailed in Chapter 4, allows flexible processing of the logarithmic receiver output. Using this computationally efficient processing algorithm it became possible to process the output from the receiver, simulating different power law transfer functions by simply loading applicable, pre-compiled lookup tables. This algorithm, using the quadratic table, ensures that no bias correction is needed. Terblanche (1997) showed that this method avoided up to 13 dB underestimation in range bin reflectivity in areas of steep reflectivity gradients, after application the 2.5 dB bias correction to the conventionally averaged data. Using the Marshall Palmer Z-R relationship of $Z = 200R^{1.6}$ it was found that the underestimated reflectivity due to the insufficient bias correction to the conventionally averaged data translated to a 18% underestimation in total storm rainfall.

The DISPLACE algorithm also formed the basis of the method developed by Mittermaier and Terblanche (1997) to generate more accurate CAPPI's for replacement of projection CAPPI's,

thus avoiding discontinuity rings. Terblanche (1997) also identified the negative impact of the "bright band" and ground clutter in radar rainfall estimation as issues that need further research.

(ii) An accurate tipping bucket rain gauge logger.

Prior to the arrival of the WRC's MRL-5 dual-wavelength radar a network of 45 tipping bucket rain gauges was deployed in the 4650 km^2 Liebenbergsvlei River catchment on a 10 km grid. This network would form a firm basis for radar-rain gauge comparisons in the years that were to come. The in-house developed event loggers (BPRP) allowed processing of the gauge data in radar volume-scan intervals as the time of each 0.2 mm tip was recorded. Detail on the development of the loggers, tests conducted on the loggers and tipping bucket rain gauges and examples of how the data were used are given in Mather et al. (1997a). Up to 16 of these tipping bucket rain gauges and loggers have been used in the present project.

(iii) Software to assist during the calibration of the radar, facilitating a common standard. These studies would add momentum to the quest to use S-band radar for rainfall estimation under the frequent convective storm conditions characterising the South African interior.

Software was developed as part of RDAS to assist in the receiver calibration of a radar. The software prompts the radar technician for the values of his measured losses and characteristics of the radar system. Based on the radar equation (e.g. Smith, 1986; Terblanche et al., 1994) the software then produces a table of signal generator settings corresponding to dBz values, rain rates (using a pre-specified Z-R relationship) and received power levels. The user is then prompted to inject the signal generator levels as a triggered pulse, delayed by the equivalent of 100 km range, into the bi-directional coupler of the radar. The digitised receiver values are recorded and by least squares regression the line is fitted on a graph with received power (dBz) on the x-axis and digitised receiver output (0-4095) on the y-axis. Thereafter the software automatically produces the calibration files to be used in the software as well as the DISPLACE algorithm's lookup tables. This process ensures that the calibration process is standard and that all losses are taken into account in exactly the same way. The chances for human error are also much reduced as manual calculations are all but redundant.

CHAPTER 3: RAINFALL DATA

3.1 THE RADARAIN RAINFALL NETWORK

A dense rainfall network providing reliable rainfall data deployed well within the range of the MRL-5 and Enterprise radars, is a fundamental necessity for research to determine the relationship between radar echoes and areal rainfall down to convective cloud scale. To meet this requirement a rainfall network was operated near the intersection of the Bethlehem-Warden and the Kestell-Reitz highway.

The rainfall network operated in this project, generally referred to at the RADARAIN network, is approximately 60 km from the MRL-5 and 40 km from the Enterprise Radars. It is situated in the Vaalbankspruit catchment on the farms Slangfontein, Rust, Sweetwaters, Welverdiend, Moederhuis, Eureka, Truia, Somerslus, Prosperity, Tweespruit and Vrede. Sixteen tipping bucket rain gauges fitted with BPRP (Hiscutt) designed event dataloggers, were deployed at the locations listed in Table 3.1. Two BPRP rainfall stations formed part of the dense network. The network was operated from September 1995 to April 1998. The RADARAIN network was usually installed during September/October and dismantled during March/April each summer season. Data were downloaded every 2 to 3 months.

Figure 3.1 displays the geographical placement of the rainfall network as well as the radar CAPPI pixels used throughout this project.

Table 3.1. Tipping bucket Rainfall Gauge location and station name.

No.	***Latitude S***	***Longitude E***	**Identification**
1	28.02.56	28.37.57	BPRP Welverdiend
2	28.02.80	28.38.10	Huts at Dam
3	28.03.20	28.38.20	Rust Runway
4	28.03.11	28.39.13	Rust Gate
5	28.03.46	28.37.70	Pines at Gate
6	28.03.06	28.38.10	Motor Gate
7	28.02.40	28.38.40	Rust Selignas
8	28.03.49	28.39.59	Rust Huts at Gate
9	28.04.11	28.37.51	Power Lines
10	28.03.90	28.38.20	Graveyard
11	28.04.10	28.38.80	Big Search
12	-- -- --	-- -- --	Stolen
13	28.04.70	28.37.30	North of Pan

14	28.04.15	28.38.10	Bull Camp
15	28.04.49	28.38.79	BPRP Slangfontein
16	-- -- --	-- -- --	Stolen
17	28.04.50	28.37.90	Pan South
18	28.04.50	28.38.10	Old Farmhouse
19	28.04.40	28.38.60	Crossroads
20	28.03.90	28.39.70	Middle Mealies

Three of the rainfall stations were stolen and one station (Middle Mealies) was damaged during the period September 1995 to February 1996.

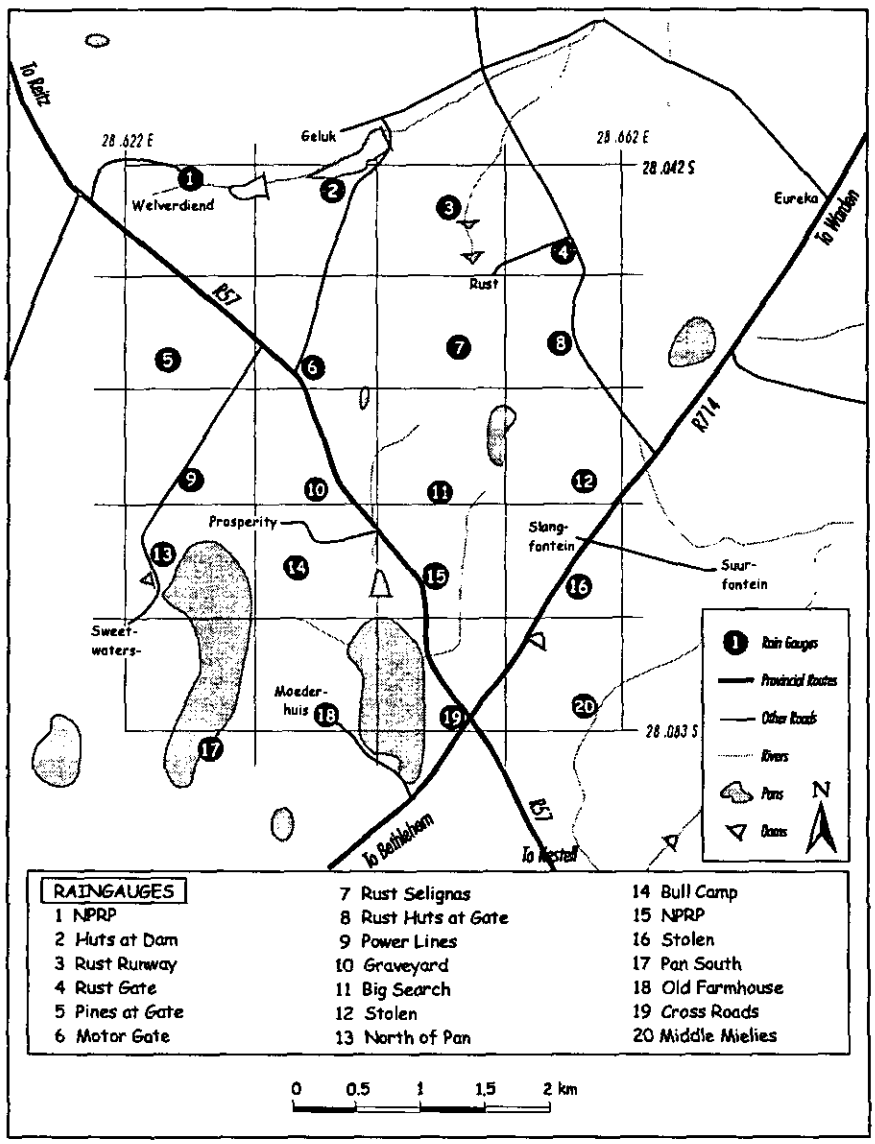

Figure 3.1: The RADARAIN network. The gridlines delineate the radar pixels.

During the first season data were read from the loggers in December 1995, February 1996 and April 1996 when the network was dismantled and taken to the Bethlehem Weather Office for maintenance. During the period December 1995 and 20 February 1996 some 500 mm of rain fell over the network. Virtually all the farm roads were impassable. Even a powerful tractor got hopelessly stuck. Project team personnel had to service most of the stations on foot. A few stations stopped recording by the 16 February 1996 due to memory limitation problems. Table 3.2 provides detail on the operational period of all the rain gauges deployed in the RADARAIN network during the project.

Table 3.2: *Periods of continuous operation of individual gauges in the* RADARAIN *network*

	'95-'96		'96-'97		'97-'98	
Gauge	First	Last	First	Last	First	Last
1	-	-	-	-	-	-
2	28-09-95	14-05-96	2-12-96	22-05-97	26-09-97	9-05-98
3	5-12-95	13-05-96	22-09-96	22-05-97	26-09-97	10-05-98
4	28-09-95	14-05-96	23-09-96	22-05-97	26-09-97	9-05-98
5	28-09-95	14-05-96	2-12-96	23-04-97	26-09-97	16-11-97
6		-	-	-	26-09-97	2-01-98
7	28-09-95	14-05-96	20-02-97	11-03-97	26-09-97	9-05-98
8	28-09-95	5-04-96	19-09-96	23-04-97	26-09-97	17-05-98
9	28-09-95	14-05-96	2-12-96	22-05-97	26-09-97	17-05-98
10	28-09-95	14-05-96	19-09-96	22-05-97	26-09-97	12-03-98
11	28-09-95	13-05-96	2-12-96	23-04-97	26-09-97	9-05-98
12	-	-	-	-	-	-
13	28-09-95	14-05-96	19-09-96	22-05-97	26-09-97	9-05-98
14	28-09-95	14-05-96	19-09-96	20-11-96	26-09-97	18-05-98
15	-	-	-	-	-	-
16	28-09-95	12-04-96	-	-	-	-
17	28-09-95	16-05-96	20-09-96	12-02-97	26-09-97	9-05-98
18	5-12-95	14-05-96	19-09-96	22-05-97	23-11-97	17-05-98
19	6-12-96	14-05-96	19-09-96	22-05-97	26-09-97	10-05-98
20	28-02-96	13-05-96	19-09-96	22-05-97	26-09-97	10-05-98

The network was re-deployed during September 1996 at the locations indicated in Table 1 and Figure 3.1. It was decided not to operate stations at the positions where theft had occurred during 1995. Servicing and inspection of the network took place every 2 to 3 months and the network was dismantled in April 1997. During the 1997/98 summer season the same procedures applied.

As part of this project the BPRP team requested the development of a rainfall-contouring package for the BPRP rainfall network. Dr C J deW Rautenbach who had developed a similar system at

UP modified and upgraded this system for use with the BPRP rainfall network. Appendix A describes the BPRP Rainfall Contouring System and provides an example.

3.2 THE RAINFALL DATA

Appendix A details all the available rainfall files compiled from the tipping bucket rain gauges deployed during the three summer seasons. This dataset also includes the CAPPI rainfall data computed during the three seasons. The dataset is available on compact disk from the BPRP office in Bethlehem as well as the University of Pretoria. The rain gauge dataset contains the individual reports per gauge per season in which the date and time of each time "tip" of the tipping bucket rain gauge was recorded. Each time the data were read or the rain gauge serviced, the time and date on the event logger were reset to the correct time in SAST. All time and date differences were noted. These time and date corrections were used to correct the logger times. Over a period of three months the uncorrected logger time could be out by as much as 10 minutes.

The tipping bucket data logger combination worked very well and proved to be a stable system. The only problems experienced were the theft of three rain gauges as well as one rain gauge at "Old Farmhouse" which was uprooted by vandals stripping the house. The team found that generally if the rain gauge was erected within sight of the farmhouse or labourers dwellings the rain gauge was not interfered with. The same did not always apply to sites we considered remote and or difficult to reach.

CHAPTER 4: RADAR DATA ANALYSIS

The RADARAIN project only became possible after significant progress had been made by the BPRP staff in the capture, analysis and processing of MRL-5 radar data. These developments are briefly outlined below and can be found in Mather et al (1997a), Mather et al (1997b), Mittermaier and Terblanche (1997), Terblanche (1997) as well as Terblanche et al (1993, 1994).

4.1 CAPPI (Constant Altitude Plan Position Indicator) DATA

The calculation of radar reflectivity CAPPI fields from radar co-ordinate reflectivity fields form the basis from which rainfall is determined. The maximum range of a specific CAPPI field is restricted by the height of the radar beam above sea level. The altitude of a radar beam is affected by:

- The curvature of the earth
- The index of refraction of the radar beam as it propagates through an atmosphere with non-homogeneous temperature and moisture fields
- The elevation angle of the radar antenna with respect to the earth surface

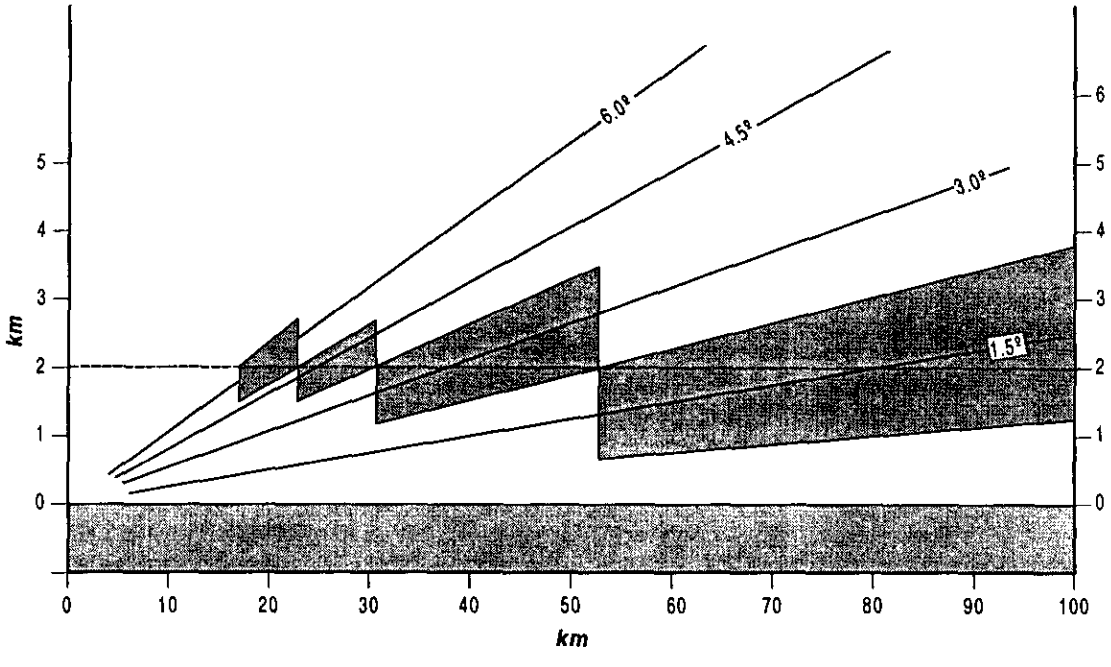

Figure 4.1: Relationship between radar antenna elevation, beam height and horizontal distance from the radar.

A description of the radar beam path with respect to the curvature of the earth, taking the refraction of the beam by the atmosphere into consideration, can be found in the textbook by Battan (1973). Figure 4.1 shows schematically how the radar elevation and horizontal distance determine a specific position in the CAPPI field. The CAPPI matrix is created by linearly interpolating (in reflectivity Z) the eight nearest radar reflectivity points of the radar co-ordinate field in radar co-ordinates (azimuth, elevation and range) to a CAPPI (latitude, longitude and altitude above sea level) position in the matrix. The grid points of the CAPPI matrix have a 1 minute longitude by 1 minute latitude horizontal resolution and a 1 km vertical resolution. The CAPPI levels are calculated in a 201 by 201 horizontal grid, centred on the radar, with 15 vertical levels, starting at 2 km and ending at 16 km above sea level.

The lowest CAPPI possible for the MRL-5 radar, at altitude 1712 m, is 4 km above sea level. The 2 and 3 km CAPPI levels are not used in this study, as they have a range of less than 40 km and are often severely affected by ground clutter. Therefore, the lowest CAPPI used, is at 4 km above sea level, which is approximately 2.3 km above ground level. Some CAPPI data generated during 1995/96 used the so-called Seed-method in which case the CAPPI's were at 2 km AGL This set was used in calculating some of the 1995/96 season's rainfall.

4.2 DISPLACE VARIATE AVERAGING

During 1995 the signal processing on RDAS was upgraded by incorporating DISPLACE averaging to avoid the significant underestimation in return power from areas of steep reflectivity gradient (Terblanche, 1996). Quality tests on the MRL-5 radar, regarding the antenna beam characteristics, were done and calibration procedures were conducted frequently (Mather and Terblanche, 1997a).

The DISPLACE method (an acronym for Digital Signal Processing for Logarithmic, Linear and Quadratic Responses) was developed by Terblanche (1995 and 1996) to facilitate the averaging of digitised logarithmic receiver output. The limitations imposed by the radar-data acquisition and networking systems in use in South Africa are listed by Terblanche et al (1994), as well as Visser and le Roux 1993. These limitations necessitated meeting the following criteria:

- During processing all data values had to be accommodated within a 16 bit word size.
- The computational efficiency of the method had to be comparable with the existing conventional averaging method.
- Modifications to radar formats and user software had to be avoided.

The basis for the DISPLACE method can be explained by the following mathematical identity:

$$\text{Log}[(a+b)/2] = \log(a+b) - \log 2$$

$$= \log a + \log(1+b/a) - \log 2$$

$$= \log a + \mathbf{\log(1 + 10^{-(\log a - \log b)}) - \log 2} \qquad (4.2.1)$$

If the logarithm of each value in a pair (a and b) is known, the logarithm of the average of the pair can be determined. The bold section in equation (4.2.1) represents a correction (or a *displacement*) which must be applied to log a. These *displacements* can be pre-computed and loaded into a look-up table as the value is only a function of (log a – log b). By successively computing averages over pairs, the average over 2^I, I=1,2,....,n values can be obtained. The advantages of this procedure are that: (1) no division is necessary to determine the final averaged value; (2) the a absolute values of the *displacement* is smaller than the larger of the pair values, and (3) only a single look up is needed for each pair of values.

Consider two samples (either in range or time), taken from a logarithmic receiver. These are proportional to 10 log P_1 and 10 log P_2 where P_1 and P_2 are the returned powers in mW. Analogous to (4.1) but for the more general case we can write:

$$10\log[(P_1^a+P_2^a)/2]^{(1/a)} = 10\log P_1 - \mathbf{(10/a)\{\log 2 - \log[1+0.7943282^{a(10\log P1 - 10\log P2)}]\}} \qquad (4.2.2)$$

From equation (4.2.2) it is clear that unbiased averages, over pairs, in dBm can be determined corresponding to receiver transference functions of the general form P^a, using the output from a logarithmic receiver. The following applies for a linear response:

$$10\log[(P_1^{0.5}+P_2^{0.5})/2]^2 = 10\log P_1 - \mathbf{20\{\log 2 - \log[1+0.8913^{(10\log P1 - 10\log P2)}]\}} \qquad (4.2.3)$$

and for a quadratic receiver we can write:

$$10\log[(P_1+P_2)/2] = 10\log P_1 - \mathbf{10\{\log 2 - \log[1+0.7943^{(10\log P1 - 10\log P2)}]\}} \quad (4.2.4.)$$

A similar equation can also be compiled for a logarithmic response:

$$[10\log(P_1) + 10\log(P_2)]/2 = 10\log P_1 - \mathbf{0.5(10\log P_1 - 10\log P_2)} \quad (4.2.5)$$

Therefore, the DISPLACE method can be used to obtain the pair averaged values (in dBz) corresponding to a logarithmic, linear or quadratic receiver when only logarithmic receiver outputs in dBz are known. This is achieved by using the same algorithm but with the appropriate *displacement* values. The application of the DISPLACE method is not restricted to conventional pair averaging. Weighted averages over pairs, as done during interpolation, can also be computed, for which the following applies in the general case:

$$10\log[bP_1^a + (1-b)P_2^a]^{(1/a)} = 10\log P_1 + (10/a)\log b + (10/a)\log[1+0.7943^{a(10\log P1 + (10/a)\log b - 10\log P2 - (10/a)\log(1-b)0}]$$

for $0 \le b \le 1$ (4.2.6)

In equation (4.2.6) an adjustment, related to the specific (non-constant) weighting factor b, must be applied to each sample before the averaging is performed on the modified samples. In the case of constant b, the entire bold section in equation (4.2.6) can be precompiled as a *displacement* value table. Whatever the case, the DISPLACE method ensures, in contrast with conventional methods, that only addition and subtraction is done between the weighing factors and the data values. For the difference between a pair we can write the following for the general case:

$$10\log[P_1^a - P_2^a]^{(1/a)} = 10\log P_1 + \mathbf{(10/a)\log[1-0.7943^{a(10\log P1 - 10\log P2)}]} \quad (4.2.7)$$

It is now possible - using the calibration relationship of a specific radar - to scale the above equations and to pre-compile tables of *displacement* values (in bold) for the difference between the digital values representing 10 log P_1 and 10 log P_2. Whenever the calibration changes, new

displacement tables need to be compiled. The specific *displacement* value relating to the required operation must now be subtracted from (or added to) the digital value corresponding to 10 log P_1. By arranging the pair of samples in a manner where 10 log P1 ≥ 10 log P2, the size of the look-up table can be halved at the expense of more arithmetic. In this case a *displacement* table consisting entirely of zeros, will result in obtaining the maximum value while a table consisting of the values 10 log P_1 – 10 log P_2 will result in the minimum value of the pair (or the 2^I,I=1,2,....,n samples under construction).

The averages obtained with the DISPLACE method without division and products are obtained with multiplication. When truncated, the *displacement* values and all other values obtained during the computation remain integers of the same magnitude as the larger of the two samples both numerically and in terms of computer word size. This is in contrast with other methods in which each digitised sample is converted to a received power equivalent using a look-up table before averaging is done (Chandrasekar et. Al., 1989), in which case the time consuming divisions must still be done. Full details on the derivations of the DISPLACE equations are available in Terblanche (1996).

4.3 THE STORM SEVERITY STRUCTURE METHOD

The Storm Severity Structure (SSS) methods based on volumetric radar data, are used to describe the structure and intensity of convective storms. Convective cells normally pass through a life cycle of developing, mature and dissipating stages. The structures of convective storms determine the characteristics of the storm, with regard to the preferred region for further development or decay. Radar reflectivity increases logarithmically with drop size. Using the vertical profile of radar reflectivity distribution to determine storm structure, will be biased towards the location of the maximum radar reflectivity. Therefore, the vertical distribution of the liquid water content is used to define the structure of a convective storm. In convective storms, the strength of the updraft determines the height reached by the liquid water and this forms the basis of the SSS method.

A strong updraft can keep the liquid water of a cell suspended at higher altitudes. Therefore, a region in a convective storm where the liquid water is predominantly located at 8 km and higher above sea level is where a significant updraft to sustain such a structure must exist. Such a liquid water vertical profile is defined as a TOP structure and is indicative of a developing convective

cell. A convective storm can be classified to be in a mature phase of development, when the liquid water content is more evenly spread throughout the vertical cloud column. In this case deep convection exists, and although a strong updraft can prevail, significant liquid water fallout and a downdraft already exists. This vertical distribution of liquid water is defined as a VOLUME structure. If the liquid water content is concentrated lower than 6.5 km above sea level, one can infer that strong updrafts no longer exist. This storm structure is also observed in dissipating convective storms or in precipitation from stratiform cloud. Visser (1999) defined such a liquid water distribution as a BASE structure. To simplify the broad range of reflectivity values, only 3 classifications as WEAK (30 to 44 dBz), MODERATE (45 to 54 dBz) and SEVERE (55 dBz and greater) is defined. A SSS classification is determined by combining the definitions of WEAK, MODERATE and SEVERE for storm intensity with TOP, VOLUME and BASE for storm structure.

The following procedures are detailed by Visser (1999):

- As a first step, the liquid water contents at all CAPPI grid points are calculated in a vertical column at each CAPPI level.
- The Vertically Integrated Liquid Water (VIL), at each horizontal grid point for each vertical column is determined and used to normalise the liquid water content distribution. The normalisation is done in such a way that the percentage liquid water present at each CAPPI is expressed as a percentage of the VIL of the vertical distribution of the column.
- The average altitude above sea level of the liquid water content distribution is then determined by:

$$\overline{H} = \sum_{i=2}^{16} i * M_i \qquad (4.3.1)$$

where i = is the altitude of the CAPPI level and M_i = the percentage of total vertical liquid water content at CAPPI level i. The standard deviation of this distribution of liquid water content is:

$$\sigma = \sqrt{\sum_{i=2}^{16} (i - \overline{H})^2 M_i} \qquad (4.3.2)$$

To classify the vertical structure according to the TOP, VOLUME or BASE classification Visser (1999) performed an analysis of the height of the maximum reflectivity $\overline{H}$, and the standard deviation σ detailed in table 4.1

Table 4.1: Classification of convective cell structure with the SSS method

$\overline{H}$, (km)	σ (km)	Maximum Z height	Structure
< 6.5 km	**< 2.0**	**Not Applicable**	**BASE (B)**
	≥ 2.0	**2-5 km**	**BASE (B)**
	≥ 2.0	**≥ 6 km**	**VOLUME (V)**
6.5 - 8 km	**< 2.0**	**Not Applicable**	**VOLUME (V)**
	≥ 2.0	**2-5 km**	**BASE (B)**
	≥ 2.0	**6 km**	**VOLUME (V)**
	≥ 2.0	**≥ 7 km**	**TOP (T)**
> 8 km	**< 2.0**	**Not Applicable**	**TOP (T)**
	≥ 2.0	**2-6 km**	**VOLUME (V)**
	≥ 2.0	**≥ 7 km**	**TOP (T)**

Visser (1999) Indicated that the maximum reflectivity is not considered if the standard deviation is smaller than 2.0, meaning that the distribution is concentrated around the average height of the liquid water. Only 3 indices are used to define the severity of a storm. The maximum reflectivity within a vertical column defines the severity for the SSS method as in table 4.2

Table 4.2: Indices used to define the intensity of a storm for the SSS method.

Max Z_{ave}	SEVERITY CLASS
30-44 dBz	WEAK (W)
45-54 dBz	MODERATE (M)
55+ dBz	SEVERE (S)

By combining the Structure with the intensity indices, 9 distinct storm Severity Structure classes are defined. The SSS classification is illustrated in table 4.3

Table 4.3: The SSS classification. Numbers 1-9 are the SSS class number.

	Weak	Moderate	Severe
Base	Weak Base (WB) 1	Moderate Base (MB) 4	Severe Base (SB) 7
Volume	Weak volume (WV) 2	Moderate Volume (MV) 5	Severe Volume (SV) 8
Top	Weak Top (WT) 3	Moderate Top (MT) 6	Severe Top (ST) 9

The project team conducted a number of case studies where the SSS classification of Visser was used in conjunction with CAPPI and other data.

4.4 THE BRIGHT BAND

The bright band has significant effects on the radar vertical reflectivity profile and may lead to erroneous CAPPI rainfall computation. Mittermaier (1999) described the dynamical and microphysical processes relevant to the bright band. Stratiform and convective precipitation can occur under a variety of dynamically-driven patterns. They are not mutually exclusive. The unstable overturning of the atmosphere by buoyant air motions is termed convection. Convective regions can consist of both convective and stratiform elements, as distinguishable by radar (Houze, 1997). The precipitation type is determined by the strengths of the vertical air motions. These in turn determine the underlying sequence of microphysical processes.

Condensation in a young or mature convective element is rapid and the liquid water content (LWC) increases accordingly. Under these conditions the larger drops grow most efficiently by collection of small cloud droplets (collision and coalescence) as well as collection by ice particles (riming). The strong updrafts allow the larger particles to remain suspended and they continue to grow by collection of cloud droplets for longer periods. Most of the precipitation from a convective cell falls within a few kilometres of the updraft core. After the onset of precipitation, the convective cell weakens. Updraft velocities decrease and the cell structure becomes more stratified. The weaker updrafts are still capable of supporting precipitation particles to grow by vapour diffusion. The LWC is significantly lower making the process of riming inefficient under these conditions.

Growing ice particles settle slowly downward in the mid- and upper regions of old convective elements resulting in the appearance of distinct layers, with markedly different microphysical processes. Such a vertical reflectivity profile is given in Figure 4.4.1. At the upper levels, growth by vapour diffusion dominates. Aggregation (clumping) of ice particles can occur in the temperature range of 0 to -15°C, with the greatest likelihood between 0 and -5°C. The layered structure of stratiform precipitation causes the reflectivity to be enhanced by radar because the reflectivity of melting snow aggregates is much higher due to the physical facts that:

- Z is proportional to sixth power of the diameter D. Many of the snow aggregates are very large, i.e. they are non-Raleigh scatterers.
- The index of refraction of the radar pulse is ~ 5 times greater for melting snow aggregates.

The relative decrease in the radar reflectivity below the melting layer, is a result of an increase in the fall speeds, decreasing the particle concentration. Sandwiched between lower reflectivity values above and below the melting layer, a bright band of enhanced reflectivity appears just below the 0°C isotherm.

The bright band is a feature of radar reflectivity data, describing the microphysical processes at work. The problem with the bright band comes when the reflectivity data are converted to rainfall using for instance the Marshall-Palmer relationship. The enhanced reflectivity values result in an over-estimation of rainfall totals. Methods of modifying the reflectivity field before converting to rainfall have been developed worldwide. Locally Mittermaier (1999) has considered using a convective-stratiform classification algorithm combined with an objective mathematical technique - singular value decomposition - to improve the quality of radar- rainfall estimates under stratiform conditions. The algorithm has sufficient potential to be operationally tested in the coming rainy season.

Apart from this work detailed by Mittermaier (1999) in a MSc dissertation, no work on the "bright band" problem was attempted. The project team was fortunate that Mittermaier (1999) did such sterling work under the guidance of Prof Pegram and Dr Terblanche. One of the case studies (980308) detailed in Chapter 5 describes the results when, presumably a bright band was present. Unfortunately Mittermaiers' methods could not be applied in this case study.

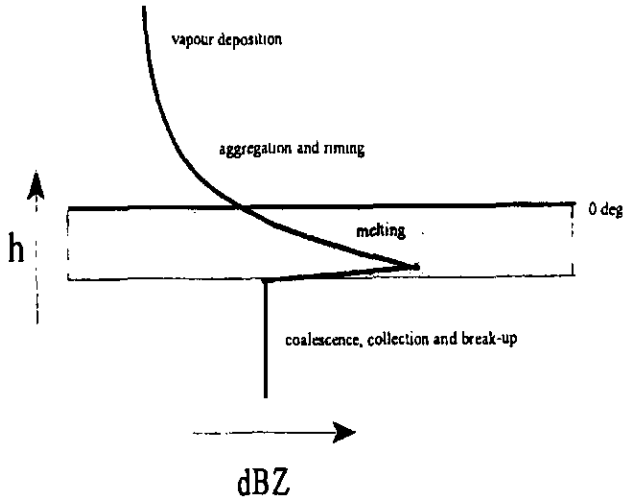

Figure 4.4.1: Schematic of the vertical reflectivity profile characteristic of stratiform precipitation showing the dominant microphysical processes at work.

4.5 DISTROMETER DATA

In an attempt to determine a specific Z-R relationship for the MRL-5 S/X band RADAR operated near Bethlehem, the drop size distribution (DSD) was measured by a distrometer operated in a dense rain gauge network near Bethlehem. This distrometer measures the number of droplets that precipitates each minute in each of 20 droplet size categories, and from these categories the DSD's can be estimated.

After estimating the DSD's (different sets for different rain rates), an average set of DSD's is calculated using all the available distrometer data collected. This approach does not take any cloud or dynamical processes into account. It is generally accepted that these processes could affect the DSD's considerably. However, single Z-R relationships for all types of rainfall probably result in errors.

DSD's calculated for both convective and stratiform rainfall over the dense rainfall network are compared. In order for rainfall to be classified as stratiform or convective rainfall, a method first

had to be developed to facilitate this classification. A one dimensional cloud model (Stuart 1996, personal communication) was developed to derive a measure of the convectivity of the atmosphere for a 12 hour time period. This model uses the upper air sounding data for Bethlehem for the periods over which the distrometer data were collected. The buoyancy of the atmosphere as well as the wind shear were utilised to calculate a simplified Richardson's number for each 12 hour period. Considerable differences were found to exist between DSD's observed from rainfall precipitating from convective and stratiform cloud.

The simplified Richardson's number, adapted from Weisman and Klemp (1986), is defined as:

$$R = \frac{B}{\frac{1}{2}U^2}$$

where B = Estimated Bouyant Energy U = Measure of the vertical wind shear

Following Weismann and Klemp (1986) the following division was used:

Stratiform clouds **< R = 10 <** **Convective clouds**

Analysis of the CAPPI data for each group, in order to determine specific Z/R relationship, was considered. The research was discontinued because of equipment problems on the one hand but primarily because the research team considered that other problems such as the bright band, ground clutter and attenuation were significantly more important than determining a "new" Z-R relationship.

The great variability in observed rain rates from convective cloud over the dense network also indicated that a locally derived DSD and Z-R relationship will require a long observation period with absolutely no certainty of success.

CHAPTER 5: RAIN GAUGE AND RADAR-DERIVED RAINFALL INTER-COMPARISONS

5.1 RAINFALL CHARACTERISTICS OF THE RADARAIN AREA

Most rainfall in the eastern Free State occurs as convective development (Court, 1979). Convective storms develop mainly between 14:00 and 20:00 (Mather and Terblanche, 1993). Convection is triggered mainly by topography in combination with surface heating and most storms propagate from west to east in the area (Steyn and Bruintjes, 1990).

Stationary storms can cause severe flooding and loss of life especially of people living in low lying areas. Examples are the Free State floods (Triegaardt et. al.1991), Moreletta and Apies River floods in Pretoria (Weather Bureau, 1991), the Umzindize River (Visser, 1999) and several flooding events in the Ladysmith area which occur on an annual basis.

Prediction and tracing of these storms still presents a major problem for flood managers. Weather radars and satellite images are valuable remote sensing methods to evaluate these storms.

5.2. SEASONAL RAINFALL

In all of the work described below, the Marshall Palmer Z-R relationship of $Z=200R^{1.6}$ was used. Radar rainfall rates were calculated for radar bins which correspond with the geographical positions of the rainfall gauges depicted in figure 3.1. Following this procedure mean radar rainfall for an area of approximately 4 x 5 km was calculated and used for comparison with the areal mean rainfall originating from the rainfall gauge data.

For the 1995/96 and 1996/97 seasons radar CAPPI data were calculated using the procedure developed by A W Seed (1998) and applicable to 2 km heights above ground level at the radar site. The improved procedure for interpolation of the CAPPI levels was used for the 1997/98 data (Mittermaier and Terblanche, 1997). It should also be noted that the CAPPI data used for the areal averages were supplied by the BPRP team during the course of the project and should not be confused with the data recalculated from the **mdv** formatted files supplied after December 1998 and used in all of the case studies.

Rainfall Characteristics for the 1995/96: 1996/97 and 1997/98 Summer Seasons.

Table 5.2.1. Number of days with radar data per season, total rain for season and the total rain on days with radar data.

Season	Period	Days with radar data	Total rain	Total rain on days with radar data
1995/96	951018-960223	33	823.8	425.4
1996/97	961004-970309	56	501.0	403.1
1997/98	971105-980220	28	567.8	348.3

Total seasonal rain refers to the rainfall for the period 1 October to 31 March. Radar data for the 1995/96 season were only available from 20 November 1995 to 24 February 1996 at which time the rain-gauge loggers' memories were filled to capacity. The contribution of these days to the total rainfall was 52%. The 1996/97 season had 56 days of radar data. Rainfall on these days contributed 81% of the seasonal rainfall. Radar data for the 1997/98 season were available from 5 November 1997 to 20 February 1998.

Table 5.2.2. Total rainfall for the three summer seasons from October to March as well as the percentage as compared to the long-term average rainfall.

Season	Rainfall	Percentage
1995/96	823.8	156
1996/97	501.0	95
1997/98	567.8	107

The long-term average rainfall for the period October to March is 529 mm (WB 40). The 1995/96 season received much more rainfall as compared to the long-term average, the 1996/97 slightly less while the 1997/98 season slightly above.

One of the highest flood peaks in the past 100 years occurred during a seven-day period from 9 to 16 February 1996 (Terblanche, 1996). During this period 163 mm of rain was recorded over the network. Extensive flood related damage was reported. This flood resulted in the Vaal Dam rising from 101% on the 13th to 118% on the 19th, which required very careful reservoir management. These heavy rainfalls were preceded by falls of 150 mm over the network during the period 14 to 22 December 1995 (Fig 5.4.2), resulting in a saturated catchment. No exceptional rainfalls were recorded during the 1996/97 season, the best falls being 84 mm during the period 1 to 9 March

1997. A pronounced midsummer drought is evident in Fig 5.4.2. The first of two high rainfall events during the 1997/98 season occurred during the period 31 December 1997 to 2 January 1998 when 103 mm was recorded over the network. However this was followed by a dry period lasting some 14 days. The second event from 1 February to 2 February 1998 yielded 129 mm.

5.3 USE OF "MDV" RADAR FILES

In order to provide areal information on a rainfall event using radar reflectivities the operator must start at radar pixel resolution. To investigate the reliability of the MRL-5 at pixel resolution several case studies were completed. Some of these describe days when the MRL-5 CAPPI derived rainfall did very well while case studies with poor results at pixel resolution are also illustrated. In order to do this research it was decided to use the "**mdv**" format radar images provided by the BPRP staff. These radar "**mdv**" files comprise of a vast number of images all in **mdv** format. Unfortunately the BPRP staff were unable to provide all of the **mdv** formatted radar files for all of the days during the three project seasons. The BPRP processing and archival system only became fully operational during 1998.

Eventually a cut-off date for computation of **mdv** files, using Displace Variate Averaging, was set for end June 1999. This left the UP team very little time to complete the analysis. Analysis of the **mdv** formatted files comprised the classification of rainfall/cloud systems over the project rain gauge network using the TITAN system as well as calculation and extraction of data over the rain gauge network comprising:

(i) CAPPI data at 4 km ASL
(ii) Storm Severity Structure (SSS) data.
(iii) Maximum dBz values above network grid points.
(iv) Rainfall rates based on (iii)

In order to do this the UP team had to acquire a working knowledge of LINUX and the TITAN system. Mr S Stuart from the BPRP, developed the programmes to perform these tasks in accordance with our specifications. He also devoted more than a week to training the project leader in the use of the TITAN software and the running of the program system. This process is quite complicated but fortunately LINUX allows for multi-processing, and all four programmes ran simultaneously. This processing task started in January 1999 and continued as **mdv** files

became available. Table 5.3.1 lists all the days per season for which "**mdv**" files became available.

Table 5.3.1. List of all the MRL-5 Radar Files in **mdv** format:

Season 1		Season 2		Season 3		
1995/96		1996/97		1997/98		
95/11/28	96/01/23	96/10/21	97/03/01	97/10/11	98/01/01	98/02/11
95/11/29	96/01/24	96/10/22	97/03/02	97/10/14	98/01/02	98/02/12
96/12/13	96/01/25	96/10/23	97/03/03	97/10/15	98/01/03	98/02/13
95/12/14	96/01/26	96/10/29	97/03/04	97/11/08	98/01/04	98/02/14
95/12/15	96/01/27	96/10/30	97/03/05	97/11/09	98/01/05	98/02/15
95/12/16	96/01/28	96/10/31	97/03/06	97/11/10	98/01/06	98/02/16
95/12/17	96/02/01	96/11/06	97/03/07	97/11/11	98/01/07	98/20/17
95/12/18	96/02/02	96/11/08	97/03/08	97/11/12	98/01/08	98/02/19
95/12/19	96/02/05	96/11/17	97/03/09	97/11/13	98/01/09	98/02/20
95/12/20	96/02/09	96/12/02		97/11/14	98/01/13	98/02/21
95/12/21	96/02/10	96/12/03		97/11/15	98/01/14	98/02/22
95/12/22	96/02/11	96/12/06		97/11/16	98/01/15	98/02/23
95/12/23	96/02/12	96/12/08		97/11/27	98/01/16	98/02/24
95/12/24	96/02/13	96/12/09		97/11/28	98/01/17	98/02/25
95/12/25	96/02/14	96/12/10		97/12/04	98/01/18	98/02/26
95/12/26	96/02/15	96/12/11		97/12/05	98/01/19	98/02/27
95/12/27		96/12/12		97/12/06	98/01/20	98/02/28
		96/12/15		97/12/24	98/01/21	98/03/01
		96/12/17		97/12/27	98/01/23	98/03/08
		96/12/18		97/12/28	98/01/25	98/03/10
				97/12/29	98/01/29	98/03/21
				97/12/30	98/01/30	98/03/22
				97/12/31	98/01/31	98/03/23
						98/03/24
						98/03/25
						98/03/26
						98/03/27

Details on the classification of images are in section 5.5 and the use of SSS data are detailed in section 5.7.

5.4 SEASONAL INTER COMPARISONS

Figure 5.4.1 shows a scatter plot on a logarithmic scale of radar derived daily rainfall for the three seasons. A total of 117 days were available when both radar and rain gauge data could be used. The data are clustered fairly closely around the diagonal. Large deviations, however, are evident.

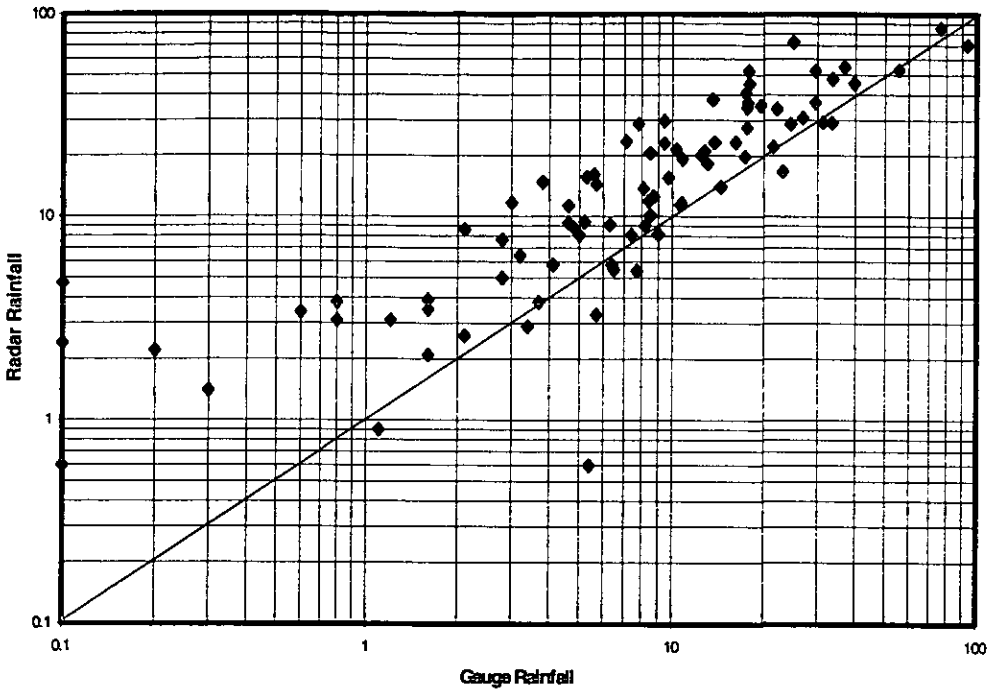

Figure 5.4.1: Scatter plot of the CAPPI and gauge daily totals for all the summer seasons, October to March, 1995/96, 1996/97 and 1997/98.

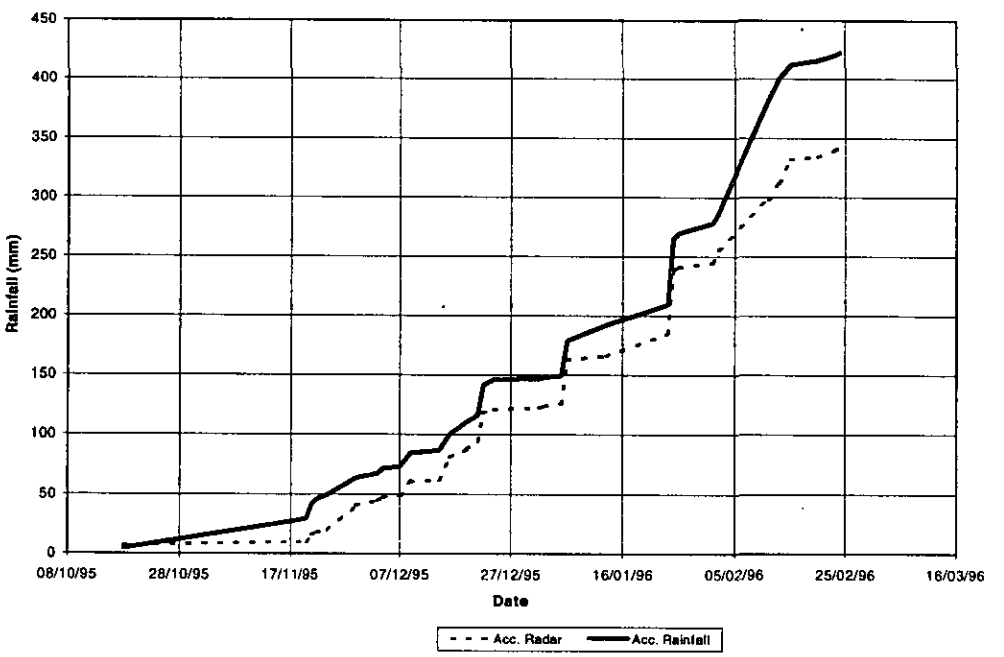

Figure 5.4.2: Accumulated mean RADARAIN network CAPPI and gauge rainfall for the 1995/96 summer season.

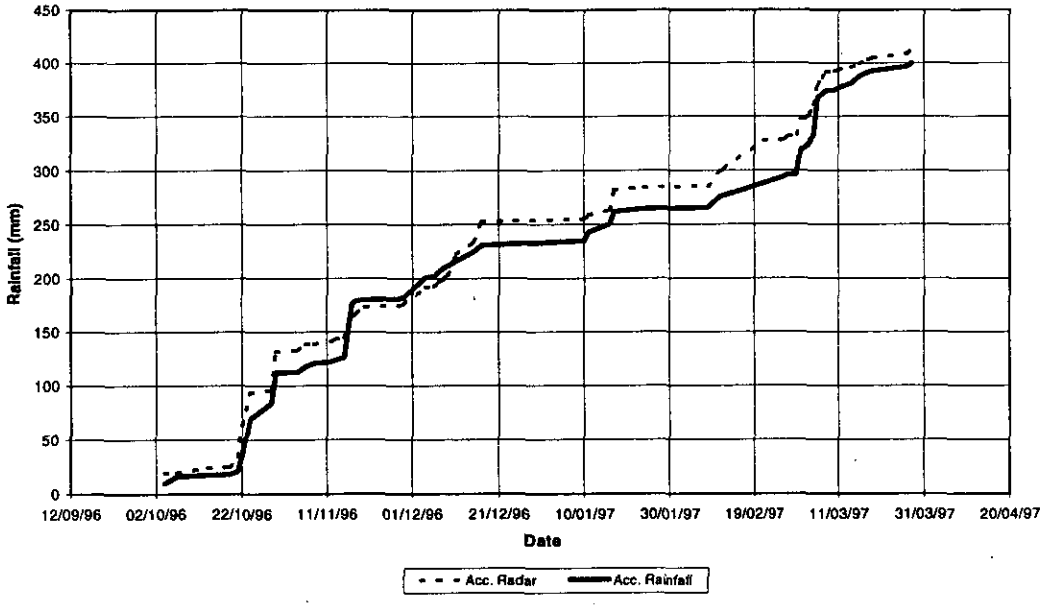

Figure 5.4.3: As figure 5.4.2 but for 1996/97.

Figures 5.4.2 to 5.4.4 compares the accumulated rainfall (radar and gauge) for the three seasons. The ratio (gauge/radar) was 1.2 for the 1995/96 season, indicating that the radar was underestimating the rainfall. The curves (fig 5.4.2) followed each other reasonably well until 11 February, after which the curves deviated appreciably.

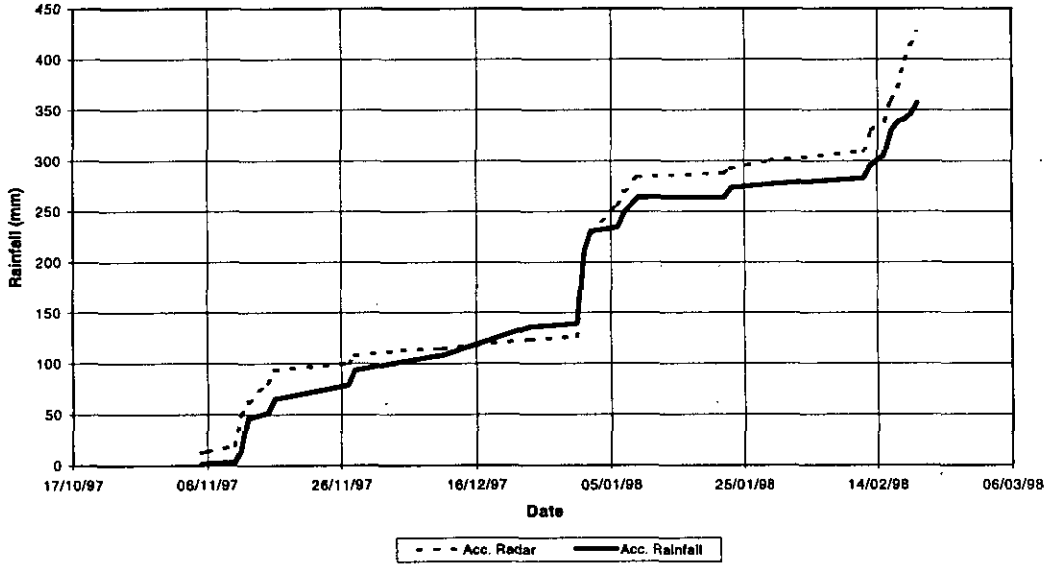

Figure 5.4.4: As figure 5.4.2 but for 1997/98.

The 1996/97 season (figure 5.4.3) shows a very good comparison, with a ratio of 0.9 at the end of the season. This season has the largest data set with 57 days, which could be the reason for the better comparisons.

The 1997/98 season (figure 5.4.4) shows a deviation between the two curves during the early part of the season, then a good comparison towards the end of January, and thereafter a deviation in mid January and towards the end of the season. Noticeable in figure 5.4.4 is the good comparison of the heavy falls at the beginning of January 1998.

5.5 CLASSIFICATION OF RADAR IMAGES

The TITAN (version 5) software is a very powerful radar image analysis system. The authors gained enough experience with the system to begin to appreciate its full potential. It allowed the authors to view each rainfall system as it moved over the RADARAIN network. In all, 32 576 radar scans were available. In order to arrive at a classification, the authors viewed the images until cloud development started over the radar area and then scan per scan. It was decided to classify rain-system states over the network on an hourly basis. Generally the most dominant states were used. The final results of the classification plus some useful comments are listed in Appendix B. The classification of rainfall systems as viewed by the TITAN display are described in table 5.5.1.

Table 5.5.1. Classification of rainfall systems over the RADARAIN network for days listed in table 5.3.1.

Code	Class	Description
I	Isol	Isolated cells with dBz > 30. Cell size < 20 kms in diameter
C	Clusters	Multi-cell clusters of diameter greater than 20 km in various stages of development but having diameters generally less than 60 km
CL	Clusters Large	Multi-cell clusters of large horizontal extent greater than 60 km in diameter
L	Line	Clusters organised in a linear structure exceeding 60 km in length with a width less than a third of the length. The line must remain recognisable as a line for at least one hour. Otherwise it reverts to C or CL
G	General	Reflectivities generally low (dBz <40). No large organised structures should be present. The horizontal rainfall system must cover at least 25% of the radar area.

In hindsight, it would have been useful to include an additional class, namely S for a "Stratiform" image field. These often occur ahead or behind large rainfall structures and CAPPI derived rainfalls are of the order of 1mm/hour or less. Our experience also indicated that a computer based classification system over an important catchment would be beneficial to hydrological applications of radar images.

Using all the CAPPI 4km ASL data computed from the **mdv** formatted radar files the author found the distribution depicted in table 5.4.2.

Table 5.5.2. Contribution of the different classes of days to the Total Rainfall.

	Percentage of total rainfall	Number of cases
Isol	18.7	103
Clusters	20.4	61
Large Clusters	38.8	66
General Rain	22.1	85

The largest contribution to the rainfall during the periods of the classification came from the large cluster cases. As might have been expected, the smallest contribution was from the isolated cases.

Figures 5.5.1 to 5.5.4 show scatter plots of radar and gauge rainfalls for the different classes of days. Isolated cases show the worst spread around the diagonal, with cluster, large cluster and general rain a better spread. In the cluster and large cluster cases there is a tendency for the radar to over-estimate the rainfall.

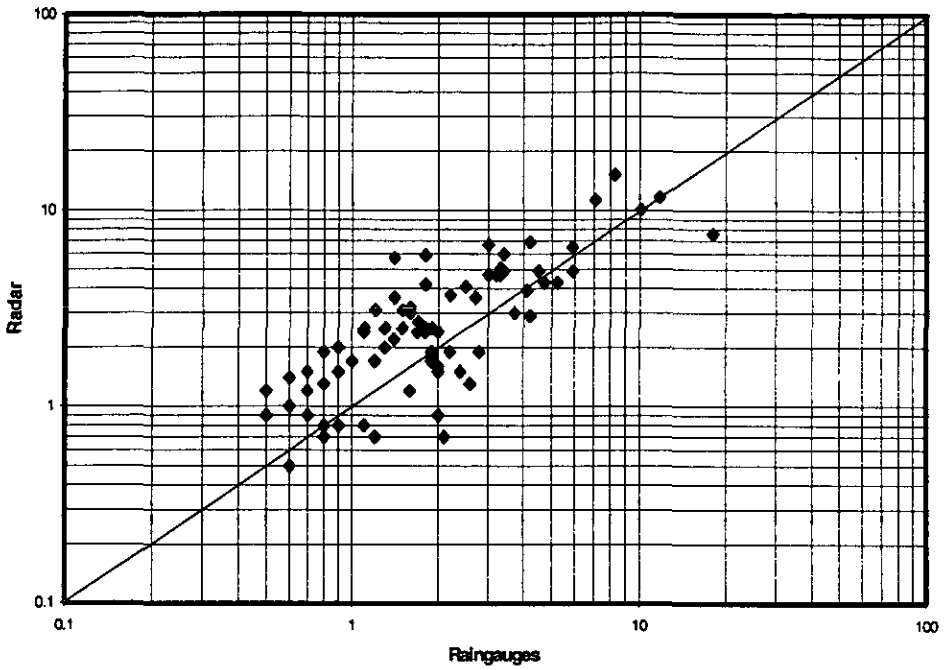

Figure 5.5.1: Scatter plot for hourly General rain CAPPI and gauge totals for the summer seasons 1995/96, 1996/97 and 1997/98.

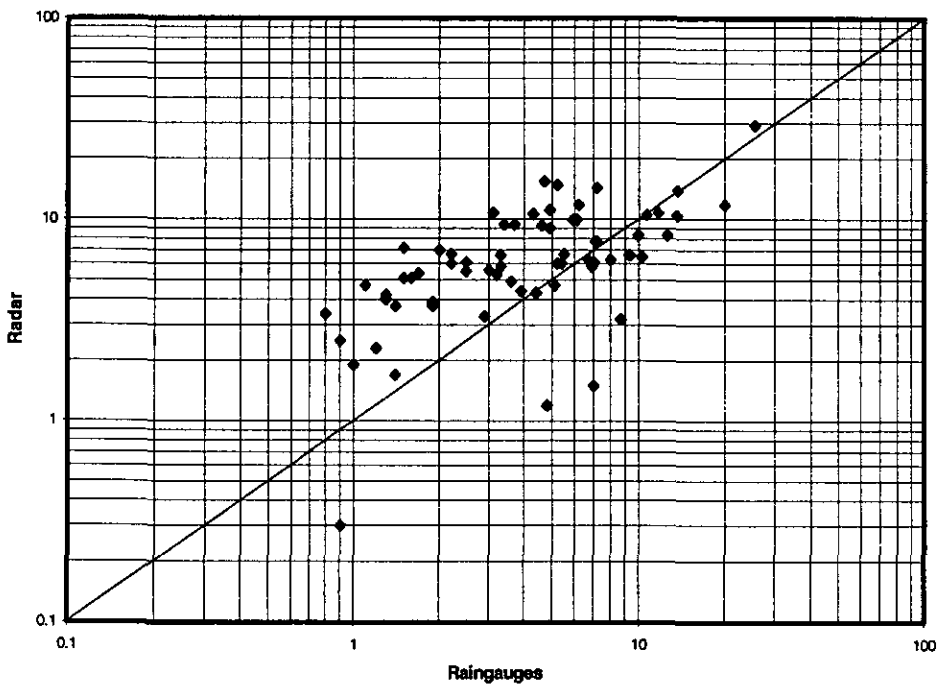

Figure 5.5.2: As figure 5.5.1 but for hourly Large Clusters.

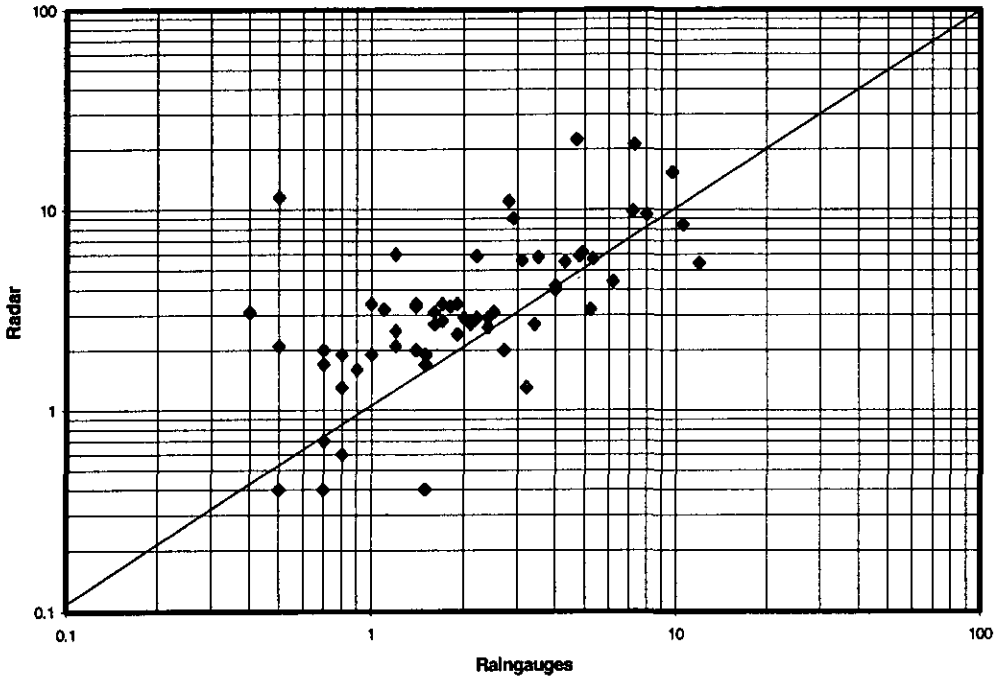

Figure 5.5.3: As figure 5.5.1 but for hourly Clusters.

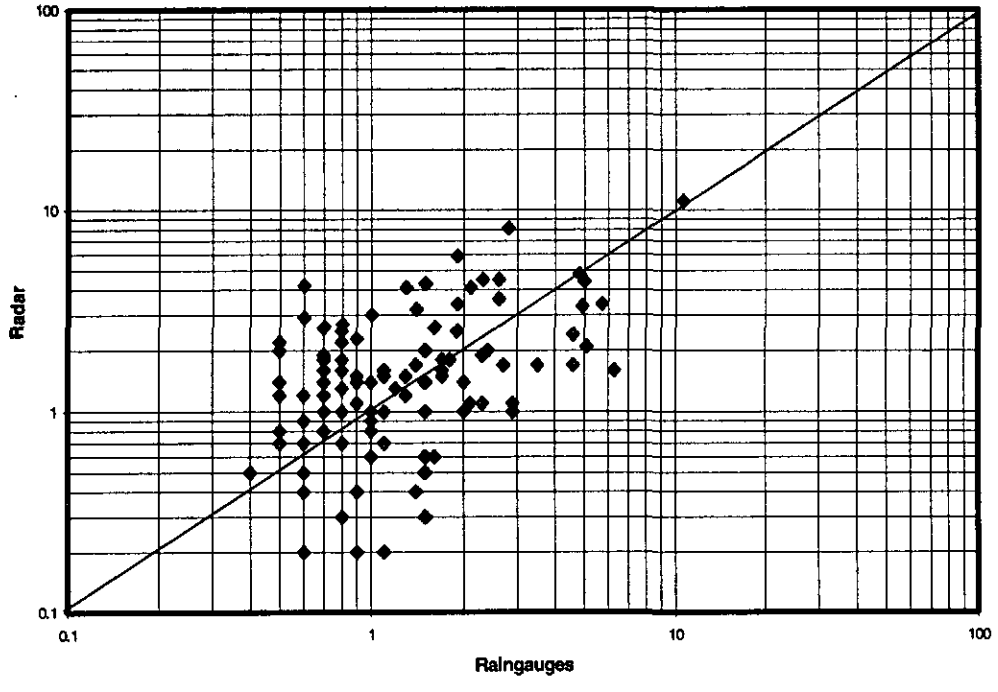

Figure 5.5.4: As figure 5.5.1 but for hourly isolated rain systems.

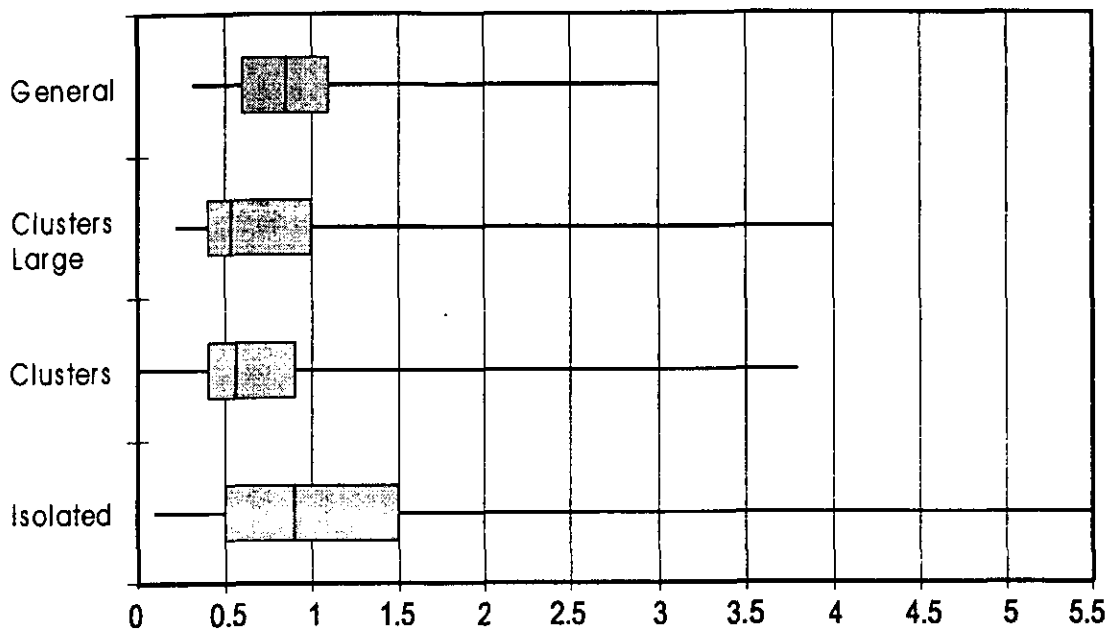

Figure 5.5.5: "Box and Whiskers" plot of the ratios (gauge/radar) for the four categories of hourly rain systems.

Figure 5.5.5 shows a "box and whiskers" plot of the ratios (gauge/radar) for the four category of days. The spread is greater for the isolated cases, with half of the cases lying between 0.5 and 1.5. The best spread occurs for the general rain cases where half of the data lies between 0.6 and 1.1.

5.6 CASE STUDIES AND AVERAGES

In the case studies 5.6.1 to 5.6.7 the rain gauge network and CAPPI data are averages computed from hourly totals.

Figures 5.6.1 to 5.6.7 compare the accumulated rainfall for the radar and rain gauges for the entire network for selected case studies. The case studies present cases with high intensity rainfall occurring for a length of time, i.e. the best cases in the data set.

A colour figure denoted by "CHAPTER 5.6 CASE STUDY (2) 1996-01-25 00:11:28", which forms part of Case Study 2, is a composite radar image created with the TITAN display system. The position of the RADARAIN network is shown as a small yellow block with the letters NTW, in black, just south east of the network. This image serves to bring the scale of events, in relation to the network, into perspective.

Case 1 1997-12-31 – 1998-01-02

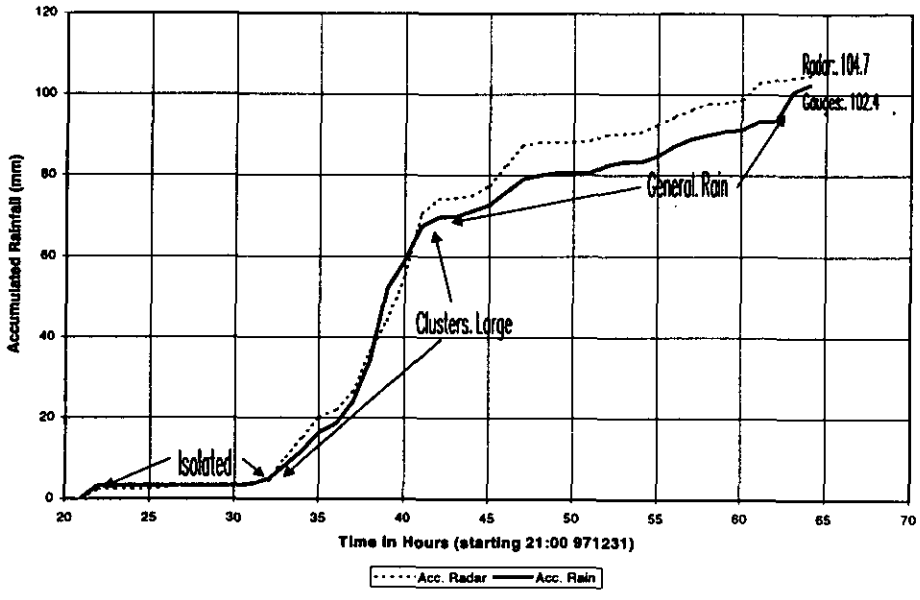

Figure 5.6.1: Accumulated CAPPI and gauge rainfall for the period 21h00 on 1997-12-31 to 19h00 on 1998-01-02.

The rain event started at 21h00 on the 31 December 1997 and lasted until 16h00 on 2 January 1998. This rain event started off as isolated rain over the network and developed to large clusters with high rainfall intensities during the morning of 1 January 1998. The event was classified as general rain from the night of 1 January 1998 until the end of the event on the 2 January 1998.

The rainfall comparisons (figure 5.6.1) between the radar and the rain gauges on this occasion were very good, ending with a ratio of 0.98. Noticeable are the very good comparisons during the high rainfall intensities. The authors are of the opinion that in this case a bright band did not occur, or was not present near the RADARAIN network.

Case 2 1996-01-24 – 1996-01-25

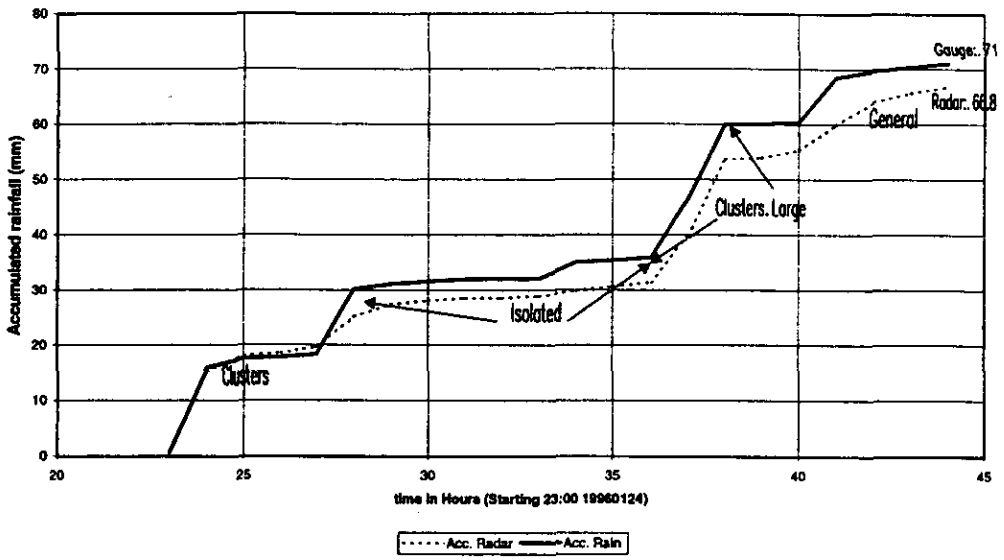

Figure 5.6.2: As figure 5.6.1 but for 23h00 on 1996-01-24 till 19h00 on 1996-01-25

This event started off as clusters, changed to isolated during the morning of the 25 January 1996 with clusters during the afternoon, and followed by general rain towards the evening. The radar under-estimated the rainfall, although the curves followed each other reasonably well (figure 5.6.2). The ratio was 1,06 at the end of the event.

Case 3 1995-12-16 – 1995-12-18

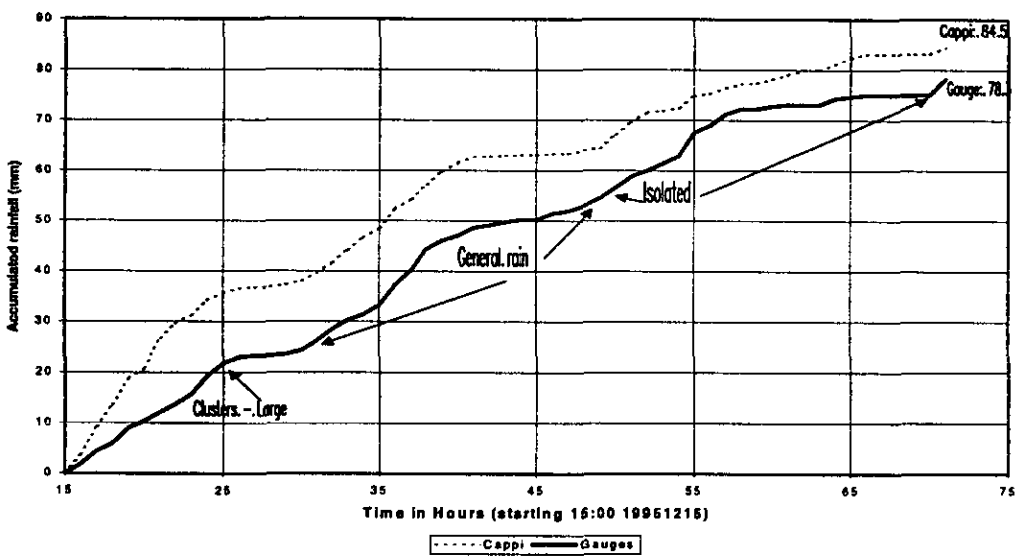

Figure 5.6.3: As figure 5.6.1 but for 15h00 on 1995-12-16 to 23h00 on 1995-12-18.

More than 78 mm of rain fell during this event, which started off as isolated, changing to clusters and thereafter, general rain on 17 December 1995, followed by isolated rain towards the end of the event. The radar over estimated the rainfall (figure 5.6.3), ending with a ration of 0.92.

Case 4 1998-03-08

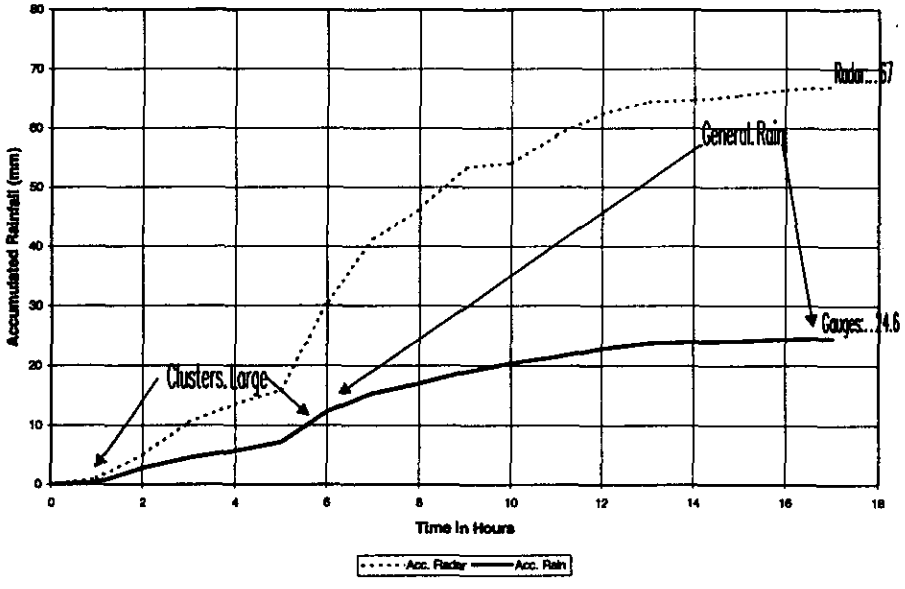

Figure 5.6.4: As figure 5.6.1 but 00h00 to 17h00 on 1998-03-08.

The development started off as large clusters which turned into general rain towards the end of the event. As can be seen from figure 5.6.4 the comparison between radar and rainfall was bad with a ratio of 0,36. This case will be further analysed using data for individual rain gauges/ radar pixels.

Case 5 960210 -960211

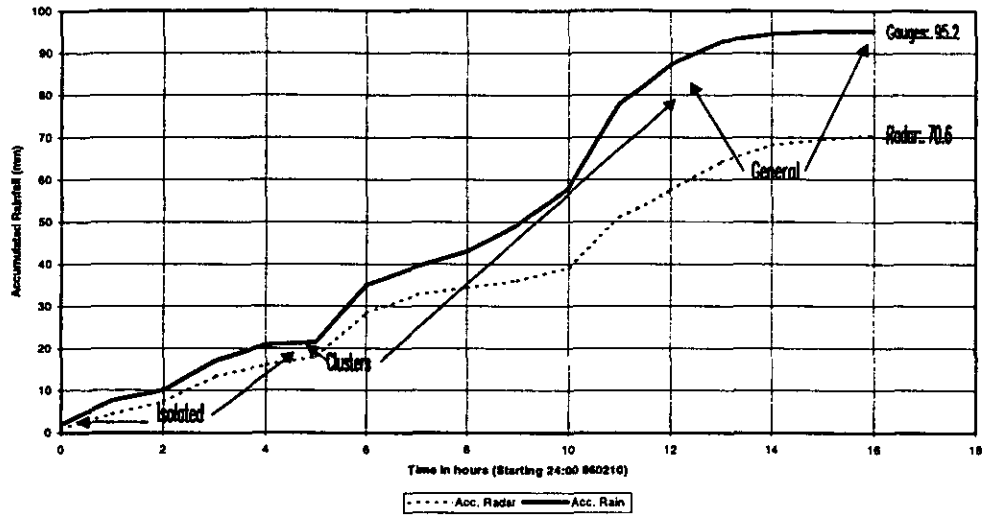

Figure 5.6.5: As figure 5.6.1 but for 00h00 on 1996-02-10 to 16h00 on 1996-02-11.

The flood events started during this period and lasted till 15 February I996. A total of 95 mm was recorded during this rain event. (figure 5.6.5)

On 10 February 1996 the development was classified as isolated, turned into large clusters and ended as general rain. The radar underestimated the rainfall, ending with a ratio of 1.34. This is difficult to understand and is further investigated at radar pixel level.

Case 6 1996-02-13 – 1996-02-14

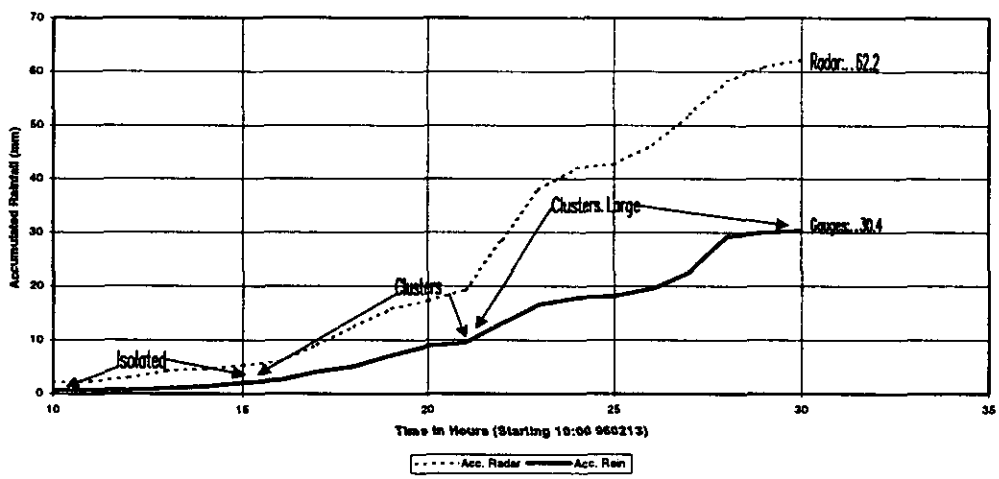

Figure 5.6.6: As figure 5.6.1 but for 10h00 on 1996-02-13 to 06h00 on 1996-02-13.

The rainfall event during this period was classified as isolated at first, later on turning into large clusters. A total of 30 mm was recorded over the network during this period.

The radar overestimated the rainfall (figure 5.6.6) by a considerable margin. The ratio was 0.5 at the end of the event.

Case 7 1996-02-15

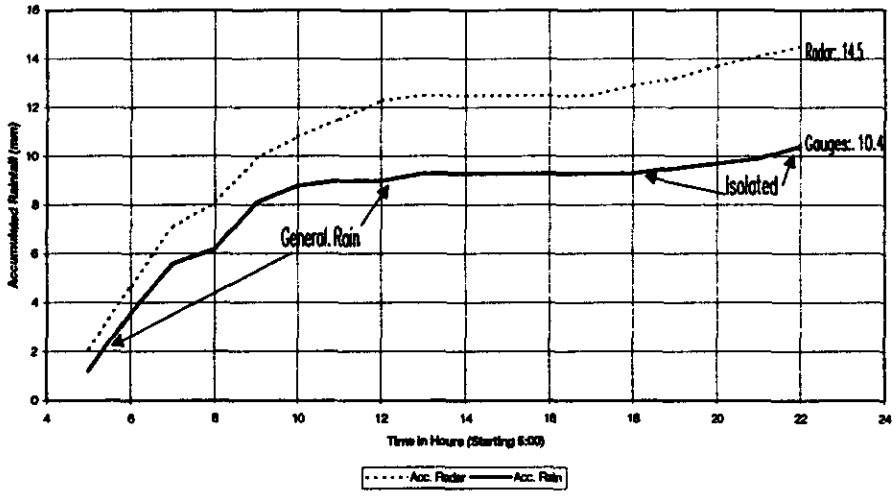

Figure 5.6.7: As figure 5.6.7 but for 05h00 to 22h00 on 1996-02-15.

This day (figure 5.6.7) was classified as general rain for the whole period except at the end when the system moved out of the study area.

The radar overestimated the rainfall with a ratio of 0.71. Taking the flood period (from 1996-02-09 to 1996-02-16) as a whole, the ratio turned out to be 0.92, which was acceptable.

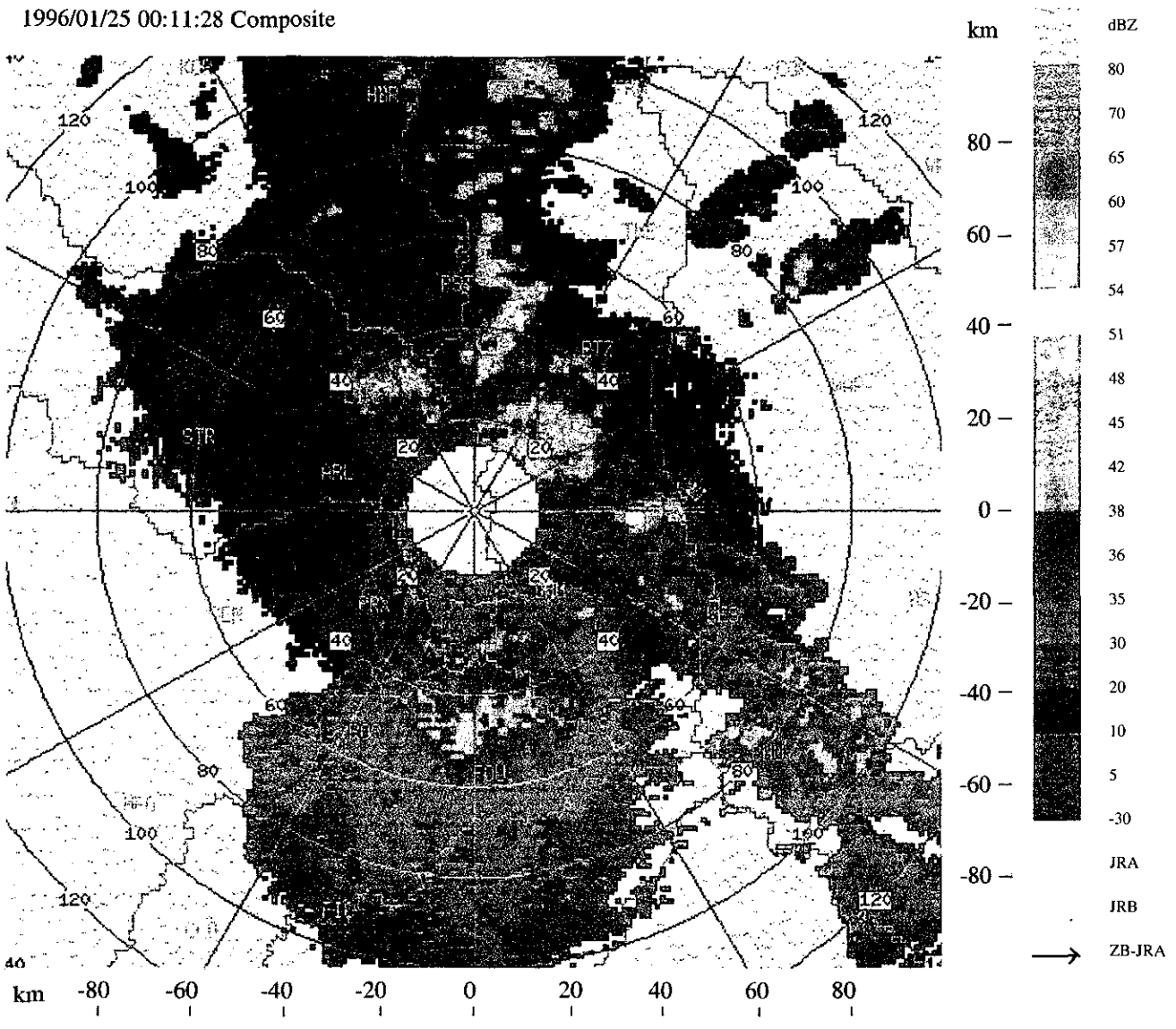

CHAPTER 5.6 CASE STUDY 2 1996-01-25 00:11:28

5.7 RAINFALL ANALYSIS WITH SSS DATA

Use of conventional CAPPI data provides little information on the storm structure or its evolution. This information is available if one uses the TITAN software to its full potential but is only practicable for a post mortem case study. Even in the "Nowcasting" environment full use of the TITAN system needs at least one full time operator. The SSS method developed by Visser (1999) provides a means to classify a storm at radar pixel level in terms of its structure and intensity and can be computed in near real time for incorporation in a rainfall computation scheme – or so the authors thought.

In the case studies detailed in section 5.8, some use was made of the SSS classification. It appears that the most rainfall events occur when the storm water mass in the storm has descended to lower levels during the dissipating stage of the storm when SSS class 1 (weak base) was identified as seen in table 5.7.1. Fairly high rainfall rates (in scan times) occurred when a class 4 (moderate base) occurred.

Considering all of the 32576 scan intervals, for which a SSS classification was done, the authors found a distribution, as depicted in table 5.7.1. This distribution of SSS classes covers the entire study period at each of the radar pixels over the RADARAIN network..

Table 5.7.1: Number of SSS classes observed on all days listed by table 5.2.1

		Number of Pixels
Total number of pixels used		651520
Number of pixels not classified during scan intervals when at least one pixel was classified		14209
SSS = 1	Weak Base (WB)	30795
SSS = 2	Weak Volume (WV)	313
SSS = 3	Weak Top (WT)	537
SSS = 4	Moderate Base (MB)	1509
SSS = 5	Moderate Volume (MV)	58
SSS = 6	Moderate Top (MT)	47
SSS = 7	Severe Base (SB)	113
SSS = 8	Severe Volume (SV)	18
SSS = 9	Severe Top (ST)	21

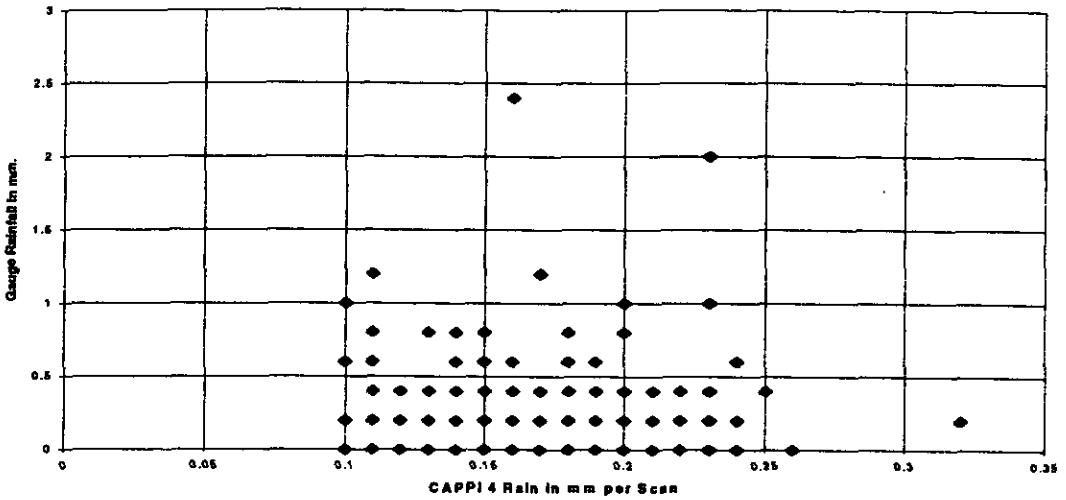

Figure 5.7.1: Scatter plot CAPPI and gauge rainfall at pixel 10 for class SSS = 0.

Base structures comprise the vast majority of classifications (32 417). With only 1 004 pixels classified as either volume or top, the classification leads to the conclusion that significant water volumes do not stay for long at higher levels in convective cloud.

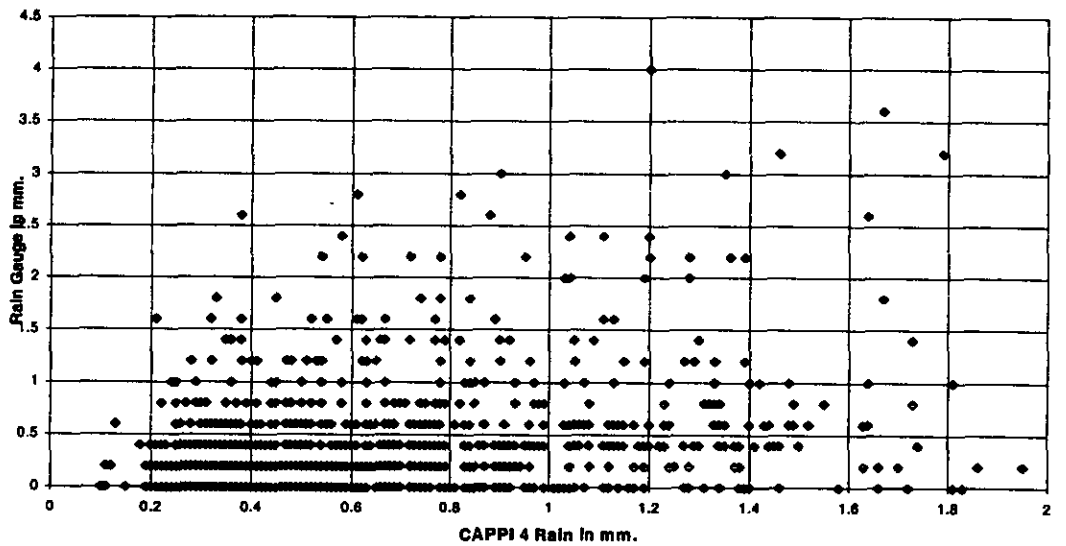

Figure 5.7.2: Scatter plot CAPPI against gauge rainfall at pixel 10 for class SSS = 1.

The low number of volume structures (389) also seem to indicate that the water mass descends rapidly down the cloud structure. The overwhelming majority of the Base Structures (1, 4 and 7) may also indicate that a far greater amount of raindrop generation takes place lower in the cloud structure.

The SSS data available for all three seasons were analysed in order to determine whether SSS classification can assist in producing better rainfall estimates from CAPPI data. In the analysis and because of the huge number of scan intervals available, it was decided to use only SSS classification at the 10^{th} radar pixel. To eliminate the large number of unclassified incidents SSS values were only considered when CAPPI determined rainfall was 0.1 mm or greater per scan interval at pixel 10. In figure 5.7.1 a scatter plot for SSS=0 is displayed of CAPPI derived rainfall against the gauge rainfall for the scan.

Only those scan data points when the CAPPI rainfall was at least 0.1 were used. Altogether 922 such events occurred. The scatter plot does not show this number because the gauge rainfall are in steps of 0.2 mm. It does show that no real structure exists and that significant rainfall (>2.0 mm/scan) occurs without the pixel attaining a classification. However the 7 out of 922 incidents are insignificant in number. Considering figure 5.7.1 it is fairly safe to assume that with a SSS=0 classification only very light rain is possible from, probably stratiform, cloud/ rain structures.

In figure 5.7.2 a scatter plot CAPPI rain against gauge rainfall for SSS=1 is displayed. Only scans when CAPPI rain was 0.1 mm or more at a pixel were considered. In this case we found a total number of 1614 incidents. Again the absence of structure is disappointing. It is interesting to note that the maximum CAPPI rainfall for a SSS=1 classification remained below 2 mm/scan and with the vast majority below 1 mm/scan. Rain gauge rainfall maximum of 4 mm/scan occurred but rainfall figures generally stayed less than 2 mm/scan. A large number of events occurred when no rainfall was recorded at rain gauge 10 but with CAPPI derived rainfall at pixel 10 indicating significant rainfall. It should be remembered that the rain gauge covers an insignificant area of the 1x1 km radar pixel. The large number of events when CAPPI rainfall between 0.5 and 1.5 mm/scan with rain gauge rainfall less than 0.5mm indicates that the CAPPI rainfall over estimates rainfall for lower rainfall rates. A slightly larger threshold could be introduced.

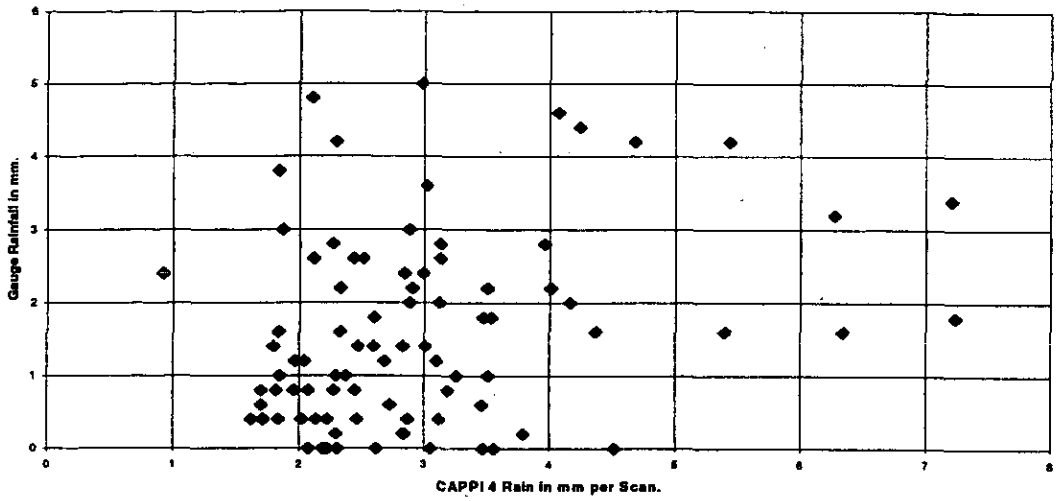

Figure 5.7.3: Scatter plot CAPPI and gauge rainfall at pixel 10 for class SSS = 4.

When figure 5.7.3 is considered for SSS=4 some structure appears. All in all 87 events happened with CAPPI rain at least 0.1 mm/scan and SSS=4. In this case we are dealing with a Moderate Base structure. Overestimation by the CAPPI rainfall is still evident but it is clear from the scatter plot that a SSS=4 classification indicate significant rainfall. Considering that there are some 15 scan intervals per hour, even the lower CAPPI rain rates point to 30 to 45mm/hr.

For higher SS classifications the numbers drop significantly. Table 5.7.2 lists the number of incidents at pixel 10 as well as CAPPI and rain gauge figures.

Table 5.7.2: Number of SSS events at pixel 10 with extreme CAPPI rainfall points.

SSS	Number	CAPPI	Rain gauge	CAPPI	Rain gauge
2 WV	16	2.80	6.40	0.32	5.00
3 WT	22	0.36	1.20	0.39	0.60
5 MV	1	1.92	1.20		
6 MT	2	1.56	0.00	0.36	0.00
7 SB	5	9.50	1.00	0.33	5.40
8 SV	1	1.01	3.20		
9 ST	1	9.80	1.60		

With moderate and severe structures, especially volume and top it seems heavy precipitation is probable, but not necessarily in the same scan interval or at the same location. Analysis of these

structures considering the complexity introduced if different location and later scan intervals are considered was not attempted.

5.8 CASE STUDIES AT RADAR PIXEL AND RAIN GAUGE RESOLUTION

Radar- and gauge rainfall intercomparisons at individual gauge resolution allows the introduction of the Storm Severity Structure data. It also allows use of the rainfall rates as determined from the maximum dBz value in the CAPPI matrix above the pixel. For the analysis 32 576 MRL-5 volume scans in '**mdv**' format were available. During the three seasons there were 123 days with rain recorded over the network. The MRL-5 radar completes 15 volume scans per hour. For the 123 rain days a total of 15 x 24 x 123 volume scans are possible. A total of 32 576 volume scans in **mdv** format, or approximately 50% were available for analysis.

Each of the 32 576 scans covering the entire radar coverage were reduced to 20 radar pixels over the network depicted by figure 3.1. A total of 32 576 x 20 data points were available for analysis. It was impossible to do a radar- gauge rainfall intercomparison at all of these points. The approach taken in the case studies was to select one or more rainfall station/s, which had continuous or reliable data for the period under consideration. In Chapter 3 the rainfall gauge data are reviewed while full details on the gauge rainfall are available in Appendix A.

A complication which exists is the fact that the gauge data are all recorded in South African Standard Time (SAST) while the majority of the "**mdv**" files are in Universal Time (UT). However some "**mdv**" files were only available in SAST due to computer programme complications at the NPRP. The inconsistency in the recording time standard between gauge and **mdv** format radar data was one of the major complications in the analysis of the data. All the data were reworked into UT. This process can be complicated, as the dates needed to be adjusted for all times between 24h00 and 02h00 SAST. Care must also be taken at the beginning of a new month. All the radar CAPPI data are in scan intervals and the software developed by Stuart (1998) records beginning, centroid and end dates and times for each scan. The rainfall gauge data originating from the locally developed "event data logger" records the date and event time of each "tip" of 0.2mm. Computation of a proper CAPPI rainfall and gauge rainfall record, per scan interval, requires careful programming.

5.8.1 Case Study 1. 1998-01-01 to 1998-01-02

Using the displace variate averaging system of Mittermaier et al (1997) the CAPPI rainfall was calculated over the RADARAIN network for all the available **mdv** formatted radar files. Because **mdv** formatted files were only available for some 50% of the rain days, the team decided to use new dataset for case studies. This was done to describe how the network fared as a whole in section 5.5. Here we illustrate how the system did performed at the individual pixel/rain gauge level. This is important as all calculations should start at this level when computing areal or catchment rainfall. It is also a stated objective of this project to investigate the radar rainfall relationship down to cloud or storm scale.

One of the most significant rainfall events developed on 1998/01/01 and lasted well into the next day. Two pixel/rain gauge combinations were selected namely 11 and 13. In figure 5.8.1 the radar CAPPI rainfall and the rain gauge rainfall are displayed for pixel/gauge 11. Figure 5.8.2 shows the same for pixel/gauge 13. On this day the classification indicated that general (G) and large clusters (CL) dominated for most of the day.

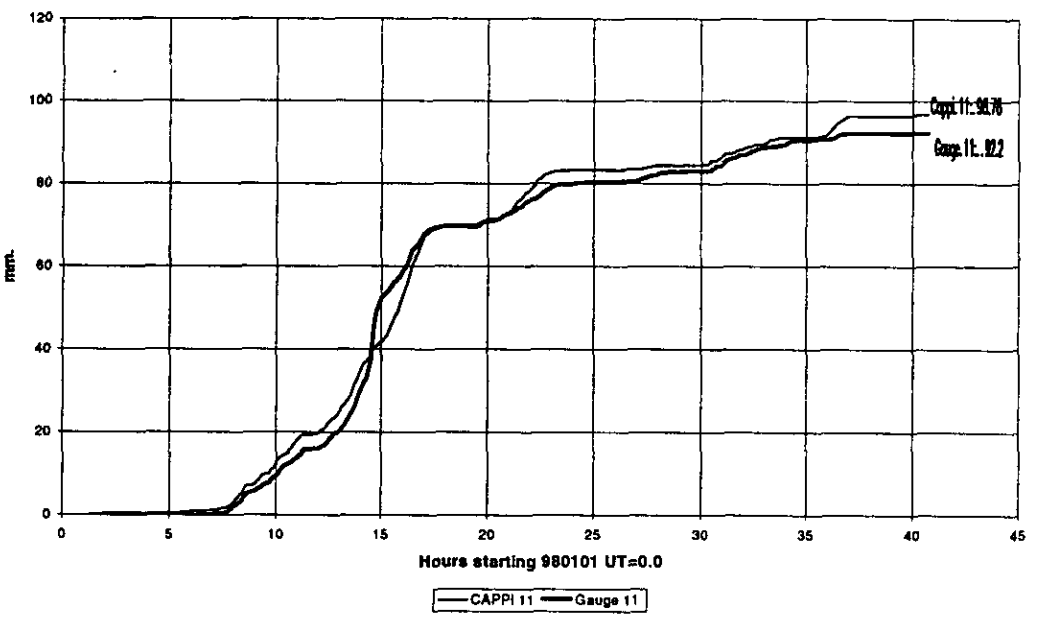

Figure 5.8.1: Accumulated CAPPI and Gauge rainfall at pixel/gauge 11 on 1998-01-01 and 1998-01-02.

In the case of pixel/gauge 11 (figure 5.8.1) the relationship is probably as good as it can get. In both figures it is noted that the rain rate between 12h00 and 15h00, as measured by the gauge, is somewhat steeper than that measured by the CAPPI pixel. Considering that convective elements are nearly always present in large long lasting storm structures one would expect these variations.

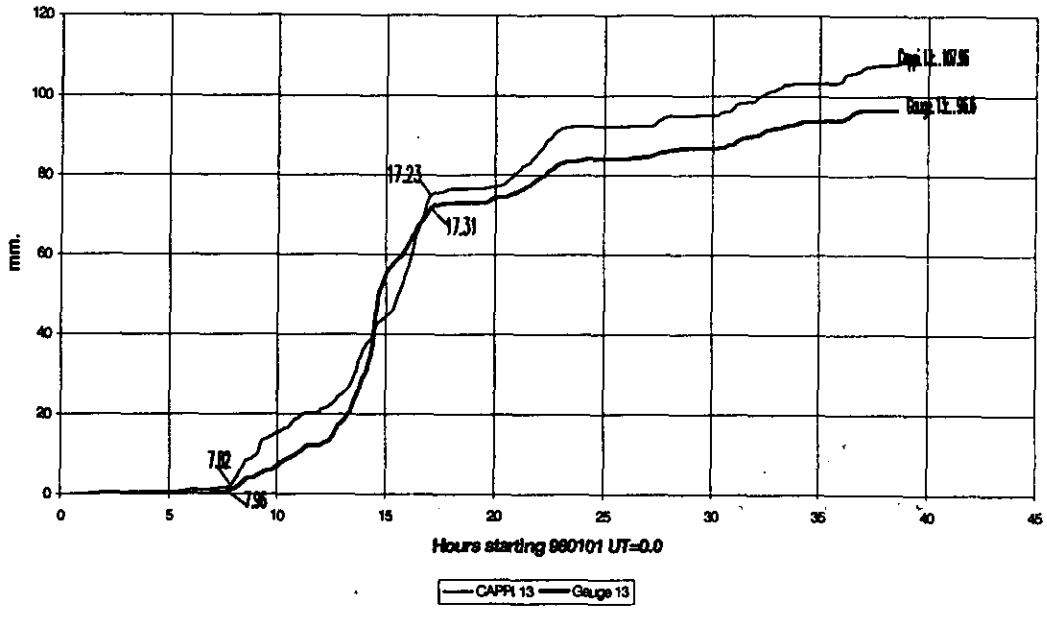

Figure 5.8.2: As figure 5.8.1 but for pixel/gauge 13.

In the case of pixel gauge 11 the CAPPI total for this event was 96.76 and gauge 11 recorded 92.2 which gives a CAPPI/gauge ratio of 1.05. At pixel 13 (figure 5.8.2) the totals were 107.96 and 96.6 respectively which leads to a ratio of 1.12. This is very good. Considering that the rainfall that occurred on the first two days of January 1998 is precisely the type of system that, provided the catchment is saturated and the rivers flowing, may result in extensive flooding. To measure at this accuracy on catchment scale is but to dream of. Unfortunately things don't always go that well.

5.8.2. Case Study 2: 1998-03-08

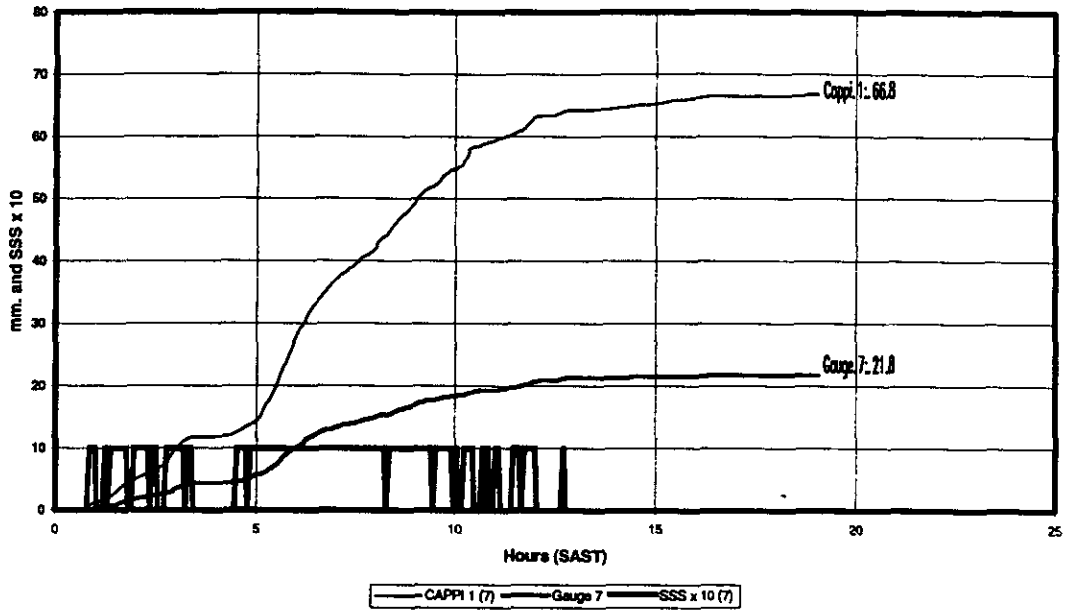

Figure 5.8.3: Accumulated CAPPI and Gauge Rainfall and SSS x 10 values, at pixel/gauge 7 on 1998-03-08. The CAPPI's are at 4 km ASL.

In complete contrast to Case Study 1, on 8 March 1998 the CAPPI derived rainfall failed, overestimating the gauge rainfall. In figure 5.8.3 (pixel and gauge 7) the CAPPI (4 km ASL) accumulated rainfall is 66.8 mm while at gauge 7 a total of 21.8 was observed. The SSS classification per scan interval (x10) is also plotted in figure 5.8.3. During the period approximately 01h00 to 13h00 SAST on this day the storm structures never exceeded SSS=1. The cloud systems producing the rainfall were Weak Base structures, especially during the period 05h00 to 12h00 SAST when the CAPPI rainfall reported steady uniform rain. Ratio between CAPPI and gauge rainfall was 3.06. A 300% overestimation is unacceptable. The SSS classification does not help to explain this anomaly.

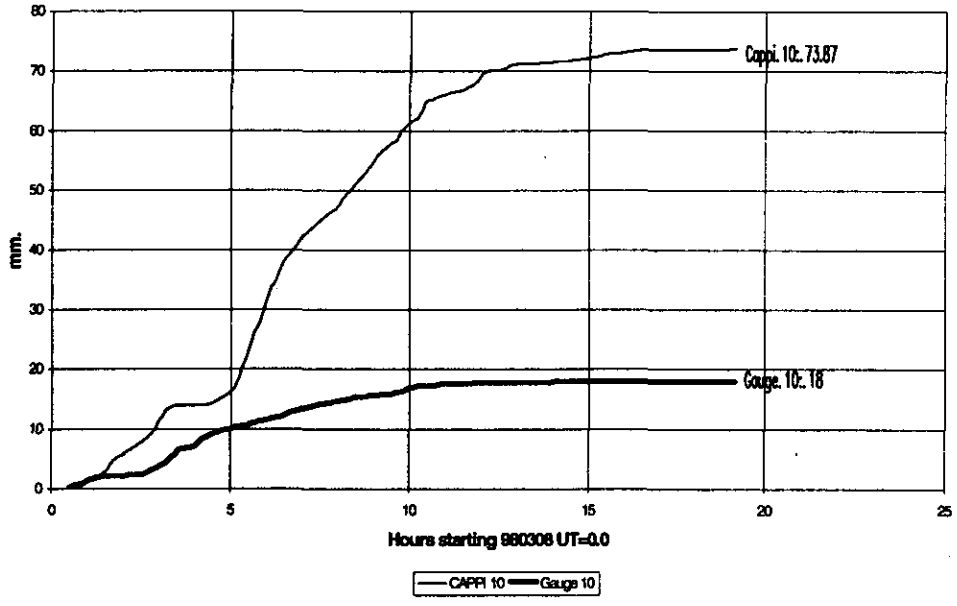

Figure 5.8.4: As figure 5.8.3 but for pixel/gauge 10.

Figure 5.8.4 does the same for CAPPI and gauge data at pixel 10. No real difference exists between these figures except that the accumulated CAPPI totals (73.87) at pixel 10 are somewhat higher but at the same time the accumulated gauge rainfall at gauge 10 is lower (18.0) than the figure for gauge 7. In this case the ratio at 4.1 is even higher. An interesting feature of figure 5.8.4 is the short period approximately 03h00 to 04h00 SAST when gauge 10 reported steady rain while the CAPPI's at pixels 7 and 10 as well as the gauge at 7 did not report significant precipitation.

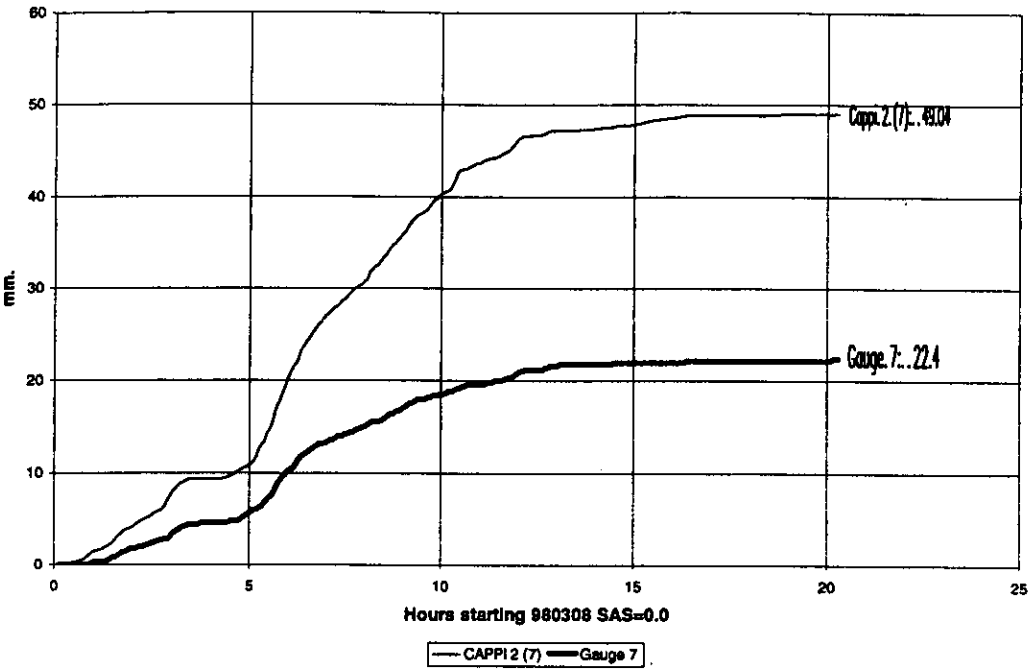

Figure 5.8.5: As figure 5.8.3 but CAPPI level at 5 km ASL and at pixel/gauge 7.

The SSS classification provided little help to explain this problem and the next most likely candidate is the bright band. The CAPPI rainfall for this day was recalculated but in this case for the next higher CAPPI level (5 km ASL). Figure 5.8.5 details the result for pixel/gauge 7. Clearly the CAPPI derived rainfall rates are lower. CAPPI accumulated totals are now at 49.04 mm. These are still far too high with a ratio of 2.19. It appears a clear case of a significant bright band as described by Mittermaier in Chapter 4. Unfortunately Mittermaier's procedure to eliminate the bright band was unavailable. This day was an extreme case and deserves further research. However it appears that on days with steady rain when the SSS classification indicates Weak Base structures and no others present which point to convection, care should be taken to filter the bright band.

5.8.3 Case Study 3: 1996-02-11

On 11 February 1996 the situation was the complete reverse of the second Case Study (using pixel/gauge 9) as is depicted by figure 5.8.6. Now the CAPPI's seriously underestimated the gauge rainfall. A total of 103.8 mm. was recorded at gauge 9 on this day all within 18 hours. Considerable flooding also occurred in the Vaal- and Wilge rivers following these rains. Yet contrary to most of the data investigated, the CAPPI's underestimated by a ratio of 0.64. CAPPI rainfall accumulations at 4 km ASL were 66.5 mm while the figure for CAPPI level 5 km ASL

was considerably lower at 44.7 mm. In complete contrast to the so called bright band case (Case Study 2) it turns out that the higher CAPPI level rainfall is even worse. The rainfall rate and scan accumulations using the maximum dBz value in the CAPPI column was also computed. It follows an identical line with the 4 km ASL CAPPI generated rainfall and totals to 67.3 mm. Obviously the maximum reflectivities all originate near or at the 4 km ASL level. The SSS classification is also plotted in figure 5.8.6. As with the other Case Studies Weak Base structures are the only ones present.

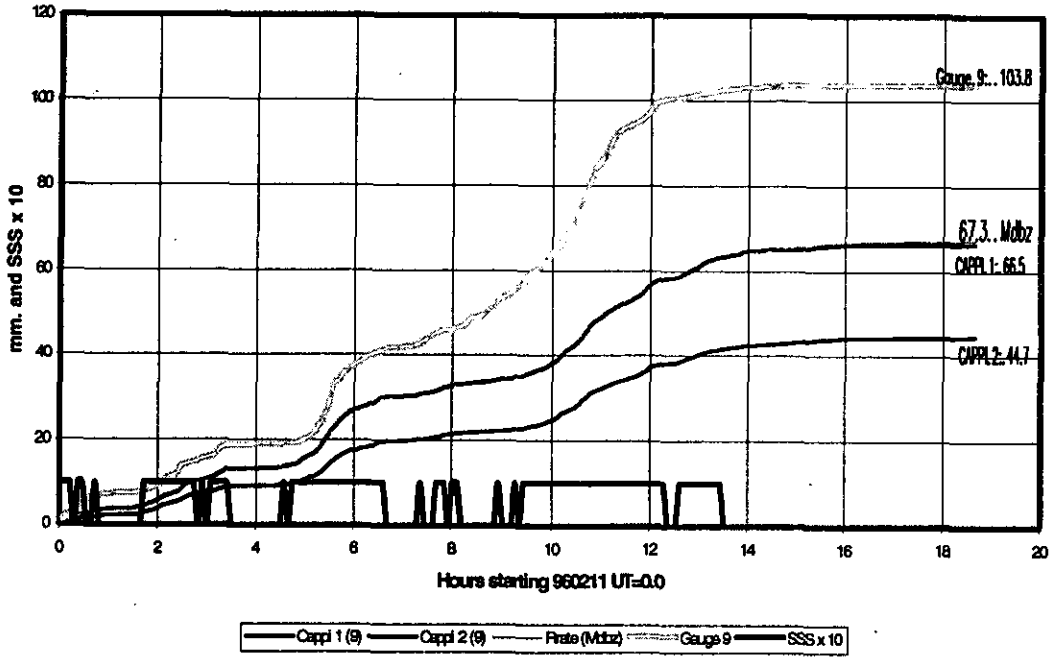

Figure 5.8.6: Accumulated CAPPI and gauge rainfall at pixel/guge 9 on 1996-02-11. CAPPI's at 4 and 5 km ASL as well as the rainfall from the maximum dBz reflectivites are shown.

It would seem to be an almost inverse bright band situation. It was noted (Terblanche, 1996) that when large spheres exist and the sphere diameter (D) is such that $D > 0.8\lambda$ with λ the wavelength a decrease in reflectivity due to Mie scattering occurs during the onset of melting. This is the only explanation we can think of for what happened on this day. BPRP staff are confident that the radar calibration was stable and that no procedural or computational modifications occurred.

5.8.4 Case Study 4: 1997-03-08

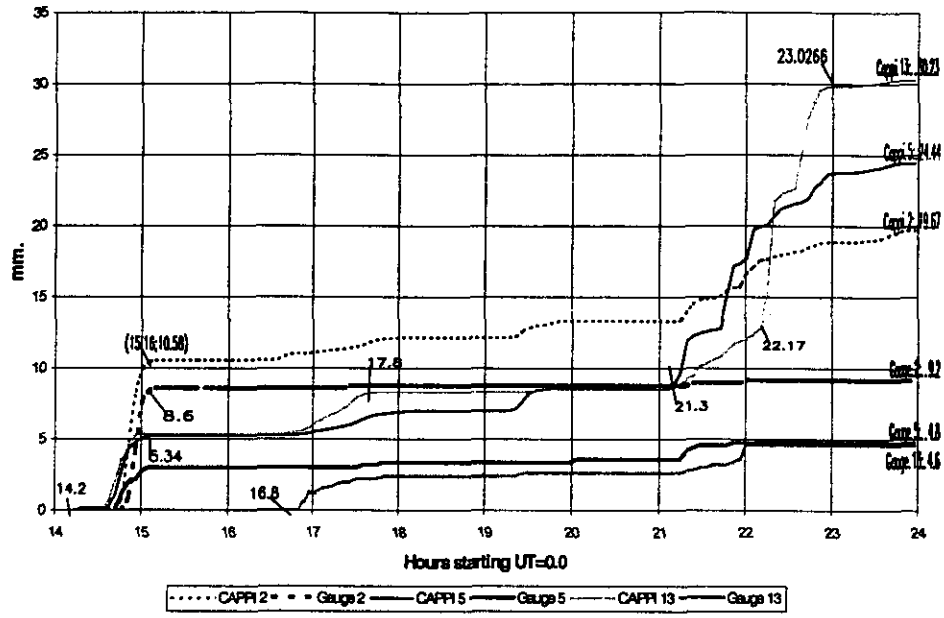

Figure 5.8.7: Accumulated CAPPI and Gauge rainfall at pixels/gauges 2, 5 and 13 on 1997-03-08. The values are either time or rainfall.

This day was classified as a day with predominantly isolated convective systems over the network. Figure 5.8.7 shows the sudden onset of intense showers over pixels 2, 5 and 13 at about 143h0 UT. The rain gauges at stations 2 and 5 recorded the sudden onset of the showers at this time, while the rain gauge at 13 missed the shower altogether. Possibly the showers moved away from the rain gauges but remained within the radar pixel for a scan interval or so with the result that the CAPPI derived rainfall exceeds the gauge rainfall. During the 14h30 shower at pixel/gauge 2 the shower must have been centered close to the gauge as the CAPPI 2 and gauge 2 totals were within 2 mm. Gauge 13 and CAPPI 13 shows good correspondence with the shower which started at about 17h00 UT. Both CAPPI's 13 and 2 recorded an intense shower which had started about 2130 UT, lasting about 30 minutes. Considering the accumulations it is obvious that the totals computed from the CAPPI's overestimated with ratio's between 2.3 (2) and 6.57 (13). In this case it is clear from the rain rates and the onset and stop times of the showers that the CAPPI data may in fact do much better than the rain gauges.

Isolated showers over a catchment, even if they happen to be quite intense, producing some 50 mm/day are of minimal concern for hydrological purposes. It is however satisfying if it can be presumed that the radar does better than the rain gauge.

5.8.5 *Case Study 5: 1996-01-24 to 1998-01-25*

The rainfall systems responsible for the rain were classified as isolated. Figure 5.8.8 plots the rainfall for the period from about 23h30 UT on 1996-01-24 to 20h00 on 1996-01-25 at pixel/gauge 2. Intense showers occurred between 23h34 and 23h54 on 1996-01-24 as well as between 12h13 and 13h38 on 1996-01-25. In the first case the rain rates are approximately 22 mm/hr for both the CAPPI and Gauge. For the second interval, 19 mm/hr for gauge 2 and 22 mm/hr for the CAPPI rainfall at pixel 2.

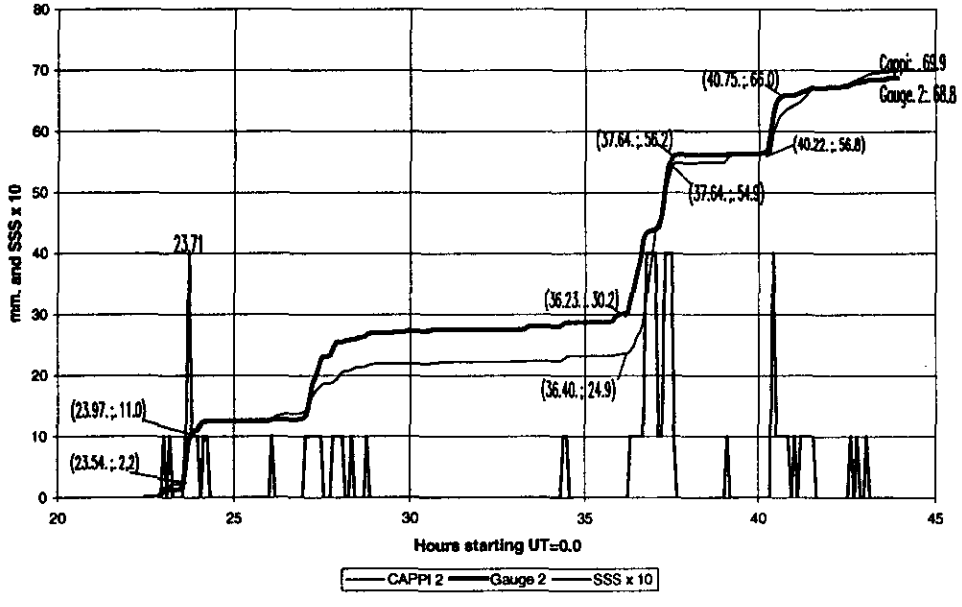

Figure 5.8.8: Accumulated CAPPI and gauge rainfall at pixel/ gauge 2 for the period 22h30 on 1996-01-24 to 23h00 on 1996-01-25.

A third intense shower occurred between 16h13 and 16h45 producing a rain rate at gauge 2 of approximately 17 mm/hr. Except for the first, approximately 30 minutes of the shower starting at 12h13, all the intense showers were accompanied by a SSS=4 (Moderate Base) storm structure. Nearly all of the other showers depicted by figure 5.8.8 were associated with SSS=1 (Weak Base) storm structures. The accumulated CAPPI and gauge rainfall was 69.9 and 68.8 mm respectively. This ratio (CAPPI/Gauge) of 0.984 is exceptional.

The plots for pixel/gauge 10 and 19 captured the same showers (figures not shown). Gauge (pixel) 10 had accumulated totals of 84.4 and (69.6) producing a CAPPI/gauge ratio of 0.824 while at gauge (pixel) 19 the totals were 51.4 and 47.5 respectively resulting in a CAPPI/gauge ratio of 0.924. The accumulated rainfall rates produced at these three pixels shows that the CAPPI and gauge data compare well for isolated storm systems when the rainfall rates are appreciable and shows that CAPPI derived rainfall for isolated but active convective systems can be reliable. The fact that the more intense showers were associated with a MB (SSS=4) classification indicates that this SSS classification in association with an area classification of "ISOL", produce reliable CAPPI rainfall.

CHAPTER 6: CONCLUSIONS

Conclusions are subdivided into general conclusions where the achievement of the project objectives are discussed, and a section where a system for radar derived rainfall is proposed.

6.1 GENERAL CONCLUSIONS

The first objective of RADARAIN was:

- *To develop greater understanding of the space-time characteristics of convective precipitation over the highveld regions of South Africa using the MRL-5 10/3 cm and other radar data.*

Considerable understanding of the space-time characteristics of convective precipitation over the northeastern Free State has been gained. The potential of the S band MRL-5 radar to measure rainfall down to pixel scale has been adequately demonstrated. Under conditions when a bright band or large melting spheres are absent the accuracy of the S band CAPPI data was surprisingly good. The case studies provided ample examples where CAPPI/gauge ratios were as good as between 90 and 110%.

The best results were obtained under conditions of general rain or when large well-organised cloud clusters were present. It is precisely these systems which produce hydrologically significant rainfall. Results indicate that rainfall from these systems can be measured far more accurately than is possible with a conventional gauge network. Real time reporting gauge networks on catchment scale do not exist in South Africa. However the MRL-5 S band radar data used in this study can produce better rainfall estimates over a large area in near real time.

Considering the results for smaller scale convective systems normally classified as isolated systems, it was satisfying to note that the CAPPI data faired well when the convective rainfall reached rates in the order of 10 to 20 mm/hour. For isolated systems producing lower rain rates the authors postulate that the CAPPI data still have the potential to produce far better rainfall estimates than a sparse rainfall network.

On time scales extending to a season the comparison between the CAPPI derived rainfall totals and the gauge data shows that radar does have the potential to provide accurate seasonal rainfall distribution. These results should interest managers in the agricultural sectors and can play a vital role in drought management. Daily area rainfall figures from the CAPPI data are generally good. The fact that these can be produced within a short period after cut-off time is a significant advantage over any other system current in South Africa.

The introduction of the SSS method to provide information on the vertical profile of precipitating systems helped considerably to understand some of the rainfall characteristics as viewed by the radar. In the case studies at pixel resolution the use of the SSS classification showed that rainfall is generally associated with lower level structures. The authors failed to find any significant links between higher level structures and CAPPI (4km ASL) rainfall. The SSS classification may well be useful to identify the presence of the bright band when used in conjunction with the CAPPI matrix.

The second objective of the RADARAIN project was:

- *Develop and apply measuring techniques based on 10 and 3 cm radar data in order to measure storm rainfall accurately at scales varying from cloud scale to catchment scale.*

Results from the large number of case studies and analysis of the data supported the use of the conventional Marshall-Palmer Z-R relationship. The classification of rainfall producing systems over the network have not provided a strong enough case to modify the accepted M-P Z-R relationship, even if the statistics seem to suggest this. However a classification may be useful to assign a reliability to the CAPPI derived rainfall. Introduction of a classification class for stratiform rainfall fields in conjunction with the SSS Weak or Moderate Base structure may provide early warning of the bright band.

Results from the case studies indicate that radar derived rainfall should start at the pixel level. Averaging to produce catchment scale representative rainfall figures should start at this level.

The third RADARAIN objective was:

- *Refine the inter-calibration links between S-, X- and C- band radar's for quantitative rainfall measurement. (Use of the attenuation of X-band data for cloud and rainfall research).*

The commissioning, calibration and other operational constraints relative to the MRL-5 radar made the operation of the MRL-5 at X band wavelengths, during the RADARAIN project impossible. Research to deal with this objective therefore never got off the ground.

The final objective was:

- *To develop the means of communicating experimental radar/satellite based rainfall data to potential users, with a view to satisfying hydrological requirements.*

The authors of this report did not attempt communicating radar based rainfall. The Bethlehem Precipitation Research Project (BPRP) does this on a regular basis and has several clients who make use of the data. Experience and feedback from clients will soon see the development of effective radar rainfall communication. What is needed is for users to validate the results not so much against conventional rainfall data but rather in terms of its application and usefulness.

This project played a critical role in bringing more order to the vast MRL-5 radar data base. Furthermore, the seasonal accumulations give a practical reference (base line) on the effectiveness of radar to cover a large part of the seasonal rainfall. Projects of this nature provide an independent assessment on data quality – the value of which should not be underestimated.

6.2 RECOMMENDATIONS

Based on the experience gained during RADARAIN we feel free to make the following recommendations with respect to the operation of an S band radar for hydrological operations.

STAFF MATTERS

6.2.1 It is of absolute fundamental importance to have an experienced professional meteorologist to provide overall project leadership, give direction to the research and provide liaison with clients as well as with the authorities.

6.2.2 The project leader must be assisted by competent radar technicians in order to ensure that the radar(s) stay operational.

6.2.3 It is of fundamental importance to have a data archival and retrieval system operating in near real time. This system must be manned by dedicated computer experts. The permutations of data manipulations and computation are virtually unlimited.

6.2.4 A research and support team conducting ongoing research to improve the radar rainfall estimation and develop other products useful to the country's infrastructure is a vital necessity to ensure continuous quality of the products. An end research user remains the best guarantee for quality.

PROCEDURES TO DERIVE RADAR RAINFALL

6.2.5 Current procedures followed with the processing of MRL-5 data in terms of calibration, computation of CAPPI's using the displace variate averaging process are probably amongst the best available anywhere.

6.2.6 Computing rainfall from CAPPI data using the Marshall Palmer Z-R relationship for active convective systems over the northeastern Free State is satisfactory. However the research on the classification of rainfall systems could be adapted and computerised for active convective systems in order to provide error bars to the computed CAPPI rainfall.

6.2.7 For rainfall systems classified as isolated convective the Storm Severity Structure (SSS) system developed by Visser (1999) should be used with CAPPI derived rainfall rates to validate intense showers.

6.2.8 When it comes to systems classified as uniform stratiform (often classified as general rain) the SSS classification should be used to identify pixels with weak bottom (WB SSS=1) structure. If the maximum dBz value in the CAPPI matrix also occurs near the lowest CAPPI level (4km ASL) then the algorithm developed by Mittermaier (1999) should be used to test for the "bright band".

6.2.9 It is recommended that the "bright band" algorithm of Mittermaier be tested thoroughly.

6.2.10 No computer-based processes using conventional radar derived parameters were found which could explain the anomalously low CAPPI rainfall of Case Study 3 (960211). It is recommended that a small rain gauge network, producing real time rainfall rates, be operated at a suitable distance from the radar. Data from this network should be used to identify and research similar anomalies.

REFERENCES

Alexander W J R, 1990.
Flood Hydrology for Southern Africa. *The South African National Committee on Large Dams, Pretoria.*

Atlas D, 1964.
Advances in radar meteorology. *Advances in Geophysics, Vol 10, Academic Press, New York, USA.*

Atlas D, 1990.
Radar in Meteorology. *Battan Memorial and 40th Anniversary: Radar Meteorological Conference, AMS, Boston, USA.*

Battan L J, 1973.
Radar observation of the atmosphere. *The University of Chicago Press, Chicago, USA.*

Breit G and Tuve M A, 1926.
A test for the existence of the conducting layer. *Phys. Rev., 28, 554-575.*

Carte A E and Held G., 1978.
Variability of hailstorms on the South African plateau. *J.Appl.Met., 17, 365-373.*

Chandrasekar V., Bringi V N., Gray G R and Keeler R J, 1989.
Efficient Differential Reflectivity Processing using Logarithmic Receivers. *J. Atmos Ocean Tech. 6, 4, 663-670.*

Court A P, 1979.
a: The contribution of general rain , scattered rain and isolated rain in the Bethlehem area. *Progress Report 5, Bethlehem Weather Modification Experiment. Weather Bureau. 27pp.*
b: Rainfall characteristics of classification systems used by the BEWMEX Project. *Progress Report 14. Bethlehem Weather Modification Experiment. Weather Bureau, Pretoria. 19pp.*

Dixon M and Wiener G, 1993.
TITAN: Thunderstorm Identification, Tracking, Analysis and Nowcasting- a Radar-based Methodology. *J. Atmos. Ocean Tech. 10(6), 785-797.*

Doviak R J and Zrnic D S, 1984.
Doppler Radar and Weather Observations. *Academic Press, 458 pp.*

Fleischer S L M., 1980.
Radar observations in the BEMEX area. *BEWMEX Progress Report 21, 47.*

Gagin A., Rosenfeld D. and Nozice H, 1986.
Report on the analyses of convective rain cells in the region of Bethlehem, R.S.A as a basis for a rainfall enhancement experiment.
Report to the Water Research Commission, Pretoria.

Harrison M S J, 1974.
An Introduction to the Bethlehem Weather Modification Experiment. Part 1. *Technical Paper No. 1, Weather Bureau, Pretoria.*

Held G., 1978.
The probability of hail in relation to radar echo heights on the South African Highveld. *J.Appl.Met., 17, 755-762.*

Held G., 1982.
Comparison of radar observations of a devastating hailstorm and a cloudburst at Jan Smuts Airport. *Cloud Dynamics eds. E M. Agee and T Asai, D Reidel Publ. Co. Dordrecht.*

Held G and Carte A E., 1973.
Thunderstorms in 1971/72. *CSIR Research Report 322, 1-77.*

Houze R.A. Jr., 1997.
Stratiform precipitation in regions of convection : A meteorological paradox ??? *Bull. Amer. Met. Soc.*, 78(10), 2179-2196.

Krauss T W, Bruintjes R T and Verlinde J., 1987.
Microphysical and radar observations of seeded and non-seeded continental cumulus clouds. *J.Climate Appl. Meteor. 26,585-606.*

Kroese N J, Mittermaier M P and Terblanche D E, 1997.
The flood event during February 1996 in the Vaal River catchment: A radar, rainfall and stream flow study. *5th International Conference on Southern Hemisphere Meteorology and Oceanography. Preprints, Pretoria, SA. P13.*

Langleben M P and Gunn K L S, 1952.
Scattering and absorption of microwaves by a melting ice sphere. *Sci. Ret. MR-5., Montreal, Stormy Weather Group. McGill Univ.*

Marshall J S., Lagille R C and Palmer W Mc K, 1947.
Measurement of rainfall by radar. *J. Meteor. 4, 186-192.*

Marshall J S and Palmer W Mc K, 1948.
The distribution of raindrops with size. *J. Meteorol., 5, 165-166.*

Mather G K and Terblanche D E., 1993.
The National Precipitation Research Programme. Final Report. 1990-1992. *WRC Report, Pretoria.*

Mather G K., Terblanche D E and Steffens F E, 1997a.
The National Precipitation Research Programme, Final Report: 1993-1996. *WRC Report No. 726/1/97*

Mather G K, Terblanche D E, Steffens F E and Fletcher L, 1997b.
Results of the South African Cloud-Seeding Experiments Using Hygroscopic Flares. *J. Appl. Meteor.*, **36**, 1433-1447.

Mie G, 1908.
Contribution to the optics of suspended media, Specifically colloidal metal suspensions. *Ann. Phys. 25, 377-445.*

Mittermaier M P, 1997.
Bright-band studies in South Africa. *Preprints 28th Radar Meteorological Conference, AMS, Austin, USA.*

Mittermaier M.P., 1999.
Characteristics of the radar vertical reflectivity profile. *Unpublished MscEng dissertation.* University of Natal, Durban.

Mittermaier M P and Terblanche D E, 1997.
Converting weather radar data to Cartesian space: A new approach using DISPLACE averaging. *Water SA, 23(1), 45-50.*

Mittermaier M P, Terblanche D E, Hiscutt F O, Dicks D J and de Waal K P J, 1997.
A real-time data-processing algorithm and communication system implemented on an upgraded Water Research Commission MRL-5 radar. *5th International Conference on Southern Hemisphere Meteorology and Oceanography Preprints, Pretoria, SA. P15.*

Rayleigh Lord, 1871.
On the scattering of light by small particles. *Phil. Mag. 41, 447-452*

Rosenfeld D., 1988.
Evaporation of rain falling from convective clouds as derived from radar measurements. *J.Applied Meteor., 27, 209-215.*

Rosenfeld D and Gagin A., 1989.
Factors governing the total rainfall yield from continental convective clouds. *J. Appl. Meteor., 28, 1015-1030.*

Ryde J W., 1941.
Echo intensities and attenuation due to clouds, rain, hail sand and dust storms. *Rep. No. 7831, General Electric Laboratory, Wembley, England, 48 pp.*

Seed A, 1998.
The impact of radar and rain-gauge sampling errors when calibrating a weather radar. *Meteorl. Appl. 3, 43-52.*

Skolnik M I, ed., 1970.
Radar Handbook.*McGraw-Hill, New York.*

Skolnik M I, 1981.
Introduction to radar systems. *International Student Addition, McGraw-Hill, Johannesburg, RSA.*

Smith P L, 1986.
On the sensitivity of weather radars. *J. Atmos. Oceanic. Technol.*, 3, 704-713.

Smith P L and Joss J, 1997.
Use of fixed exponent in "adjustable" Z-R relationships. *Preprints 28th Radar Meteorological Conference, AMS, Austin, USA.*

Steyn P C L and Bruintjes R. T., 1990.
Convective cloud characteristics for the Bethlehem area. *Water SA, 16-2, 115-118.*

Terblanche D E, 1995.
Simulating Linear, Logarithmic and Quadratic Responses from a Radar's Logarithmic Receiver by a Simple Digital Signal Processing Method. *Preprints, 27th Conf. On Radar Meteorology, AMS, Vail, 769-770.*

Terblanche D E, 1996.
A Simple Digital Signal Processing Method to Simulate Linear and Quadratic Responses from a Radar's Logarithmic Receiver. *J. Atmos. Oceanic. Technol.*, 10, 785-797.

Terblanche D E, 1996.
Digital signal processing of data from conventional weather radar: The DISPLACE method. *PhD Thesis, Faculty of Engineering, University of Pretoria, 86pp.*

Terblanche D E, 1997.
Radar Meteorology in South Africa. *Preprints 28th Radar Meteorological Conference, AMS, Austin, USA.*

Terblanche D E, Pienaar H G and de Waal K P J, 1993.
Radar/rainfall studies over the north-eastern Free State. *Sixth South African Hydrological Symposium, Pietermaritzburg, 87-94.*

Terblanche D E, Hiscutt F O and Dicks D J, 1994.
The upgrading and performance testing of the Bethlehem weather radar. *S.A. J. Sci.*, **90**, 588-596.

Triegaardt D O, van Heerden J and Steyn P C L, 1991.
Anomalous Precipitation and Floods during February 1988. *Technical Paper No. 23, Weather Bureau, Pretoria.*

Visser P J M, 1999.
The use of Volumetric Scanned Weather Radar Reflectivities for the identification of Convective Storm Characteristics. *Dissertation for MSc degree.*

Weather Bureau, 1991.
Caelum: A history of notable weather events in South Africa; 1500-1990. *The Weather Bureau, Department of Environmental Affairs, Pretoria.*

Weisman M L and Klemp J B, 1986.
Characteristics of isolated convective storms. *Mesoscale Meteorology and Forecasting. American Meteorological Society. Boston. 331-358.*

APPENDIX A: RAINFALL AND CAPPI DATA

(Compiled by R Burger)

The dataset is available on CD at the NPRP or at Department of Earth Sciences (Meteorology), UP. It contains files with rain gauge and Radar CAPPI data.

A. RADAR DATA

A1. GENERAL

- The MRL-5 S-band radar data was used to obtain the rainfall rates (m/hr) at each pixel.
- Rain rates were calculated using the Marshall-Palmer relationship [$Z=200*(R^{1.6})$]
- A minimum cut off threshold of 18dBz was used.
- A maximum cut off threshold of 55dBz was used, higher values considered as hail.
- During the first two seasons, (95-96 & 96-97), CAPPI's were calculated using the method of Seed (1996). CAPPI's for 2km and 3km are listed.
- During the last season, (97-98), Displace Variate Averaging CAPPI's was calculated at 4km ASL.
- Rain rates are rounded off to the nearest integer.
- The scan times for the first two seasons are rounded off to the nearest minute.

A2. FILE FORMAT

2.1 File location/names files are located at:

/radardat/ssN (N = 1,2,3 (denotes the season))

- first season ['95-'96]

TyymmddC.PRN

yy = year

mm = month

dd = day

C = CAPPI LEVEL

- second season ['96-'97]

SyymmddC.PRN

yy = year

mm = month

dd = day

C = CAPPI LEVEL

- third season ['97-'98]

Ryymmdd.PRN

yy = year

mm = month

dd = day

A2.2 File content

6-DEC-1995 14:04:00 00 00 00 00 01 00 02 00 00 00 00 00 00 00 00 00 00 00 01 00

Can be intepreted as:

date-95/12/06

time-14:04:00

rain rate (mm/h) of the 20 pixels covering the

area (each one has a corresponding rain gauge)

B. GAUGE DATA: ALL TIMES ARE IN SAST

B1. GENERAL

- The rain gauge network consists of 20 rain gauge positions. Of these 15 were active during the project.
- Every gauge corresponds to a specific radar pixel.
- The tipping bucket rain gauges were all calibrated to tip for every 0.2mm rain. For each tip a time stamp is recorded on the logger.
- Time corrections were applied to the raw data. During data collection the gauge time and the real time was recorded. A linear correction was applied to the raw data logger times.
- When two consecutive time stamps are separated by less than 2 seconds a double tap is presumed. Double taps were removed from the data.

B2. THE TIME-CORRECTED RAIN GAUGE DATA

B3.1 File name

Files are located at:

Gaugedat/ssN/L0XX

N = 1/2/3 (denotes the season)

XX = gauge number (1-20)

B.3.2 File content: L002 95 10 05 15 38 46 0.200 271

L002 = Gauge number

date = 95/10/05

time = 15:38:46

measured rainfall = 0.2mm

day of the year = 271

C. ANALYSED GAUGE DATA

C1. GENERAL

Considerable analysis was performed on the rain gauge data. Process and file description follow:

C2. yymmdd.tot

This files contains the daily gauge rainfall total. It corresponds with the **mdv** formatted radar file. The total rainfall is an accumulation starting and stopping at the first and last radar file scan times.

It has the following format:

20 1.6 (20 = number of the rain gauge; 1.6 = total rainfall per day)

C3. AyymmddC.AVE

C=level of CAPPI (if applicable)

This file contains the average (per scan) of the guage and the radar over the area covered by the gauges. Only gauges which measured rainfall (> 0.0mm in the yymmdd.tot) and the corresponding radar pixels were used.

It has the following format: 06-012-1998 14:23:00 02 01

date = 6/12/98

centroid time = 14:23:00

02 = average rain rate of a gauge network

01 = average rain rate of radar network

C4. RGyymmdd

This file contains the total rain measured (mm) by the rainfall gauges during the radar scan interval.

It has the following format:

06-012-1998 14:23:00 0.0 0.0 0.0 0.0 0.0 0.0 0.0 0.0 0.0 0.0 0.0 0.0 0.0 0.0
0.0 0.0 0.0 0.0 0.0 0.0

date = 6/12/98

centroid time = 14:23:00

rainafall at the 20 gauge position

5. aveyymmddC => using the average gauge rain rate over area

frgyymmddC => using the CAPPI rain rates

comrateCAPC => the combined percentages of average rain rates for the entire season

C=level of CAPPI (if applicable)

These files contains the percentage of total rain rates which were measured in the different Classes detailed below.

The file has the following format: 50.5 14.23 16.13

interval [49mm/h - 52mm/h] (In steps of 3mm)

14.23 = % of the gauge rain rates happened in this interval

16.13 = % as above for the CAPPI rainfall

6. Gyymmdd

This file contains the rain rates in mm measured by the different gauges during the radar scan interval. It is the gauge equivalent of the radar cappi files (***.PRN).

The file has the following format:

6-DEC-1995 14:04:00 00 00 00 00 01 00 02 00 00 00 00 00 00 00 00 00 00 00 01 00

Can be interpreted as:

Date - 95/12/06

Centroid time in SAST - 14:04:00

The scan interval reduced to 4 minutes rain rate (mm/h) of the 20 gauges

APPENDIX B: Hourly Classification of Rainfall Systems over the RADARAIN Network.

Legend:
I : Isolated
C : Clusters
CL : Clusters Large
L : Line
G : General

Date	Time	Class	Comments
95/11/28	10:00	G	
	14:00	G	Weak general rain. Big cluster SW of network
	15:00	CL	
	16:00	CL	
	17:00	CL	
	18:00	CL	
	20:00	C	
95/12/14	10:00	I	
	11:00	I	
	12:00	I	
95/12/15	02-03:00	I	Band 30-35 dBz 40
	15:00	I	
	20:00	I	Very weak
95/12/16	13:00	G	Weak < 30 dBz. Cluster moving SE
	14:00	G	Weak, large cluster W section
	15:00	G	" "
	16:00	CL	Large area ± 45 dBz
	17:00	CL	
	18:00	I	Large clusters around
	19:00	CL	
	20:00	G	Embedded convection
	21:00	G (CL)	" "
	22:00	G (CL)	" "
	23:00	G	
	24:00	G	
95/12/17	00:02:26	G	
	01:00	G	
	02:00	G	Dissipating
	05-06:00	G	Moving from NW
	07-09:00	G	Embedded convection
	10:00	G	Weak
	11-16:00	G	Embedded convection
	17:00	G	" cluster moving east
	23:00	G	Weak redevelopment
	24:00	G	Embedded Convection
95/12/18	01:00	C	
	02:00	G	Embedded convection cells
	03:00	C	Fast moving clusters

	05-08:00	I	
	09-10:00	I	
	12-14:00	I	
	16-18:00	I	
	23:00	C	
	24:00	I	
95/12/19	02:00	C	
	03:00	L	
	09:00	I	
	20:00	G	Light rain band
	21:00	G	
	22:00	G	
	23:00	G	Clearing
95/12/22	07:00	I	
	08:00	I	
	10:00	I	
	11:00	G	Network lies between large clusters
	12:00	CL	
	13:00	CL	
	14:00	G	Network lies between clusters
	15-16:00	CL	General rain with large clusters > 50 dBz centre
95/12/24	13:00	G	Generally < 30 dBz
	14:00	C	*Storm splitting*
	15:00	C	
	16-18:00	I	
	20:00	G	Storm outflow leaving
95/12/25	14:00	I	Between large clusters
	15-16:00	I	
	20-21:00	I	
	22:00	C	
	23:00	I	
95/12/26	01:00	I	
	02:00	I	
	03:00	C	
	04:00	I	
	07:00	I	
	08:00	I	
	12:00	I	
	13:00	C	
	15:00	I	
	16:00	I	
96/01/25	00:00:56	C	
	01-02:00	C	Stratiform layer
	03:00	I	" "
	04:00	C	)
	05:00	I	) Storms moving from NNE
	06:00	I	)
	09:00	I	)
	10-12:00	I	
	13:00	C	

	14:00	CL	
	15:-16:00	I	
	17-18:00	CL	
	19:00	G	
96/01/26	03-04:001	I	
	14-15:00	I	
96/01/27	09:26:53	G	
	10:00	G	Stratiform layer < 30 dBz
	11-15:00	G	" "
	16:00	G	Isol > 40 dBz
	17:00	G	" "
	18:00	G	Dissipating
	19:00	I	
	20:00	I	
96/01/28	01:00	1	
96/02/01	14:00	C	
	15:00	I	
	16:00	I	
	17:00	I	
	18:00	I	
	19:00	G	Storm stratiform layer
	20:00	G	" "
96/02/02	15:00	L	Line NE to SW 60 km in length
	16:00	C	Line forms cluster
	17:00	C	
96/02/05	13:00	I	Intense cluster dBz > 60 moving SE to NW west of network
96/02/09	17:00	I	
	18:00	I	
96/02/10	10:00	I	
	14:00	I	
	15:00	I	
	23:00	0	Large cluster east of network
	24:00	I	
96/02/11	01:00	I	
	02:00	C	
	03:00	CL	)
	04:00	C	) Clusters forming and breaking dBz ± 40 +
	05:00	CL	)
	06:00	CL	)
	07:00	CL	)
	08-9:00	I	Large CL to West
	10:00	CL	
	11:00	CL	)
	12:00	CL	) Large clusters moving East
	13:00	CL	)
	14:00	CL	

	15:00	G	Stratiform layer 20-30 dBz
	16:00	G	" "
96/02/13	09-13:00	I	
	15-16:00	I	
	17:00	C	± 40 dBz
	18:00	C	
	19:00	C	
	20:00	I	
	21:00	I	
	22:00	CL	
	23:00	CL	
	24:00	CL	
96/02/14	00:01:48	CL	
	01:00	C	
	02-04:00	CL	
	05:00	I	
95/02/15	04:00	G	Leading edge of cluster.
	05-06:00	C	
	07:00	G	
	08-09:00	G	< 40 dBz
	10:00	G	< 30 dBz
	11-12:00	G	
	18-22:00	I	< 40 dBz
96/10/21	14:00	I	
	15:00	C	Explosive development over the network!
	16:00	I	
96/10/22	05:00	I	Stratiform field
	06:00	I	"
	07:00	I	"
	08:00	G	"
	09:00	G	"
	10:00	I	
	11:00	I	
	12:00	C	
	13:00	CL	
	14:00	C	
	16:00	C	Convection cells embedded in stratiform field
	17:00	I	
	18:00	C	
	19:00	C	
	20:00	C	
	21:00	G	
	22:00	G	
	23:00	G	
96/10/23	01:00	I	
	02:00	G	< 20 dBz
	08:00	I	Large cells NE to SE of the network
	10:00	I	
	13:00	C	

	14:00	L	Line NNW – SSE 70 + km in length
	15:00	C	
	16:00	C	
	17:00	CL	1650 – 1659 Strong bow shaped pattern approaching network dBz > 50
	18:00	CL	Hook shape at 17-08-30
	19:00	CL	)
	20:00	CL	) Moving E
	21:00	G	Moving E dissipating
96/10/29	13:00	G	DBz < 30
	14:00	G	Isol cluster dBz > 30
	15:00	G	
	16-18:00	G	Isol cells dBz > 40
	19:00	G	Isol – 40 dBz
	20-21:00	G	
	22:00	G	Large convective structure by end period dBz > 40
	23:00	G	Clearing from West
	24:00	G	
96/10/30	01:00	G	
	02:00	G	Embedded convective cells
	03:00	I	
	06:00	L	Broken NW-SE line move dBz > 45
	07:00	C	Line breaking
	08:00	C	
	11:00	L	Broken line NE-SW approaching
	12:00	I	Line breaking into cells
	14-15:00	G	Cells > 50 dBz embedded
	16-17:00	CL	Large clusters in general rain area
	18:00	G/ CL	Large clusters dissipating
	19:00	G	
	20:00	G	< 30 dBz
96/11/06	17:00	G	Stratiform layer dBz < 30
96/11/08	02:00	I	
	08:00	C	Line braking into clusters
	09:00	C	" "
	11:00	I	
	12:00	I	
	13:00		
96/11/17	01:00	L	Line > 60 km in length
	02:00	C	
	03:00	G	Stratiform layer
	06:00	G	Stratiform layer
	13:00	I	
	14:00	I	
	18:00	I	
	19:00	G	
	20:00	G	
	21:00	CL	
	22:00	C	
	23:00	C	
	24:00	C	

96/12/02	11:03:53	I	
	12:00	I	
	14:00	0	Strong line 100 km in length towards the SW
	15:00	0/I	Large line NW to SE 20 km to the SW
	16:00	L	Line passed over network 15:33
	17:00	G	Large stratiform cloud field dBz < 30 behind line
	18:00	0	" " dissipating
	23:00	I	
	24:00	I	
96/12/03	00:03:49	I	
	01:00	I	
	02:00	I	
	03:00	I	
	11:00	I	
96/12/08	19:44:59	I	
	20:00	I	
	21:00	I	
	22:00	I	
96/12/09	09:00	I	
	10:00	I	
	13:00	I	Stratiform shield dBz ± 30
	14:00	I	
	15:00	C	Cluster west of network dBz > 60 passing to the North
	16:00	C	
	17:00	I	
96/12/11	14:00	I	
	15:00	C	
	16:00	C	
	17:00	G	
	23:00	I	General rain south of radar
	24:00	I	
96/12/12	00:01:05	I	
	01:00	I	
96/12/17	14:00	I	Mainly isolated cells almost C. Isolated merging to clusters
	15:00	C	
	16:00	C	Large line NW-SE N of network
	17:00	I	
	18:00	I	
	19:00	C	
97/03/01	15:00	I	
	19:00	I	
	20:00	I	
97/03/02	04:00	G	Leading edge of cluster approaching
	05:00	CL	
	06:00	CL	
	07:00	C	Clusters moving E breaking up
	08:00	I	

	10:00	I	
	13:00	I/G	Leading edge of a cluster
	14:00	C	
	15:00	I	
	24:00	I	
97/03/03	01:00	I	
	02:00	I	
	22:00	I	
	23:00	I	
	24:00	I	
97/03/04	02:00	I	
	03:00	I	
	04:00	I	
	20:00	I	Leading edge of a large bow shaped pattern
	21:00	C	
	22:00	I	
	23:00	G	Stratiform fields
	24:00	G	" "
97/03/05	01-03:00	0	Stratiform remains
	08:00	G	Leading edge of a cluster
	09:00	C	
	10:00	0	Stratiform fields
	11:00	0	" "
	12:00	G	) Embedded cells dBz < 40
	13:00	G	)
	14:00	G	)
	15:00	G	Small cluster over net dBz = 40
	16:00	G	" "
	17:00	G	
	18:00	G	Clusters dissipating
	19:00	G	"
	20:00	G	
	21:00	G	Embedded clusters dBz > 36
	22:00	G	" " dBz > 45
	23:00	CL	Embedded cells dBz > 45
	24:00	G	DBz > 39
97/03/06	01:00	G	DBz < 30
	02:00	G	DBz > 39
	03:00	G	Embedded cells dBz > 45
	04:00	G	" dBz > 45
	05:00	G	Clearing from W dBz > 39
	06:00	G	20 < dBz < 30
	07:00	I	
	08:00	I	
	12:00	I	
	13:00	I	
	14:00	I	
	15:00	I	
97/03/07	10:00	I	
	13:00	I	
	14:00	I	

97/03/08	15:00	I	DBz > 50 Cells moving from S
	16:00	I	
	17:00	I	
	18:00	I	
	20:00	I	Cells now moving from SE
	22:00	I	
	23:00	I	
	24:00	0	Stratus fields
97/03/09	02:00	I	
97/10/11	02:00	G	
	03:00	C	dBz > 60 in some cells
	04:00	G	" "
	05:00	G	Dissipating. Some convection cells
	18:00	0	Big system approaching from W
	19:00	G	Stratiform field
	20:00	CL	) Moving fast to E
	21:00	CL	)
	22:00	I	
97/10/14	17:00	I	
	19:00	0	Large line with cyclonic curl west of radar. Perfect bow shape 15 km west of network about 40-50 km in length.
	20:00	L	Bow shape breaking up.
	21:00	CL	Strong evidence of micro cyclone
	22:00	CL	
	23:00	G	Convection elements 40-45 dBz
	24:00	CL	
97/10/15	01:00	G	Convective elements moving E and dissipating
97/11/08	15:48:07	I	
	16-18:00	I	
	21:00	I	
	22:00	I	
	24:00	I	
97/11/09	00:01:30	I	
	01:00	I	
	04:00	I	
	05:00	I	
	18:00	I	
97/11/10	03:00	I	
	10:00	C	± 20 km dBz > 50
	11:00	I	
	14:00	I	Edge cluster
	16:00	I	
	23:00	I	
97/11/11	07:00	I	
	08:00	I	
	14:00	I	Explosive developing
	15:00	I	
	16:00	C	> 50 dBz over network. Splitting?

	17:00	I	
	18:00	C	
	19-23:00	I	
97/11/12	09-13:00	0	Large fields developing NW / SW
	14:00	0	Large fields approaching
	15:00	CL	Large cluster dBz > 65 dBz north of network.
	16:00	CL	
	17:00	CL	
	18:00	G	
	19:00	G	
	20:00	G	Dissipating
97/11/13	17:00	C	Mainly to South
	24:00	I	
97/11/14	01:00	I	
	13:00	I	
97/11/15	04:00	I	
	05:00	I	
	16:00	CL	
	17:00	G	
	18:00	G	Dissipating
	19:00	G	"
	20:00	G	"
	21:00	I	Embedded cells
	22:00	I	
	23:00	I	
97/11/16	09:00	I	
	12:00	C	Peak dBz > 60
	13:00	C	Peak dBz > 60
	14:00	I	
	15:00	I	Nice line 85 km west
	16:00	L	Line reached Network by 1555 orientated N/S
	17:00	C	Line breaking up (class C)
	18:00	I	Dissipating
	20:00	I	Cell approaching
	21:0	I	
97/11/27	12:00	I	
	13:00	I	
	14:00	I	
	15:00	G	Stratiform field ahead cluster
	16:00	C	
97/11/28	07:00	I	)
	08:00	I	) Isolated cells moving fast front NW
	11:00	I	)
	12:00	I	)
	18:00	I	
	19:00	L	Line from Lindley to east of Kestel. Lindley area dBz > 60. Weak part of line over network. Systems now moving to E NE
97/12/05	17:00	G	Large clusters around

	19:00	I	
	20:00	I	
	21:00	I	
	22:00	I	)
	23:00	I	) Image poor
	24:00	I	)
97/12/24	09:00	G	With convective elements
	10:00	G	Main system north of network
	12:00	I	
	15:00	I	
	16:00	I	Broken line (160 km) E – W just south of network at 1603
	17:00	L	Signs of mesosyclone north of network at 1645-1650
	18:00	I	
97/12/27	18:00	I	
97/12/28	15:00	I	
	16:00	G	Network under stratiform field from a cell with dBz > 65 This cell is moving NE splits at 1638 with right hand member developing.
	17:00	I	Big cells remain north of network
	18:00	C	" " NW of network. Rain from Stratiform fields.
97/12/29	14-20:00	0	Big cell dBz > 65 moving from South. First seen in Lesotho 90 km south of Radar 1957, dBz >70. Tracks due north keeps dBz 60-70 (Supercell?)
	21:00	I	This storm keeps it shape and dBz > 70 at 2200. Now 60 km 25°E of N
	23-24:00	0	At 2240 still has a core dBz > 65 now at 15°E of N 90 km from Radar. Leave radar range at 23.05 10°E of N dBz >57
97/12/30	01:00	I	
98/01/01	02:00	I	< 30 dBz
	06-07:00	G	Light extended from cluster
	08-10:00	CL	Border between CL and G
	11:00	G	
	12:00	I	
	13-17:00	G	Core dBz = 50
	18:00	G	Dissipating → E
	19:00	G	Light intermittent
	20:00	G	Light dBz < 30
	21-23:00	G	Developing again
	24:00	G	Light
98/01/02	03:00	I	
	04:00	I	
	05:00	I	
	06:00	I	
	07:00	C	
	08:00	I	
	09:00	I	
	10:00	I	
	12:00	I	
	13:00	I	
	16:00	I	
	17:00	I	

98/01/03	01-24:00	0	For 03/01 and 04/01: Small dBz < 30 spots appear. May miss them in the classification. If rain then class I
98/01/04	23:00	I	
09/01/06	03:00	I	
	04:00	I	
	05:00	I	
	09:00	I	
	10:00	I	
	11:00	C	
	12:00	I	
	13:00	C	
	14:00	C	
	18:00	I	
	19:00	I	
	20:00	I	)
	21:00	G	) Light with embedded clusters
	22:00	C	)
	23:00	C	)
	24:00	I	
98/01/07	01:00	I	
	02:00	I	
	05:00	CL	
	06:00	CL	
	07:00	C	
	08:00	I	
	09:00	I	
	10:00	I	
	11:00	I	
	12:00	I	
	13:00	I	
	14:00	I	
	15:00	I	
	16:00	I	
	17:00	I	
	18:00	I	
98/01/08	18:00	I	
98/01/09	02:00	I	
	04:00	I	
	08:00	I	
	10:00	C	
	11:00	C	
	13:00	C	
	14:00	CL	
	15:00	CL	
	16:00	CL	Moving East
98/01/13	19:00	I	Weak < 30 dBz
	20:00	I	
	21-24:00	I	
98/01/14	08-09:00	G	

	10:00	G	Dissipating
	17:00	0	General rain SW to W of Network
	18:00	G	Lights sectors
	21:00	G	Bands general rain light
	22:00	G	
98/01/15	01:00	G	
98/01/18	11:00	I	
98/01/19	18:00	I	
	20:00	C	Edge only
	21:00	C	Line approaching
	22:00	G	Stratiform fields
	23:00	G	" "
	24:00	G	Dissipating - moving E
98/01/20	02:00	I	Stratiform field
	07:00	I	In stratiform field
	15:00	C	Mainly to the N
	17:00	I	
98/01/23	01:00	G	
	02:00	G	Dissipating
	12:00	I	Developed over network moving rapidly E. Example of cell splitting.
	13:00	I	
	14:00	I	
	15:00	I	
	19:00	0	Line approaching
	20:00	L	Line ESE – WNW (100 kms) over network at 1921
	21:00	I	
98/01/29	11:00	0	Large cells SW of radar
	14:00	I	
	15:00	CL	Entering network from West
	16:00	CL	Main activity North of network
	17:00	C	
	18:00	I	
98/01/30	12:00	I	Weak echoes
	15:00	I	Weak ± 30 dBz
	16:00	I	
	18:00	I	
98/01/31	00:01:49	0	Light rain /echoes 40 km
	09-11:00	I	Echoes < 30 dBz
	13:00	I	" "
98/02/11	07:00	G	Stratiform field ahead of cells
	08:00	I	DBz < 30
	09:00	I	"
	10:00	I	"
98/02/12	05:00	C	
	06:00	C	

	07:00	I	) In large Stratiform field
	08:00	I	)
98/02/13	04:00	C	Storm Splitting
	05:00	I	" "
98/02/14	18:00	I	DBz < 35
98/02/15	14:00	I	DBz > 50
	15:00	C	Near stationery complex mainly south of network
	16:00	I	In Stratiform field
	24:00	G	Stratiform fields from complex to the NW
98/02/16	01:00	I	In large Stratiform field
	02:00	CL	Large complex with embedded clusters
	03:00	CL	
	04:00	CL	
	05:00	CL	
	06:00	C	
	07:00	G	Near large cluster
	08:00	G	Imbedded clusters in Stratiform field
	10:00	I	
	11:00	C	
	12:00	C	
	13:00	G	
	14:00	G	Dissipating
	19:00	I	
	21:00	G	Stratiform field
	22:00	I	
	23:00	G	Stratiform field
	24:00	I	
98/02/17	01:00	G	Low dBz < 20 (Stratiform field)
	02:00	G	" "
	03:00	C	" "
	04:00	G	" "
	05:00	I	
	08:00	I	
	10:00	I	
	11:00	I	
	12:00	I	
98/02/19	16:00	CL	
	17:00	CL	
	18:00	I	In Stratiform field
	19:00	I	"
	20:00	I	"
	21:00	I	
	22:00	I	
	23:00	C	
	24:00	I	
98/02/20	01:00	I	
	02:00	I	
	03:00	I	
	10:00	I	

	15:00	C	
	16:00	I	
	17:00	C	
	18:00	C	
	19:00	I	
98/02/21	01:00	I	
98/02/22	01:00	I	
	02:00	I	
98/02/23	14:00	I	
	15:00	I	
	16:00	0/I	
98/02/26	23:00	I	
98/02/27	01:00	I	Stratiform band
98/03/01	05:00	I	
	12:00	I	
	13:00	I	
	14:00	I	
	15:00	CL	
	16:00	G	Stratiform fields from cluster dissipating
	17:00	G	New cluster from W
	18:00	CL	
	19:00	CL	Action mainly N of network
	20:00	G	Mainly Stratiform fields
	21:00	C	
	22:00	C	
	23:00	I	
98/03/08	01:00	G	
	02:00	G	
	03:00	CL	Mainly stratiform layer with embedded cells
	04:00	G	
	05:00	G	
	06:00	CL	In large rainfield
	07:00	CL	" "
	08:00	CL	More than 95% of image has echoes
	09:00	CL	In large rainfield
	10:00	G	Embedded convective cells 74 dBz
	11:00	CL	Rainfield slowly going S down to about 70% coverage
	12:00	G/C	Mainly general with clusters of convective systems
	13:00	G	Embedded convective systems
	14:00	G	Dissipating
	15:00	G	Some convective cells
	16:00	G	
	17:00	G	But clearing from W by 1630
	19:00	I	
98/03/24	01:00	I	
	02:00	I	
	03:00	I	Edges only

98/03/25	05:00	I	Possible
	13:00	I	
98/03/26	13:00	I	
	14:00	I	Large rain field in SW
	17:00	G	Systems moving very slowly
	19:00	G	Adjacent to CL
	20:00	C	
	21:00	CL	
	22:00	C	
98/03/27	15:00	C	
	19:00	G	CL moving to N
	20:00	G	Convective elements
	21:00	G	Dissipating
	23:00	I	

APPENDIX C

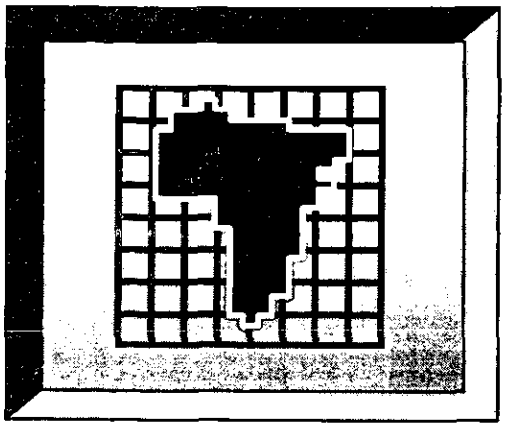

LIEBENBERGSVLEI / VAALBANK

GRID GRAPHICS
PRESS ANY KEY TO CONTINUE

Precipitation graphic system

The graphic software package runs under the DOS operating system. It provides the user with a wide range of options including grid resolution, contour spacing, contour labeling, shading and vector graphics. The mathematical process covering the interpolation of unevenly spaced rainfall to a selected grid field is described by:

Rautenbach, C.J.deW. (1996) The construction of a data point concentration dependant weight function for interpolation to rainfall grid fields. *SA Tydskrif vir Natuurwetenskap en Tegnologie*, **15**, no. **4**, 168-171.

The following are required for running the system:

- PC (486+), RAM (8mb+), Direct link with a laser printer with PCL2 or HPGL

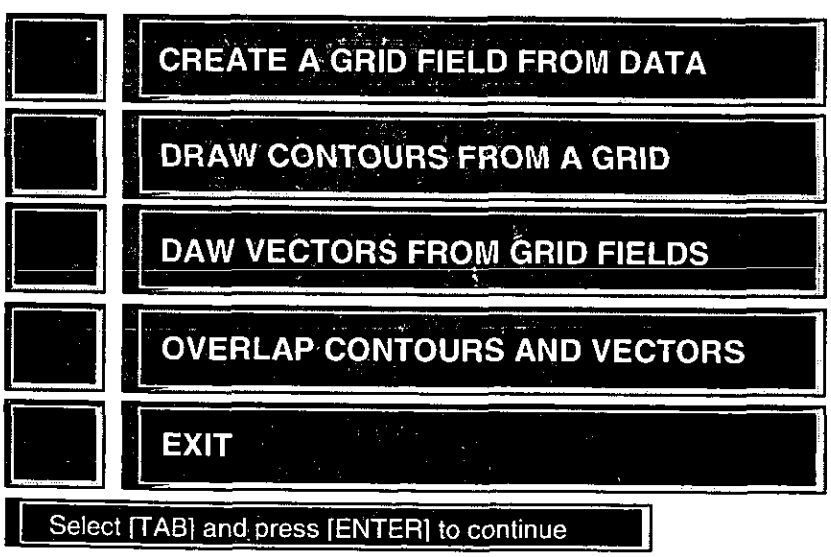

CREATE A GRID FIELD FROM DATA

	INPUT DATA FILE	Indata.doc
	OUTPUT GRID FILE	Ingrid.doc
	HEADER OF GRID FILE	INTERPOLATING DATA TO GRIDFIELD
	NUMBER OF X-GRIDS	50
	NUMBER OF Y-GRIDS	70

	MIN X-VALUE	28.1
	MAX X-VALUE	28.85
	MIN Y-VALUE	-28.42
	MAX Y-VALUE	-27.48

CONTINUE ENTER OPTION →

Select [TAB] and press [ENTER] to change - [ESC] to exit

DRAW CONTOURS FROM GRID

	INPUT FILE NAME	Ingrid.doc
	HEADER OF GRAPH	LIEBENBERGSVLEI / VAALBANK
	PRINTER: ON / OFF	OFF
	MIN ON VAL	0
	MAX ON VAL	80
	CONTOUR INTERSPACE	5
	SMOOTH DATA : ON/OFF	ON
	OBS VALUES : ON/OFF	ON

	PLOT FREQUENCY	25
	SHADING: ON/OFF	OFF
	MIN SHADE	15
	MAX SHADE	25
	PERC. SHADE	20

CONTINUE ENTER OPTION →

Select [TAB] and press [ENTER] to change - [ESC] to exit

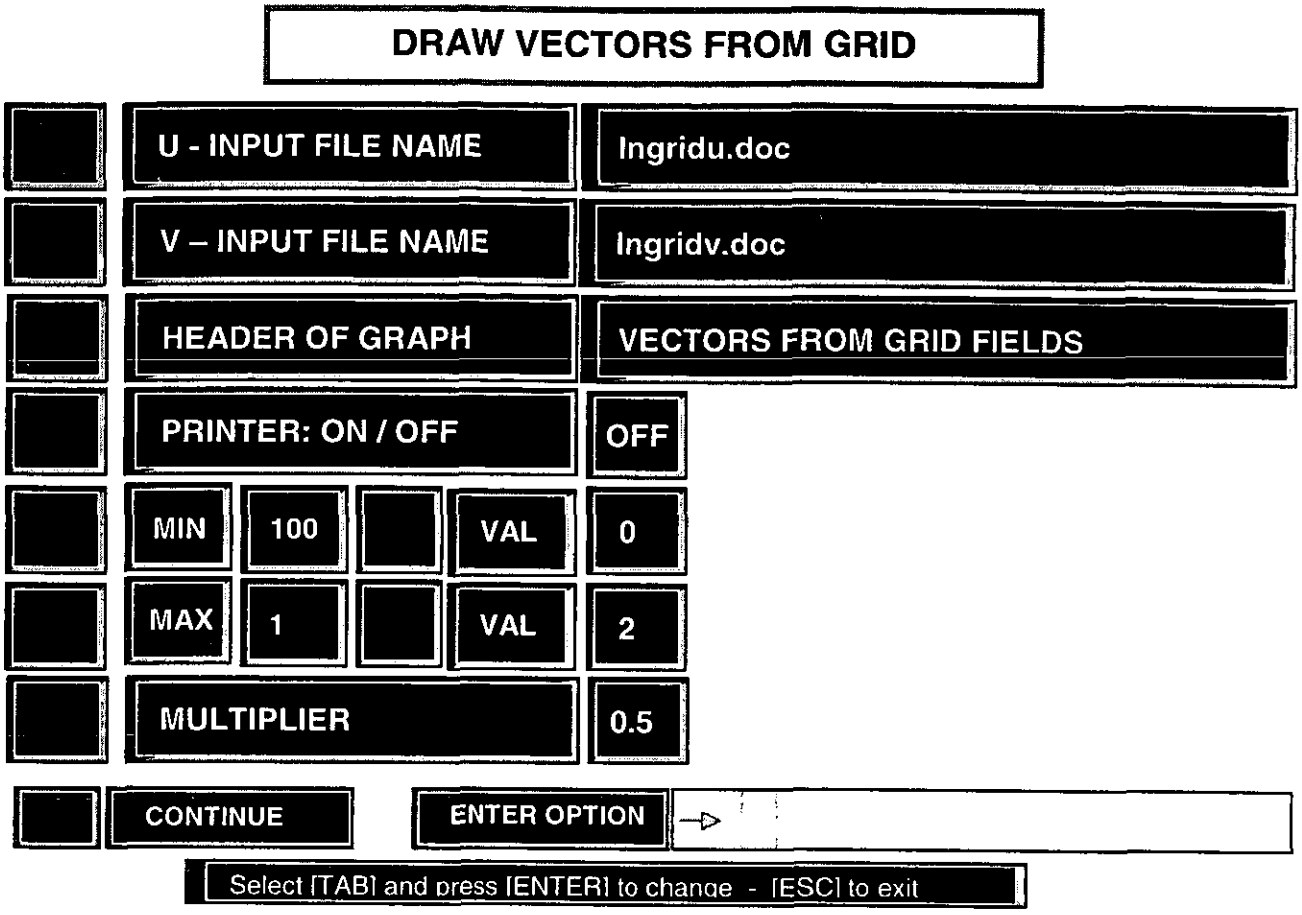
DRAW VECTORS FROM GRID
U - INPUT FILE NAME
Ingridu.doc
V – INPUT FILE NAME
Ingridv.doc
HEADER OF GRAPH
VECTORS FROM GRID FIELDS
PRINTER: ON / OFF
OFF
MIN
100
VAL
0
MAX
1
VAL
2
MULTIPLIER
0.5
CONTINUE
ENTER OPTION
Select [TAB] and press [ENTER] to change - [ESC] to exit

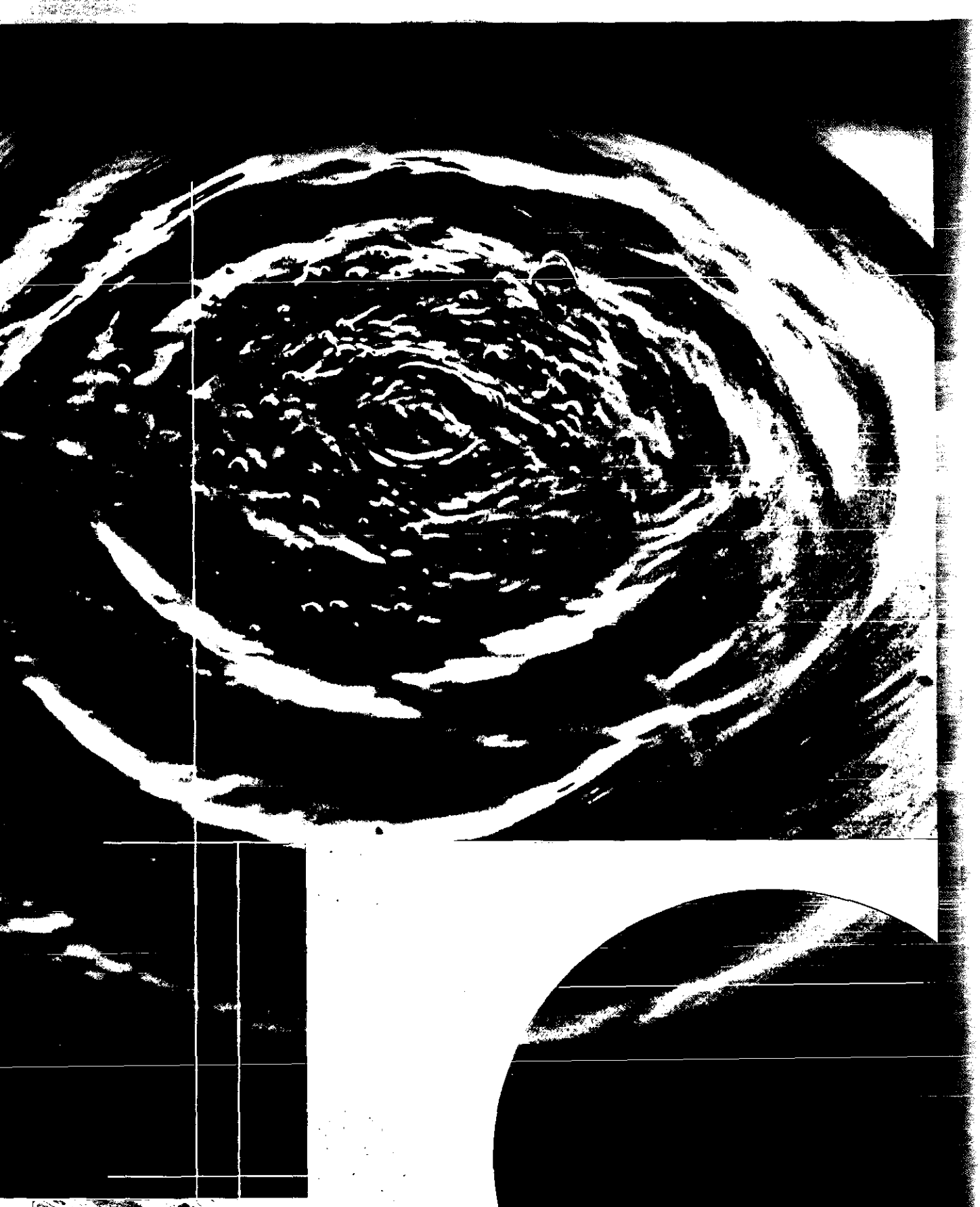

Water Research Commission
PO Box 824, Pretoria, 0001, South Africa
Tel: +27 12 330 0340, Fax: +27 12 331 2565
Web: http://www.wrc.org.za